Structural and Functional Insights into the Type II Secretion System of *Vibrio cholerae*

by

Chelsea Rule

A dissertation submitted in partial fulfillment
of the requirements for the degree of
Doctor of Philosophy
(Microbiology and Immunology)
in the University of Michigan
2016

Doctoral Committee:

Associate Professor Maria B. Sandkvist, Chair
Associate Professor Matthew R. Chapman
Professor Victor J. DiRita, Michigan State University
Assistant Professor Nicole Koropatkin

“Before a mad scientist goes mad, there's probably a time when he's only partially mad. And this is when he's going to throw his best parties.”

-Jack Handey

“An expert is a person who has made all the mistakes that can be made in a very narrow field.”

-Niels Bohr

To Cameron, я люблю тебя

Acknowledgments

Thank you Maria for your support and mentorship throughout this process. Your feedback and encouragement has been invaluable, and I deeply appreciate the significant effort that you have spent on my success.

My committee members, Vic DiRita, Matt Chapman, and Nicole Koropatkin, have been incredibly helpful and positive throughout my time at Michigan, and I thank them for their ideas and time. Thanks to many of the Microbiology & Immunology department office staff members, especially Heidi Thompson, for fielding my many questions and providing assistance with financial and administrative matters throughout my time here.

I would also like to give a big thanks to my lab-mates (past and present), who have helped me immensely throughout graduate school. Aleksandra Sikora was a huge inspiration and a fantastic mentor during my rotation in the Sandkvist lab. Thanks to Aleksandra as well as Tanya Johnson, Marcy Patrick, Miranda Gray, and Shilpa Gadwal for technical assistance and excellent company. It has been a joy working alongside Ursula Waack, Khalil Chedid, and Aurelia Syngkon. Lab would not have been nearly as enjoyable without the fun conversations I had with you all! Special thanks to my previous undergraduate research mentees Alana Pinksky and Ryan Thomas, who I know are destined for great things. To all my

other friends who have supported me through everything, thank you. You guys rock.

My family has also been integral to my success. My dad inspired, supported, and encouraged me his whole life, and is responsible for much of my motivation to pursue a PhD. My brother has been a great friend since I can remember and has always believed in me. Oates and Garfunkel are the best furry companions I could ever hope for, and have heard a lot of scientific research talks by now.

Last, but certainly not least: thank you, Cameron. I literally have you to thank for keeping me alive through this entire process. Your love and support has been so important throughout graduate school, and I absolutely could not have done this without you. Here's to a new chapter in our lives, and let us never smell LB again.

Table of Contents

List of Figures

List of Tables

Abstract

The bacterium *Vibrio cholerae* is the causative agent of cholera, a severe, acute diarrheal disease endemic throughout parts of the world. *V. cholerae* uses the type II secretion (T2S) system to transport the virulence factor cholera toxin to the extracellular milieu, which is primarily responsible for the disease's hallmark massive, watery diarrhea. This widespread T2S system is structurally homologous to the type IV pilus (T4P) system. In this study, I use a suite of biochemical and genetic techniques to further elucidate the mechanism of the ATPase that powers T2S, EpsE, as well as the overall role of the T2S system in cell envelope stability.

EpsE contains a unique metal-binding (C_M) domain that coordinates zinc via a tetracysteine motif. The C_M domain is conserved among homologous T4P ATPases that power pilus assembly, but not T4P retraction ATPases. In order to assess the contribution of the C_M domain to T2S, we removed the domain or substituted combinations of cysteine residues in the tetracysteine motif. All of these mutations abrogate EpsE's ability to support T2S and have a dominant negative effect on secretion in the presence of WT EpsE. Additionally, EpsE's ATPase activity is abolished upon zinc depletion *in vitro*. However, swapping the residues between the two dicysteine motifs with those from the homologue XcpR from *Pseudomonas aeruginosa,* resulting in the substitution of 17 out of 29 residues, has no significant effect on EpsE. Thus, while zinc coordination is essential for

function, the C_M domain may not play a species-specific role in EpsE and other T2S ATPases.

The *eps* genes encoding proteins required for T2S are putatively essential in *V. cholerae*, and *eps* inactivation results in widespread cell envelope defects, in addition to loss of secretion. To investigate the possibility that suppressor mutations facilitate *eps* gene inactivation, we used high-throughput genome sequencing to identify secondary mutations in *V. cholerae eps* mutants. Two independently constructed *eps* mutants contain distinct inactivating mutations in the T2-secreted protease VesC that may protect the cell from unwanted proteolysis by mislocalized VesC, suggesting one mechanism by which *V. cholerae* creates permissive conditions for acquiring *eps* mutations.

Chapter 1:

Introduction

Vibrio cholerae Life Cycle

Cholera is a severe, acute diarrheal disease that can cause dehydration and death within 24 hours (Wachsmuth *et al*., 1994; Harris *et al*., 2012). Although descriptions of the disease and its characteristic secretory diarrhea date back to the 5th century BCE, global spread of cholera endemics began in 1817 and continue presently (Harris *et al*., 2012). Cholera is caused by the Gram-negative bacterium *Vibrio cholerae*, which has been responsible for seven worldwide cholera pandemics in the last 200 years (Harris *et al*., 2012). There were approximately 2.9 million annual cases of cholera in 69 endemic countries, including 95,000 deaths a year, between 2008 and 2012. Roughly 60% of the worldwide cholera burden during that period was in sub-Saharan Africa. Although approximately 1/3 of the world's countries are currently endemic and/or at risk for becoming cholera-endemic, this disease disproportionately affects developing nations (Ali *et al*., 2015).

V. cholerae can be subdivided into serogroups based on the lipopolysaccharide (LPS) O-antigen, and the two serogroups responsible for most of the global cholera pandemics are classified as O1 or O139 (Faruque *et al*., 1998; Kaper *et al*., 1995). *V. cholerae* O1 strains are comprised of classical and El Tor

biotypes based on their phenotypes for hemolysis, bacteriophage sensitivity, and sensitivity to polymyxin B. These biotypes can be further divided into two serotypes: Ogawa and Inaba (Kaper *et al*., 1995; Harris *et al*., 2012). The current seventh global pandemic is caused by the *V. cholerae* O1 El Tor biotype, whereas the previous six pandemics were caused by the classical biotype. The seventh pandemic El Tor strain is more widespread than those from previous pandemics, due in large part to its increased hardiness and ability to cause asymptomatic cholera (Kaper *et al*., 1995; Felsenfeld, 1965).

V. cholerae has a biphasic life cycle, as it is able to cause cholera upon infection of a human host, and is also able to survive and persist in the aquatic environment as a disease reservoir. These environmental bacteria are commonly found in brackish and estuarine water sources such as the Ganges River, either as planktonic cells, anchored to abiotic surfaces as biofilms, or attached to copepods or chironomid egg masses (Butler & Camilli, 2005; Broza, 2001; Halpern *et al*., 2003; Vezulli *et al*., 2010; Huq *et al*., 1984). *V. cholerae* is ingested from contaminated water sources, and colonization of the human small intestine and production of cholera toxin results in the profuse, watery diarrhea that characterizes cholera (Wachsmuth *et al*., 1994; Kaper *et al*., 1995). Bacteria are shed in a hyperinfectious state that facilitates rapid spread and transmission within and between households and populations, fueling local epidemics (Merrell *et al*., 2002; Alam *et al*., 2005; Tamayo *et al*., 2010).

Climate change and seasonal variations in weather patterns play key roles in cholera dynamics, and most cholera outbreaks occur during the monsoon

season and in the spring and fall (Huq *et al*., 1984; Pascual *et al*., 2000; Lobitz *et al*., 2000). These outbreaks are linked to additional factors, such as phytoplankton and zooplankton blooms, variations in salinity, and the presence of *V. cholerae* phage (Huq *et al*., 1984; Nelson *et al*., 2009). A recent cholera outbreak following an earthquake in Haiti in 2010 resulted from a combination of the likely introduction of *V. cholerae* from another part of the world, infrastructure disruption that reduced sanitation, and suitable environmental conditions for cholera spread (Talkington *et al*., 2011; Jutla *et al*., 2013).

The most prevalent treatment of cholera is oral rehydration therapy, which includes replacement of water and electrolytes lost during diarrhea. Antibiotics may be used in conjunction with oral rehydration, especially in severe cases, but the use of antibiotics also drives increasing antibiotic resistance among *V. cholerae* (Kaper *et al*., 1995; Sack *et al*., 2004). Vaccines such as Dukoral have been effective during field trials in developing countries, but there is debate on whether they are a cost-effective method of preventing epidemics and may require regular boosters (Clemans *et al*., 1986; Clemans *et al*.,1990; Sack *et al*., 2004; Harris *et al*., 2012). A simple yet effective preventative measure to control cholera epidemics involved sari filtration of water before drinking (Huq *et al*., 2010). Further investigation of *V. cholerae* virulence and environmental survival mechanisms may assist in the development of additional or alternative prevention methods and treatments for cholera.

Type II Secretion and Pathogenesis

Gram-negative bacteria have evolved many distinct protein secretion pathways in order to transport proteins outside the cell. Proteins secreted by these pathways may either be destined for the bacterial cell surface, be released to the extracellular milieu, or be injected directly into a host cell (Costa *et al*., 2015; Gerlach & Hensel, 2007).

The type II secretion (T2S) system is a widespread exoprotein transport system possessed by a large number of human and plant pathogens (Table 1.1) (Sandkvist, 2001; Cianciotto, 2005). This multiprotein apparatus spans the entire cell envelope of Gram-negative bacteria and serves to translocate proteins in a folded conformation from the periplasmic space across the outer membrane. T2S-secreted proteins play important roles in various aspects of bacterial life cycles, depending on the organism, which includes nutrient acquisition, host modification, and environmental and/or niche survival (Cianciotto, 2005). For example, *Legionella pneumophila* uses a T2S system for intracellular survival not only in macrophages but also in amoebae (Rossier *et al*., 2004; Söderberg *et al*., 2008). Inactivation of genes required for T2S results in a loss of colonization or other aspects of pathogenesis for many organisms tested (see Table 1.1 for a partial list) (Sikora *et al*., 2007; Söderberg *et al*., 2008; Johnson *et al*., 2016; Jyot *et al*., 2011; Rossier *et al*., 2004).

Table 1.1 Examples of bacterial pathogens using type II secretion systems for virulence

Organism	Disease	Secreted proteins (subset)
Vibrio cholerae	Cholera	Cholera toxin, Chitinase, Hemagglutinin Protease[a]
Pseudomonas aeruginosa	Chronic lung infection in cystic fibrosis, nosocomial and opportunistic infections	Exotoxin A, Elastase, Phospholipase C[b]
Klebsiella oxytoca	Nosocomial infections	Pullulanase[c]
Aeromonas hydrophila	Septicemia in fish, opportunistic infections	Aerolysin[d]
Legionella pneumophila	Legionnaires' disease, pneumonia	Acid Phosphatase, Lipase[e]
Escherichia coli (EHEC)	Diarrhea	Metalloprotease[f]
Dickeya dadantii	Soft rot in plants	Pectinase, Cellulase[g]
Acinetobacter baumanii	Nosocomial infections	Lipase, Protease[h]

[a]Sandkvist *et al*., 1993; Overbye *et al*., 1993
[b]Bally *et al*., 1992; Lazdunski *et al*., 1990
[c]Pugsley *et al*., 1991
[d]Howard & Buckley, 1985
[e] Aragon *et al*., 2000; Aragon *et al*., 2001
[f]Lathem *et al*., 2002
[g]Andro *et al*., 1984
[h]Johnson *et al*., 2016; Harding et al., 2016

Vibrio cholerae uses the T2S system for the secretion of cholera toxin and many additional proteins, several of which are known to contribute to pathogenesis in humans and/or environmental survival and persistence of the bacteria outside of the host (Sandkvist *et al*., 1997; Sandkvist, 2001; Cianciotto, 2005, Sikora, 2013; Kirn *et al*., 2005; Overbye *et al.*, 1993; Connell *et al.*, 1998; Davis *et al.*, 2000; Sikora *et al.*, 2011; Johnson *et al.*, 2014). Over 20 *V. cholerae* T2S substrates have been identified, including the infamous cholera toxin, biofilm matrix proteins, chitin-

binding and –degrading proteins, as well as several proteases and a lipase (Sandkvist *et al*., 1997; Sikora *et al*., 2011; Kirn *et al*., 2005; Connell *et al*., 1998).

Cholera toxin is an 84 kDa canonical AB_5 toxin which is primarily responsible for the severe diarrhea that characterizes cholera. The B subunits bind to GM_1 ganglioside receptors on the small intestinal epithelium, allowing endocytosis of the toxin followed by retrograde transport of the A subunit, ADP ribosylation and activation of adenylate cyclase, leading to an increase in cAMP and chloride ion imbalance. This results in massive water release into the small intestine, the volume of which far exceeds the intestinal capacity, thus causing profuse, watery diarrhea containing chunks of intestinal mucus, known as rice-water stool (Sack *et al*., 2004; Nelson *et al*., 2009).

Three unique serine proteases were recently identified in the *V. cholerae* T2-secretome through proteomic analyses, called Ves (Vibrio extracellular protease) A, B, and C (Sikora *et al*., 2011). Each of these serine proteases may be involved in pathogenesis, as these proteins have been detected in the stool of human cholera patients and in some pathogenesis models (LaRocque *et al*., 2008; Hatzios *et al*., 2016). VesA may specifically play a role in cholera toxin activation, a necessary step during pathogenesis; however, a strain lacking all three serine proteases could still colonize infant mice as well as WT (Sikora *et al*., 2011). VesC has been shown to modify the villus structure and induce fluid accumulation in a rabbit ileal loop model (Syngkon *et al*., 2010). The structure and function of VesB has been recently investigated, which is a unique bacterial trypsin-like serine protease containing an N-terminal protease domain and a C-terminal Ig-fold.

Although the precise function is still unknown, this study suggested that VesB may be involved in nutrient acquisition by *V. cholerae*, which may be important during pathogenesis and/or environmental survival (Gadwal *et al*., 2014).

In addition to contributing greatly to pathogenesis, several T2-secreted proteins are known to play key roles in *V. cholerae* environmental survival (reviewed in Sikora, 2013). *V. cholerae* secretes a chitin binding protein (GbpA) to attach to zooplankton and a chitinase (ChiA), which allows bacteria to utilize chitin as a nutrient source (Connell *et al*., 1998; Kirn *et al*., 2005). The *V. cholerae* T2S substrates HAP, RbmA, Bap1, and RbmC each have distinct and critical roles in biofilm matrix modification (Fong & Yildiz, 2007; Berk *et al*., 2012; Johnson *et al*., 2014; Smith *et al*., 2015). Thus, the T2S system bridges both parts of the biphasic *V. cholerae* life cycle, contributing to both disease in a human host as well as persistence as a disease reservoir in the aquatic environment.

Type II Secretion Mechanism

Protein secretion via the T2S pathway involves two steps: first, proteins cross the inner membrane using the Sec or Tat machinery and enter the periplasm, where N-terminal signal sequences are removed and proteins fold; second, proteins transverse the outer membrane using the T2S system (Pugsley, 1993; Voulhoux *et al*., 2001). The T2S apparatus in *V. cholerae* is composed of 12 proteins, called EpsC-EpsM (for extracellular protein secretion) and PilD. The *epsC-M* genes are located in a single operon in *V. cholerae*, similar to most other organisms containing T2S systems (Sandkvist, 2001). The *pilD* (also known as

vcpD or *epsO*) gene is located elsewhere in the genome, and is also required for the related type IV pilus (T4P) system (Marsh & Taylor, 1998; Fullner & Mekalanos, 1999). The T2S apparatus proteins assemble into a multiprotein complex that spans from the cytoplasm to the outer membrane, and consists of several subassemblies: the outer membrane secretin, the periplasmic pseudopilus, the inner membrane platform, and the cytoplasmic ATPase. A model of the *V. cholerae* T2S apparatus is shown in Figure 1.1, the components of which are described in further detail below. Much of what is known about the T2S machinery has been derived from a combination of biochemical analyses, individual and protein complex crystal structures, as well as cryo-electron tomography of T2S and homologous T4P components (Johnson *et al*., 2006; Korotkov *et al*., 2012; Chang *et al*., 2016.)

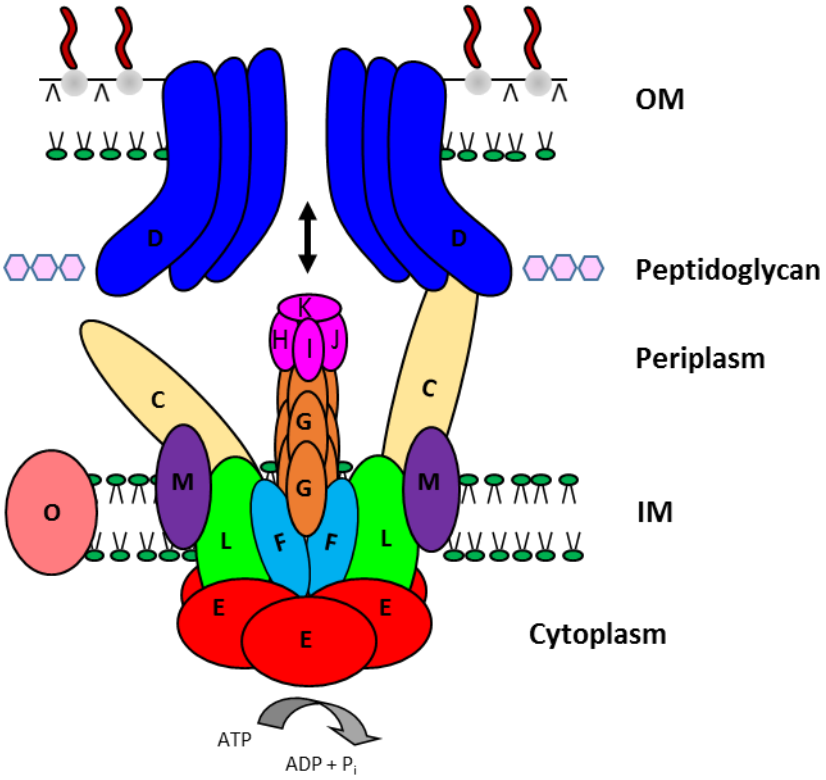

Figure 1.1 Model of the *V. cholerae* type II secretion (T2S) apparatus. This multiprotein complex spans the inner membrane (IM), periplasm, and the outer membrane (OM). The T2S apparatus is composed of the outer membrane secretin (EpsD), the inner membrane platform proteins (EpsC, F, L, and M), the major (EpsG) and minor pseudopilins (EpsH, I, J, and K), the inner membrane-associated cytoplasmic ATPase (EpsE), and the prepilin peptidase (EpsO/PilD) that is shared with the T4P system.

In the outer membrane, EpsD dodecamers form a pore through which exoproteins pass, known as a secretin. In addition to being required for T2S, EpsD is also the conduit through which the phage CTXφ is extruded (Davis *et al*., 2000; Chami *et al*., 2005; Reichow *et al*., 2010). EpsD and other homologous T2S secretins assemble into heat-stable, detergent-resistant multimeric rings (Bitter *et al*., 1998; Nouwen *et al*., 2000; Chami *et al*., 2005). The process of secretin outer membrane assembly is still not completely understood in T2S, and although many

organisms use a pilotin and/or a chaperone to promote assembly, these factors have not been implicated in EpsD assembly in *V. cholerae* (Shevchik *et al*., 1997; Condemine & Shevchik, 2000; Schoenhofen *et al*., 2005). EpsD contains a C-terminal domain which is thought to anchor proteins in the outer membrane through conserved β-strands, and an N-terminal domain located in the periplasm which may interact with other components of the T2S apparatus including EpsC and/or T2-secreted substrates (Bitter *et al*., 1998; Bouley *et al*., 2001; Douet *et al*., 2004; Korotkov *et al*., 2006; Korotkov *et al*., 2009). The structure of the EpsD secretin was recently determined using cryo-electron tomography, allowing a detailed model of the secretin to be illustrated, which consists of a cylindrical pore that looks like an inverted cup (Reichow *et al*., 2010). The secretin is gated, and it is possible that interactions between EpsD and secreted substrates results in a conformational change that opens the secretin channel (Shevchik *et al*., 1997; Sandkvist *et al*., 2001; Reichow *et al*., 2010).

EpsC putatively connects the outer membrane secretin with the inner membrane platform, and has been shown to interact with the inner membrane proteins EpsL and EpsM as well as EpsD in the outer membrane (Possot *et al*., 1999; Sauvonnet *et al*., 2000; Gérard-Vincent *et al*., 2002; Robert *et al*., 2002; Lee *et al*., 2004; Korotkov *et al*., 2006; Korotkov *et al*., 2011). The EpsC HR domain is largely responsible for determining interactions with EpsD, whereas the PDZ domain may determine substrate specificity and/or substrate targeting to the T2S system (Korotkov *et al*., 2011; Bouley *et al*., 2001; Korotkov *et al*., 2006; Pineau *et al*., 2014).

The T2S pseudopilins are named for their relatedness to the major pilin of the homologous T4P system. The T2S pseudopilus is composed of the major pseudopilin EpsG and the minor pseudopilins EpsH, I, J, and K. Together, they are thought to act as a biological piston that pushes proteins through the outer membrane secretin (Shevchik *et al*., 1997; Nunn *et al*., 1999). It is also possible that the pseudopilus more closely resembles an Archimedes' screw, in which secreted proteins bind to pseudopilin components and pseudopilus extension drives rotation and protein passage through the secretin (Nunn *et al*., 1999; Campos *et al*., 2013). The pseudopilins are processed by the prepilin peptidase, PilD (Nunn & Lory, 1993; LaPointe & Taylor, 2000; Marsh & Taylor, 1998; Fullner & Mekalanos, 1999; Sandkvist *et al*., 1997). The structure of EpsG has been solved, as well as complexes between several pseudopilins (Yanez *et al*., 2008a; Yanez *et al*., 2008b; Korotkov & Hol, 2008; Korotkov *et al*., 2009). Structural information suggests that EpsK forms the tip of the pseudopilus, and biochemical data indicates that EpsI is likely the initiator of pseudopilus assembly (Durand *et al*., 2005; Korotkov *et al*., 2008; Douzi *et al*., 2009; Korotkov *et al*., 2012). Upon overexpression of EpsG homologues, the T2S pseudopilus has been visualized as a helical fiber on the surface in some organisms, highlighting the similarity between the T2S and T4P systems (Sauvonnet *et al*., 2000; Vignon *et al*., 2003; Durand *et al*., 2003; Köhler *et al*., 2004).

The inner membrane platform consists of EpsC, EpsF, EpsM, and EpsL. EpsM and EpsL stabilize each other (Sandkvist *et al*., 1999). The structures of the periplasmic domains of EpsL and EpsM indicate that while the sequence identity

is low, these domains are structurally related (Abendroth *et al*., 2009a). EpsF, which contains three putative transmembrane domains and two cytoplasmic domains, is functionally less well-characterized than many other T2S components, although the structure of the N-terminal cytoplasmic domain has been solved, and the C-terminal cytoplasmic domain structure is putatively similar (Thomas *et al*., 1997; Arts *et al*., 2007; Abendroth *et al*., 2009b). EpsF is stabilized in the presence of EpsM and EpsL (Arts *et al*., 2007). Evidence for interactions between EpsF, EpsL, EpsE, and EpsM have been demonstrated using co-immunoprecipitation and co-purification techniques (Py *et al*., 2001; Robert *et al.*, 2005; Abendroth *et al*., 2009b). Many of the protein-protein interactions observed within the T2S complex have been confirmed with EpsE, EpsL and EpsF homologues of the T4P system (Bischof *et al*., 2016; Ayers *et al*., 2009; Georgiadou *et al*., 2012).

EpsL is a bitopic inner membrane protein containing a large cytoplasmic domain and a short periplasmic domain, and has been shown to directly interact with EpsM and EpsE (Sandkvist *et al*., 1997; Sandkvist *et al.*, 1999; Abendroth *et al*., 2005). Interactions between the cytoplasmic domain of EpsL and the N-terminal domain of the cytoplasmic ATPase EpsE have been well established, as demonstrated both by mutational analyses and co-crystallization (Sandkvist *et al*., 1995; Sandkvist *et al*., 1999; Abendroth *et al*., 2005). The cytoplasmic ATPase EpsE is associated with the inner membrane through these interactions with EpsL, and this protein will be described in more detail below (Sandkvist *et al*., 1995; Abendroth *et al*., 2005).

Type II Secretion is Powered by the AAA+ ATPase EpsE

The ATPase EpsE is a molecular motor protein that provides the energy for T2S via ATP hydrolysis (Camberg & Sandkvist, 2005). AAA+ ATPases (ATPases associated with various cellular activities), such as EpsE, belong to a diverse group of ATP-hydrolyzing oligomeric enzymes that, while maintaining some structural and functional similarities, support a wide variety of cellular processes from protein unfolding to DNA replication (Hanson & Whiteheart, 2005). EpsE is a member of the type II/IV secretion ATPase family, which includes proteins that energize protein secretion, T4P biogenesis or function, and archaeal movement via the archaeallum, which more closely resembles a T4P than a bacterial flagellum (Planet *et al*., 2001; Ghosh & Albers, 2011; Albers & Jarrell, 2015). Type II/IV secretion ATPases contain an N-terminal domain (NTD) and a C-terminal domain (CTD) connected by a short flexible linker; within the CTD, Walker A and B motifs and Asp and His boxes collectively form the nucleotide-binding pocket (Planet *et al*., 2001; Robien *et al*., 2003; Satyshur *et al.*, 2007; Chiang *et al*., 2008; Misic *et al.*, 2010; Rose *et al.*, 2011; Reindl *et al.*, 2013). EpsE belongs to the subfamily of GspE/PilB ATPases that play a role in (pseudo)pilus assembly in the T2S, T4P, or archaeal flagellar systems (Planet *et al*., 2001). Nearly all GspE/PilB subfamily members contain a tetracysteine motif ($CXXCX_{21\text{-}40}CXXC$) that coordinates zinc, whereas ATPases associated with pilus retraction, such as PilT and PilU, lack this motif (Whitchurch & Mattick, 1994; Planet *et al*., 2001; Robien *et al*., 2003; Camberg & Sandkvist, 2005; Satyshur *et al*., 2007; Misic *et al*., 2010).

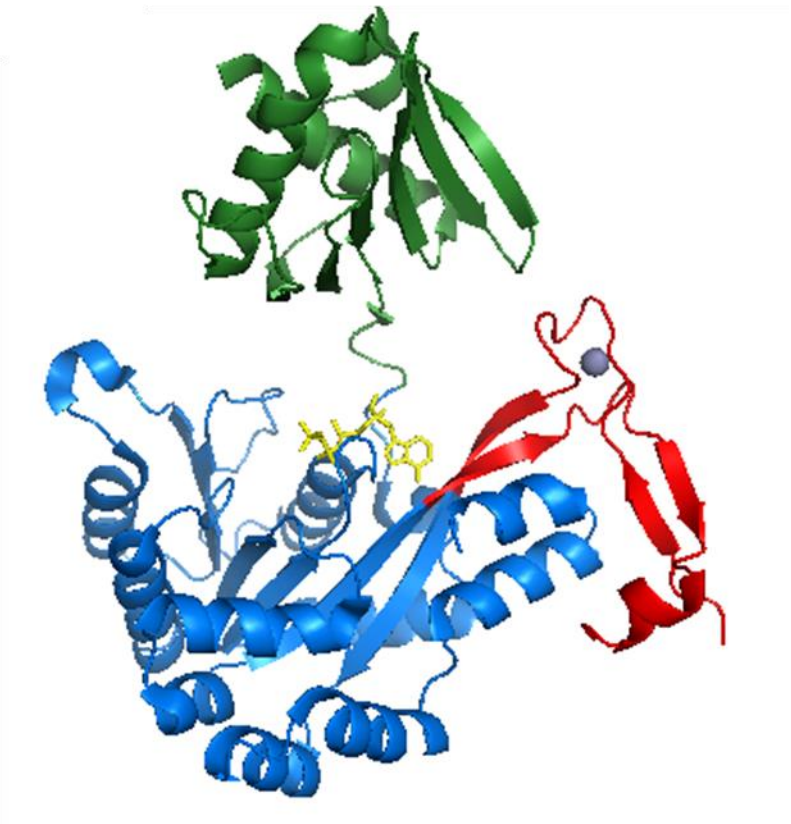

Figure 1.2 Structure of truncated monomeric EpsE. The structure of EpsE was solved lacking the first 90 amino acids (Robien *et al*., 2003; PDB 1p9w). The structure is shown in ribbon representation, where the N2 domain is colored green, the CTD is shown in blue, and the C_M domain is in red with zinc as a gray sphere. The nucleotide AMPPNP is shown in yellow.

The structure of a truncated monomeric form of EpsE was solved lacking the first 90 amino acids of the NTD, known as the N1 domain, represented in Figure 1.2 (Robien *et al*., 2003). Interactions between the N1 of EpsE and the cytoplasmic domain of EpsL are necessary for the association of EpsE with the inner membrane, and the structure of this complex has been visualized using X-ray crystallography (Sandkvist *et al*., 1995; Abendroth *et al*., 2005). Despite the observation of a small but highly active population of putative EpsE hexamers identified by gel filtration, it had been difficult to capture EpsE hexamers for

structural characterization for many years (Camberg & Sandkvist, 2005). However, hexameric models of EpsE were developed based on the structure of the known hexameric ATPases HP0525 and PilT (Robien *et al*., 2003; Patrick *et al*., 2011). Based on the latter model, several arginine residues comprising putative intersubunit interfaces were shown to be required for EpsE's function, providing further evidence of EpsE's hexamerization (Patrick *et al*., 2011). The crystal structure of hexameric EpsE was solved recently by fusing the assistant hexamer Hcp1 to the C-terminus of EpsE (Lu *et al*., 2013). Hcp1 readily forms hexamers in solution, and acts as an assistant hexamer to induce the oligomerization of EpsE (Mougous *et al*., 2006; Lu *et al*., 2013). The structures of two conformationally different EpsE hexamers were resolved, one with quasi-C6 symmetry and the other elongated with C2 symmetry, and these structures are shown in Figure 1.3 (Lu *et al*., 2013). Similarly, *Myxococcus xanthus* PilB was recently purified as a hexamer using the Hcp assistant hexamer strategy, as PilB alone also forms monomers when expressed in *E. coli* for purification (Bischof *et al*., 2016).

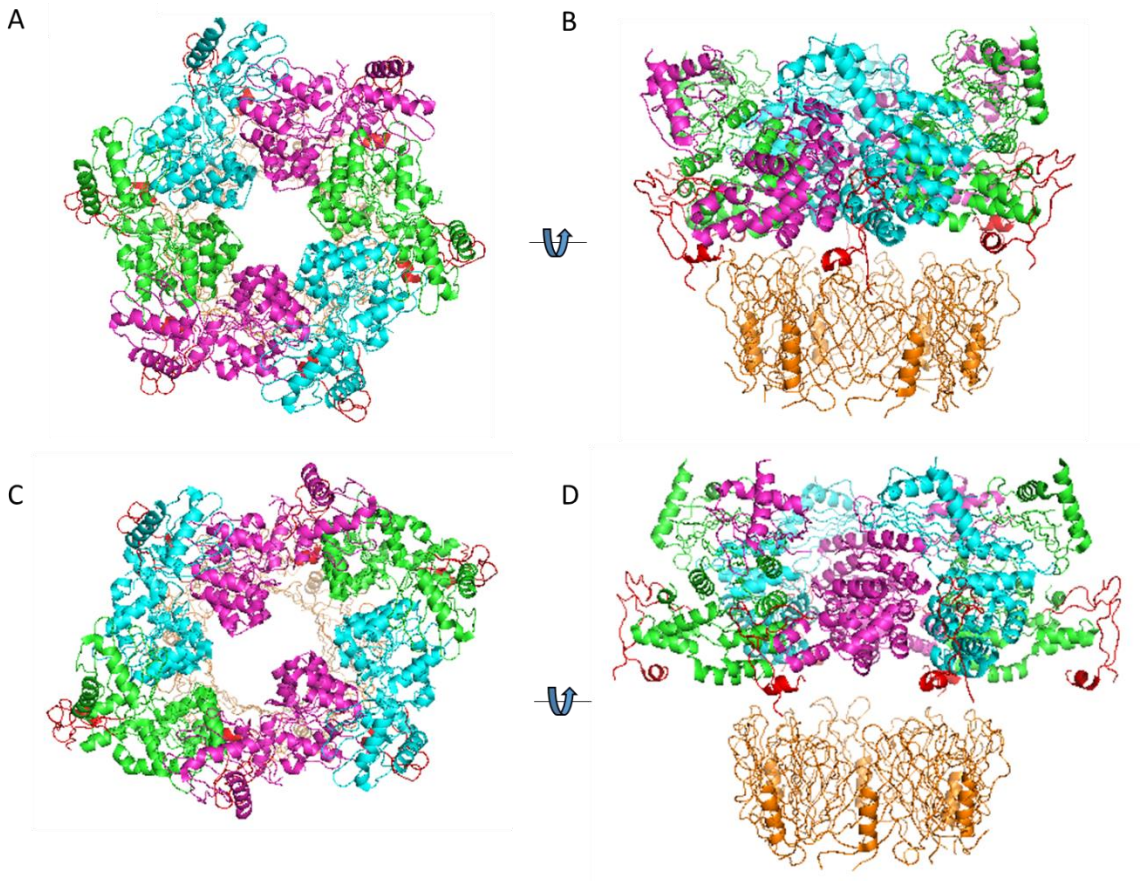

Figure 1.3 Structure of hexameric EpsE-Hcp1. Structures of fusion constructs in which the assistant hexamer Hcp1 was fused to the C-terminus of N-terminally truncated EpsE lacking the first 90 residues, with 6- and 8-amino acid linkers (Lu *et al*., 2013, PDB codes 1kss and 1ksr, respectively). The structure of EpsE-6aa-Hcp1 was solved with quasi-C6 symmetry (A, B), while the structure of EpsE-8aa-Hcp1 was solved with C2 symmetry (C, D). The six EpsE subunits (A-F) are shown in ribbon representation and colored in magenta (A, D), green (B, E), and cyan (C, F) according to symmetry, while C_M domains are shown in red and Hcp1 is colored orange throughout. A and C depict the structures from above, and B and D show the structures oriented from the side, with the EpsE N-terminus facing up.

EpsE likely functions as a dynamic hexameric complex, wherein cycles of ATP binding and hydrolysis result in conformational changes within the hexamer and alterations in interactions between EpsE and other T2S proteins to power assembly of the pseudopilus and protein secretion across the outer membrane

(Satyshur *et al.*, 2007; Misic *et al.*, 2010; Yamagata & Tainer, 2007; Patrick *et al*., 2011; Lu *et al*., 2013; Chang *et al*., 2016). As EpsE hydrolyzes ATP, energy may be transduced through the inner membrane protein EpsL to the major pseudopilin EpsG to power pseudopilus assembly (Gray *et al*., 2011). In the homologous T4P system, the EpsF homologue PilC has been shown to interact directly with the ATPase PilB that powers T4P assembly, and together with the EpsL homolog PilM may transfer the energy generated by ATP hydrolysis to power pilus extension (Takhar *et al*., 2013; Chang *et al*., 2016).

Significance and Scope of this Study

The overall goal of this research is to better understand the mechanism and the role of T2S in *V. cholerae* pathogenesis. One focus of my dissertation has been the mechanism of energy production for T2S by the motor protein EpsE. Chapter 2 centers on the role of the unique C-terminal metal binding, or C_M, domain of EpsE. This domain is conserved among pilus assembly ATPases, but not in pilus retraction ATPases or those involved in type IV secretion. My research shows that zinc is required for the function and activity of EpsE and plays an important role in protein stability. Chapter 3 details a method for measuring the *in vitro* ATPase activity of purified proteins such as EpsE that was applied throughout my research and was further used to assess the importance of particular residues within the EpsE C_M domain to the protein's activity.

In addition to studying the contribution of zinc to EpsE's function, another focus of my dissertation research has been to characterize the overall role of T2S

in *V. cholerae* cell envelope biogenesis. Previous observations from our laboratory indicated that *V. cholerae* Eps inactivation causes widespread cell envelope defects, including outer membrane leakiness and induction of a pathway involved in the cell envelope stress response, which directly or indirectly exerts a negative impact on growth rate (Sandkvist *et al*., 1997; Sikora *et al*., 2007; Sikora *et al*., 2009). Additionally, data from other groups suggest that the *eps* genes are essential in *V. cholerae* (Judson & Mekalanos, 2000; Cameron *et al*., 2008; Chao *et al*., 2013; Kamp *et al*., 2013). Since we and others have successfully constructed mutations in the *eps* genes, this suggests that perhaps the *eps* genes are only essential for *V. cholerae* under particular conditions. In Chapter 4, I address the mechanism behind these findings by using whole-genome sequencing and identify secondary mutations in *eps* mutants that may act as suppressor mutations to enable the construction of *eps* mutations.

Altogether, my research contributes to a more detailed understanding of the mechanism of T2S and its importance in *V. cholerae* virulence and persistence. Advances in our knowledge on this topic can help inform the development of additional therapeutic strategies for cholera treatment. This information may extend to other bacterial diseases caused by pathogens using the T2S system for the transport of virulence factors. Furthermore, understanding the roles of particular domains in EpsE can inform further research not only on energy production for T2S, but also for other homologous systems, such as the T4P, competence, and archaeal flagellar systems.

Chapter 2:

Zinc Coordination is Essential for the Function and Activity of the Type II Secretion ATPase EpsE

Notes:

A modified version of this chapter is currently in press for publication:

Rule, C.S., Patrick, M., Camberg, J.L., Maricic, N., Hol, W.G., Sandkvist, M. Microbiology Open. *In press*.

Abstract

The type II secretion system Eps in *Vibrio cholerae* promotes the extracellular transport of cholera toxin and several hydrolytic enzymes, and is a major virulence system in many Gram-negative pathogens that is structurally related to the type IV pilus system. The cytoplasmic ATPase EpsE provides the energy for exoprotein secretion through ATP hydrolysis. EpsE contains a unique metal-binding domain that coordinates zinc through a tetracysteine motif ($CXXCX_{29}CXXC$), which is also present in type IV pilus assembly but not retraction ATPases. Deletion of the entire domain or substitution of any of the cysteine residues that coordinate zinc completely abrogates secretion in an EpsE-deficient strain and has a dominant negative effect on secretion in the presence of WT EpsE. Consistent with the *in vivo* data, chemical depletion of zinc from purified

EpsE hexamers results in loss of *in vitro* ATPase activity. In contrast, exchanging the residues between the two dicysteines with those from the homologous ATPase XcpR from *Pseudomonas aeruginosa* does not have a significant impact on EpsE. These results indicate that, although the individual residues in the metal binding domain are generally interchangeable, zinc coordination is essential for the activity and function of EpsE.

Introduction

The type II secretion (T2S) system mediates the extracellular transport of virulence factors, such as toxins and hydrolytic enzymes, in many Gram-negative pathogens (Sandkvist, 2001; Cianciotto, 2005; Korotkov *et al.*, 2012). *Vibrio cholerae* uses the T2S system to secrete cholera toxin, which is largely responsible for the severe diarrhea that characterizes cholera, as well as at least 20 other proteins such as proteases, chitinases, lipases, and biofilm matrix proteins (Overbye *et al.*, 1993; Connell *et al.*, 1998; Davis *et al.*, 2000; Sikora *et al.*, 2011; Johnson *et al.*, 2014). Type II-secreted proteins first cross the inner membrane using the Sec or Tat general export pathways, signal sequences are then removed, and these proteins are subsequently transported across the outer membrane via T2S (Pugsley, 1993; Voulhoux *et al.*, 2001). Type II-secreted factors are important for nutrient acquisition and/or modulating the surroundings to benefit the bacteria in both the aquatic environment as well as in the human small intestine (Sandkvist, 2001; Cianciotto, 2005; Sikora, 2013).

The T2S apparatus in *V. cholerae* spans both the inner and outer membranes and is composed of 12 Eps (*e*xtracellular *p*rotein *s*ecretion) proteins (denoted EpsC through EpsM) and PilD (Overbye *et al.*, 1993; Sandkvist *et al.*, 1997; Marsh & Taylor, 1998; Fullner & Mekalanos, 1999). The cytoplasmic ATPase EpsE is associated with the inner membrane through interactions with the bitopic inner membrane protein EpsL (Sandkvist *et al.*, 1995; Abendroth *et al.*, 2005). EpsE acts as a molecular motor to provide the energy for exoprotein secretion through ATP hydrolysis (Camberg & Sandkvist, 2005). A recent study from our laboratory indicates that EpsL may provide a molecular link between EpsE and the major pseudopilin component EpsG. Protein-protein interactions between EpsG and EpsL were established through chemical crosslinking and co-immunoprecipitation followed by immunoblotting for EpsG or EpsL. EpsG prepilin processing by PilD is required for this EpsL interaction, although no other T2S proteins are necessary. The results suggest that the energy produced during ATP hydrolysis by EpsE may be transduced through EpsL to the major pseudopilin EpsG to power pseudopilus assembly for T2S (Gray *et al.*, 2011).

EpsE belongs to a large family of type II/IV secretion ATPases, including those involved in protein secretion, type IV pilus (T4P) biogenesis, competence, and archaeal flagella (archaellum) assembly (Planet *et al.*, 2001). Family members consist of two distinct domains: the N-terminal domain (NTD) and the C-terminal domain (CTD), which are connected by a short flexible linker (Robien *et al.*, 2003; Satyshur *et al.*, 2007; Misic *et al.*, 2010; Rose *et al.*, 2011; Reindl *et al.*, 2013). The CTD contains the conserved ATP-binding motifs that collectively form the

nucleotide-binding pocket, including Walker A and B motifs and Asp and His boxes (Robien *et al.*, 2003; Chiang *et al*., 2008). Within this family, EpsE and other T2S ATPases as well as ATPases required for T4P assembly form the subfamily of GspE/PilB ATPases, alternatively referred to as pilus assembly ATPases (Planet *et al.*, 2001). Members of this subfamily contain a unique domain called the C-terminal metal binding domain (C_M) that coordinates zinc through a tetracysteine motif ($CXXCX_{21-40}CXXC$) (Figure 2.1; Planet *et al.*, 2001; Robien *et al.*, 2003; Camberg & Sandkvist, 2005). The C_M domain is notably absent among T4P retraction ATPases such as PilT and PilU (Robien *et al.*, 2003; Satyshur *et al.*, 2007; Misic *et al.*, 2010; Whitchurch & Mattick, 1994). The tetracysteine motif is conserved among all T2S ATPases except for *Xylella fastidiosa* XpsE and *Xanthomonas campestris* XpsE (Robien *et al.*, 2003). The EpsE C_M domain spans residues C397-C433 in EpsE, with the amino acids in between the two dicysteines forming a hairpin turn, or loop. The C_M loop residues share low sequence homology (~30%) between homologous T2S ATPases (Robien *et al.*, 2003; Camberg & Sandkvist, 2005). Structural analysis shows that the C_M domain is located on the outside of the EpsE hexamer (Lu *et al.*, 2013).

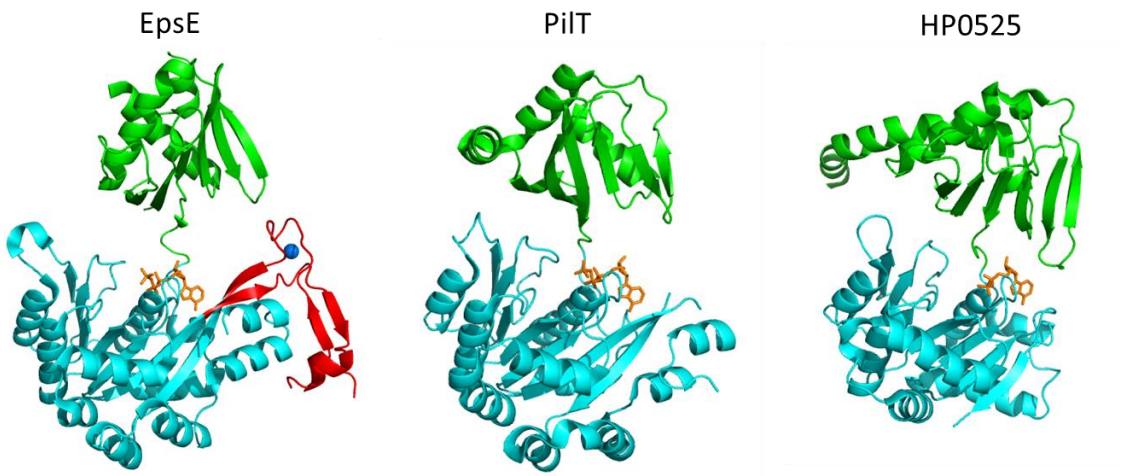

Figure 2.1 Structural comparison of type II/IV secretion ATPases. The structures of the *V. cholerae* T2S ATPase EpsE (left, PDB 1P9W), the *P. aeruginosa* type IV pilus retraction ATPase PilT (center, PDB 3JVV), and the *H. pylori* type IV secretion ATPase HP0525 (right, PDB 1G6O) are shown. N-terminal domains are colored green, C-terminal domains in cyan, and the C_M domain in EpsE is displayed in red with zinc represented as a blue sphere. Nucleotide is shown in orange.

Zinc-coordinating domains have been implicated in diverse roles such as stability, protein-protein interactions, and regulation of activity (Fekkes *et al.*, 1999; Jakob *et al.*, 2000; Salzer *et al.*, 2014). The importance of cysteine residues to the C_M domain of GspE/PilB ATPases has been previously suggested by other studies (Possot & Pugsley, 1997; Salzer *et al.*, 2014). The T2S ATPase PulE from *Klebsiella oxytoca* contains a tetracysteine motif similar to EpsE, and loses the ability to support secretion of pullulanase when at least two adjacent cysteines are replaced with serines. However, the insolubility of native PulE and lack of protein purification techniques prevented study of PulE *in vitro* (Possot & Pugsley, 1997). *Thermus thermophilus* PilF is an ATPase involved in T4P biogenesis and DNA uptake, and was recently shown to require zinc for stability of PilF hexameric

complexes but not for ATPase activity *in vitro*. Additionally, cysteine residues were important for PilF's role in piliation at high temperatures but not for transformation *in vivo* (Salzer *et al.*, 2014).

Understanding the function of EpsE and its individual domains is essential for elucidating the mechanism of T2S and its contribution to pathogenesis. In this study, we investigate the role of the tetracysteine motif and zinc in the EpsE C_M domain, as EpsE is a well-characterized ATPase involved in the secretion of cholera toxin and many hydrolytic enzymes in *V. cholerae*, an important human pathogen and established model organism. We show that zinc coordination by the C_M domain is required for the function of EpsE in T2S, but the C_M residues between the two dicysteines are interchangeable with that of a homologue. Zinc coordination provides stability to the EpsE hexamer, as removal of zinc results in a loss of ATPase activity *in vitro*, an inability to support T2S *in vivo*, and an alteration in the protein's conformation.

Results

The EpsE C_M domain is required for Type II Secretion

The C_M domain is conserved among T2S and T4P assembly ATPases such as EpsE and PilB, while it is absent in homologous T4P retraction ATPases such as PilT and type IV secretion ATPases including HP0525 (Figure 2.1), suggesting that it may be required for a process unique to T2S and T4P assembly. In order to examine the importance of the C_M domain in T2S, we designed mutations in EpsE that remove the entire C_M domain and connect the residues at the point in the CTD

where the β-strands most closely converge based on structural superposition of EpsE and HP0525, which lacks the C_M domain (Figure 2.1). We removed the entire domain including the four cysteines (EpsE ΔC_M) or replaced it with a proline residue (EpsE ΔC_MPro) in order to generate EpsE variants that resemble ATPases lacking the C_M domain. Although wild-type (WT) EpsE can complement the loss of secretion of the serine protease VesB and lipase in an *epsE*::*kan* strain of *V. cholerae*, EpsE ΔC_M and EpsE ΔC_MPro are deficient in their ability to support secretion in this mutant (Figure 2.2A, B). While EpsE ΔC_M and EpsE ΔC_MPro are expressed, they are detected at slightly lower levels than WT EpsE, suggesting a small decrease in stability (Figure 2.2C). However, both EpsE ΔC_M and EpsE ΔC_MPro exhibit negative dominance, as over-expression of these EpsE variants prevents T2S in WT *V. cholerae* (Figure 2.3A). This dominant negative phenotype may be explained by competition between WT and mutant forms of EpsE for interaction with other components within the T2S complex, or by the formation of mixed EpsE oligomers with lower overall activity. Together, these results suggest that both deletion constructs are expressed in *V. cholerae*, and that the C_M domain is necessary for EpsE's function in T2S.

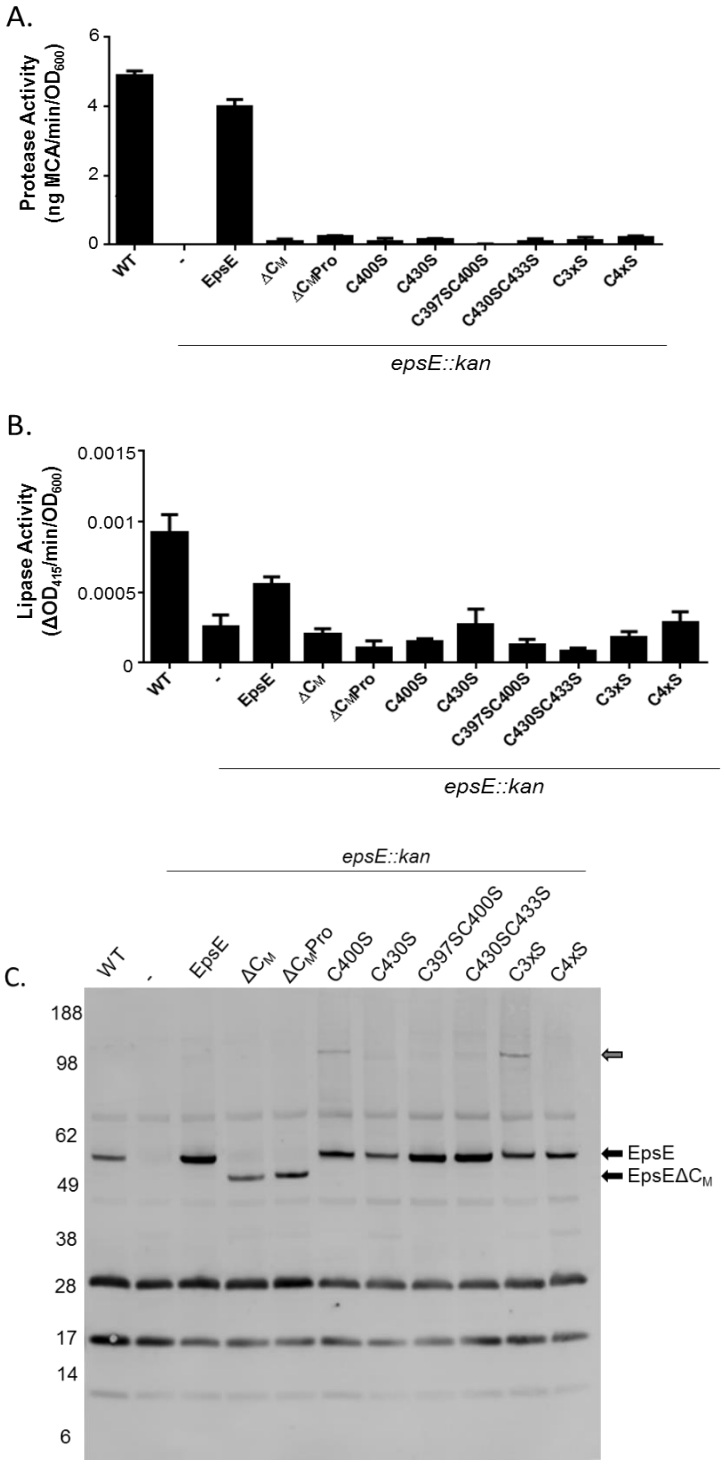

Figure 2.2 The EpsE C_M domain is required for secretion. **A.** WT and *epsE::kan* strains of *V. cholerae* TRH7000 containing empty vector (-) or pMMB plasmids encoding WT or mutant EpsE variants described on the x-axis were grown with 200µg/ml carbenicillin and 10µM IPTG. Culture supernatants were analyzed for VesB protease activity using a cleavable fluorogenic probe as described in *Experimental Procedures*. All EpsE variants showed statistical significance compared to WT EpsE ($p<0.0001$). **B.** The same overnight culture supernatants as in A were analyzed for lipase activity as described in *Experimental Procedures.* All EpsE variants showed statistical significance compared to WT EpsE ($p<0.03$) **C.** Expression of EpsE in WT *V. cholerae* TRH7000, followed by *epsE::kan V. cholerae* containing empty vector and *epsE::kan V. cholerae* expressing either WT EpsE, or variants of EpsE. Samples were analyzed by SDS-PAGE and immunoblotting for EpsE. The size of EpsE and EpsE ΔC_M are indicated by black arrows, and EpsE dimers by a gray arrow.

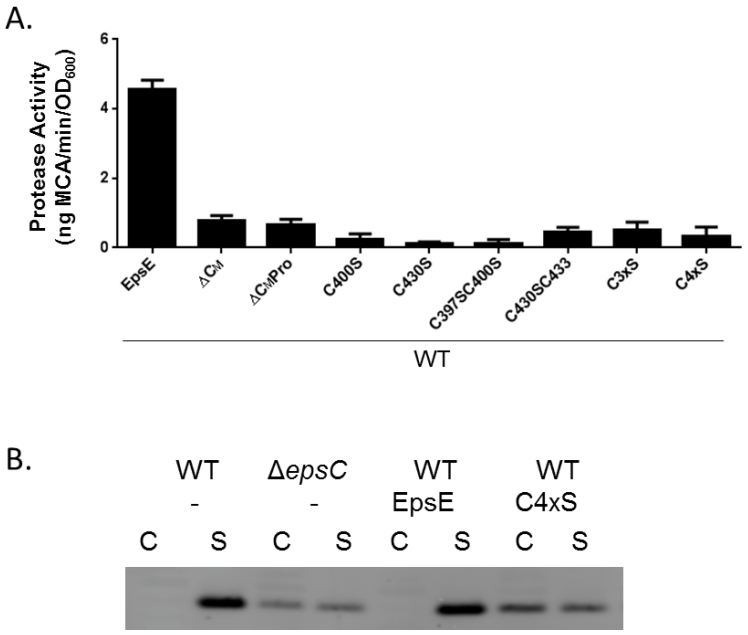

Figure 2.3. EpsE ΔC$_M$ and cysteine mutants exert negative dominance. A. WT *V. cholerae* TRH7000 containing pMMB plasmids encoding WT or mutant EpsE variants described on the x-axis were grown with 200µg/ml carbenicillin and 100µM IPTG. Samples were prepared and assayed for protease activity as in Figure 2.2. Assays were performed in triplicate and standard error is shown. All EpsE variants showed statistical significance compared to WT EpsE ($p<0.0001$). **B**. WT *V. cholerae* 3083 and isogenic Δ*epsC* containing pMMB plasmids (empty vector (-), WT EpsE, or EpsE C4xS) were grown with 200µg/ml carbenicillin and 100µM IPTG. Cells (C) and supernatants (S) were analyzed by SDS-PAGE and immunoblotting for cholera toxin.

We have previously reported that *V. cholerae* T2S mutants leak periplasmic content likely due to outer membrane damage (Sikora *et al*., 2007). Therefore, we also evaluated the ability of EpsE ΔC$_M$ and EpsE ΔC$_M$Pro to restore outer membrane integrity by determining their effect on non-specific extracellular release of periplasmic β-lactamase. We observed higher percentages of β-lactamase activity in the supernatant of *epsE*::*kan* strains containing empty vector or expressing the C$_M$ deletion variants of EpsE (35-45%) compared to WT *V. cholerae*

and the *epsE*::*kan* strain expressing WT EpsE (15-20%) further indicating that these EpsE variants are non-functional (Figure 2.4).

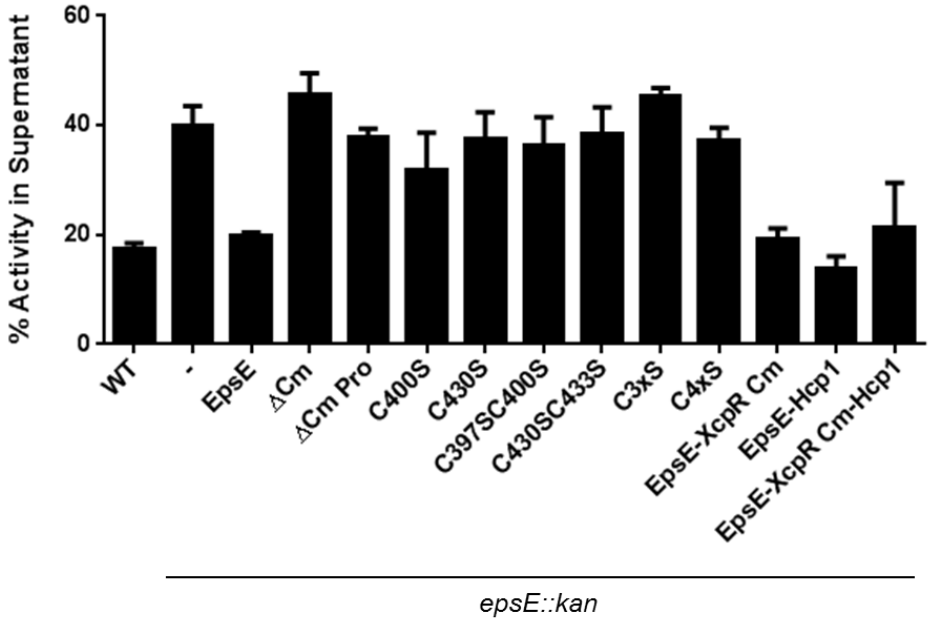

Figure 2.4 Cysteines in EpsE are required for outer membrane stability in *V. cholerae*. Overnight culture supernatants and periplasmic extracts were isolated from WT *V. cholerae* as well as strains of *V. cholerae epsE*::*kan* containing empty vector or expressing WT and C_M variants of EpsE. β-lactamase activity was measured as described in *Experimental Procedures* and expressed as the percent of total activity in the supernatant. Assays were performed in triplicate, and means and SEM are presented.

Residues in the C_M loop are interchangeable for EpsE's function in vivo *and* in vitro

After establishing the importance of the EpsE C_M domain, we then investigated the role of the 29 amino acids in between the two dicysteines. In order to understand the contribution of these residues to EpsE's function, we decided to swap the loop from EpsE with that of a homologue. This technique was selected over mutation of individual residues as it allowed us to simultaneously substitute

multiple residues and to evaluate whether the C_M loop residues participate in species-specific protein-protein interactions (Sandkvist *et al.*, 1995; Sandkvist *et al.*, 2000). We compared the C_M loop residues among several EpsE homologues and found that both the length of the loop and the specific residues vary significantly (Figure 2.5). The EpsE C_M loop contains 29 amino acids, and in order to alter the specific residues of the C_M loop without changing the length, we chose to genetically engineer a chimeric construct, EpsE-XcpR C_M, wherein the 29 C_M loop residues between the two dicysteines from EpsE were exchanged with those of XcpR from *P. aeruginosa*. The cysteines remain intact, but the exchanged region from EpsE differs from that of XcpR by 17 out of 29 residues, mostly in the central portion of the loop (Figure 2.5).

```
V. cholerae EpsE          cpdckepyeadkeqrklfdskkkep-lilyratgcpkc
P. aeruginosa XcpR        cpackepyradeaecallgvdpaap-ptlhrargcgec
A. hydrophila ExeE        cpdcraprpiteqerlamgmelapd-qqvwrpvgceqc
K. oxytoca PulE           cphcrqqepanadt--ahqmeiapg-talwqprgcaec
D. dadantii OutE          cpscrqpyvindeq--aqqtglaag-ttlyhpggcekc
L. pneumophila GspE       cshcktphelrqeekelmglkpdadvsqvfepkgcdyc
                          *  *:                     : .  **  *
```

Figure 2.5. Alignment of C_M domains in T2S ATPase homologues. Clustal Omega alignment of $CXXCX_{27-30}CXXC$ motifs of T2S ATPase homologues. Asterisks below indicate residue conservation identity, and colons and periods indicate high and low levels of residue homology, respectively.

The EpsE-XcpR C_M chimera was found to complement the loss of VesB and lipase secretion in the *epsE*::*kan* strain of *V. cholerae* (Figure 2.6A, B) and is expressed at nearly WT levels (Figure 2.6C). Although restoration of protease secretion was much more variable compared to WT EpsE, it was consistently more substantial than the C_M deletion mutant phenotypes (Figure 2.2A, B). Consistent with its ability to complement the secretion defect in the *epsE*::*kan* mutant, the EpsE-XcpR C_M chimera had no negative effect on VesB secretion when overexpressed in WT *V. cholerae* (Figure 2.6A). It is possible that either the presence of WT EpsE can overcome a slight defect in the interaction of the EpsE-XcpR C_M chimera with the T2S system or that this chimera causes a deficiency in oligomer formation or stability.

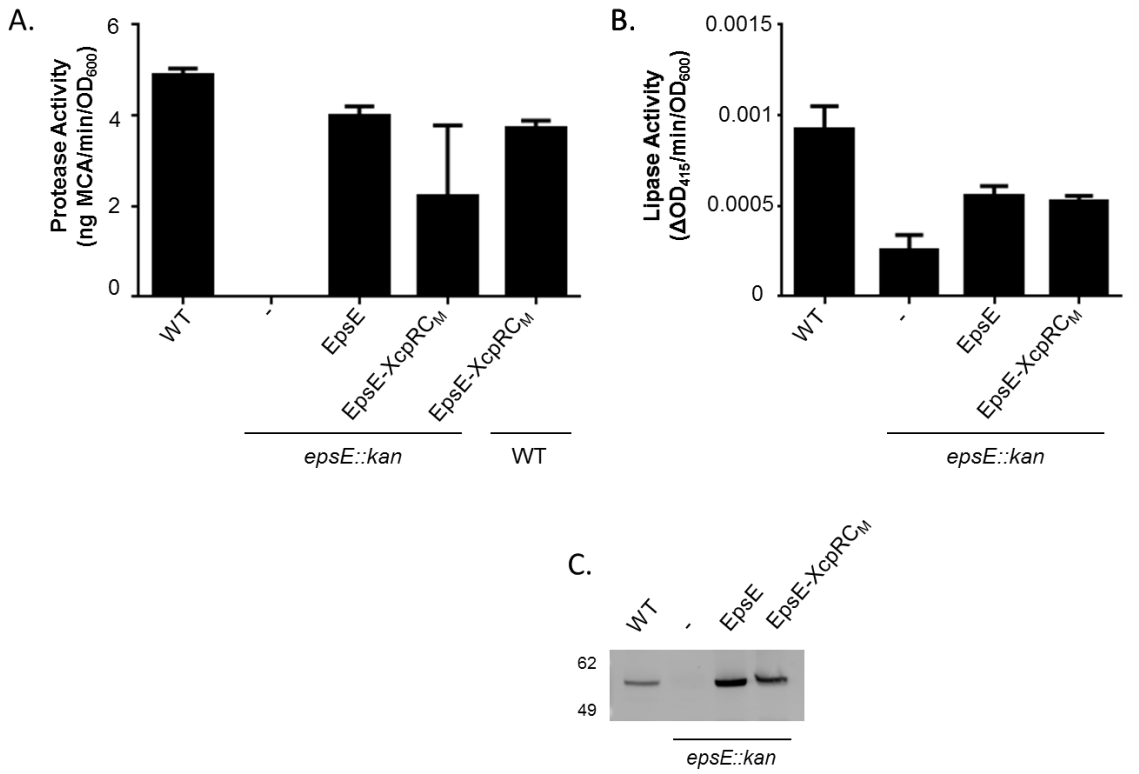

Figure 2.6 The EpsE-XcpR C_M chimera partially complements the T2S defect in *epsE*::*kan* mutants of *V. cholerae*. A. *V. cholerae* TRH7000 WT, followed by *epsE*::*kan* strains containing empty vector (-) or pMMB encoding EpsE or EpsE-XcpR C_M were grown with 200µg/ml carbenicillin and 10µM IPTG. The last bar represents WT *V. cholerae* expressing EpsE-XcpR C_M induced with 100µM IPTG to test for negative dominance. Culture supernatants were analyzed for VesB activity using a cleavable fluorogenic probe as described in *Experimental Procedures*. Assays were performed in triplicate and SEM is shown. No statistically significant difference between WT EpsE and EpsE-XcpR C_M was detected using a T-test ($p = 0.37$). **B**. Overnight culture supernatants were assayed for lipase activity as in Figure 2.2B. No statistically significant difference between WT EpsE and EpsE-XcpR C_M was detected using a T-test ($P = 0.064$). **C**. Expression of EpsE in WT *V. cholerae* TRH7000 (lane 1), followed by empty vector (lane 2), WT EpsE (lane 3), or EpsE-XcpR C_M expressed in *epsE*::*kan V. cholerae* (lane 4) and induced with 10µM IPTG. Samples were analyzed by SDS-PAGE and immunoblotting for EpsE.

EpsE hexamers have a greatly increased ATPase activity over monomeric EpsE, suggesting that EpsE likely functions as a hexamer *in vivo* (Sandkvist & Camberg, 2005). The crystal structure of EpsE was first solved as a helical filament, but modeled as a hexamer based on the structure of *H. pylori* HP0525 (Yeo *et al*., 2000; Robien et al., 2003). In a later study, a refined hexameric model was proposed based on *P. aeruginosa* PilT and tested by mutagenesis of residues predicted to participate in subunit-subunit interactions (Patrick *et al*., 2011). We recently constructed a fusion protein consisting of Hcp1, a hexameric protein from *P. aeruginosa* (Mougous *et al.*, 2006), fused to the C-terminus of EpsE (Lu *et al*., 2013). This resulted in a stable EpsE hexamer with increased ATPase activity that was amenable to purification, crystallization and structure determination. Similarly, the C-terminal Hcp1 fusion strategy has also been recently used to purify the hexameric form of the homologous T4P assembly ATPase PilB (Bischof *et al*., 2016). To determine whether stabilization of the EpsE-XcpR C_M chimera by the "assistant hexamer" Hcp1 can overcome a possible oligomerization defect, we fused Hcp1 to EpsE-XcpR C_M and compared its ability to support secretion with EpsE-Hcp1 in the *epsE*::*kan* mutant. We found that the EpsE-XcpR C_M–Hcp1 chimera fusion with the loop swap is able to support T2S to the same extent as EpsE-Hcp1 (Figure 2.7), suggesting that most of the residues in the EpsE C_M domain can be interchanged with those of a homologue without having a negative impact on EpsE's ability to support T2S.

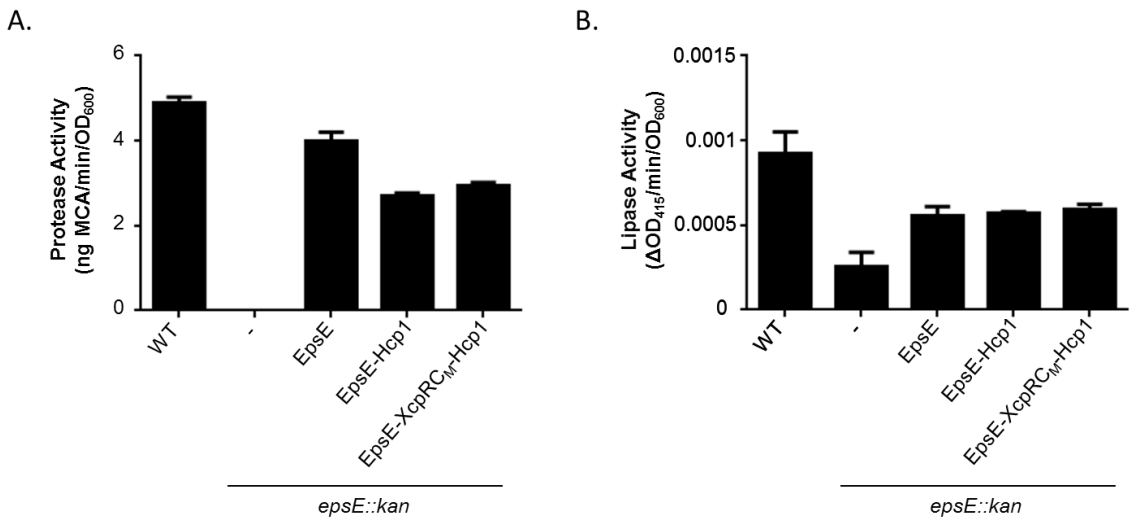

Figure 2.7 EpsE-Hcp1 and EpsE-XcpR C_M–Hcp1 fusions support secretion in *V. cholerae*. **A.** WT and *epsE::kan* strains of *V. cholerae* TRH7000 containing empty vector (-), pMMB encoding EpsE, EpsE-Hcp1, or EpsE-XcpR C_M–Hcp1 were grown with 200µg/ml carbenicillin and 10µM IPTG. Supernatants were analyzed for VesB activity using a cleavable fluorogenic probe as described in *Experimental Procedures*. Assays were performed in triplicate and standard error is shown. **B.** Lipase assays were performed on overnight culture supernatants as in Figure 2.2B. Assays were performed in triplicate with standard errors displayed.

In order to verify that the fusions are stable and do not break down into native EpsE, we analyzed cell extracts by SDS-PAGE and immunoblotting for EpsE and Hcp1 (Figure 2.8). The results show that both WT and chimeric EpsE-Hcp1 fusions remain intact *in vivo* and migrate according to their predicted molecular weights similarly to EpsE-Hcp1-His_6 purified by metal affinity and size-exclusion chromatography from *E. coli* cell extracts (Figures 2.9, 2.10). Thus, the complementation of the T2S-defect in the *epsE*::*kan* mutant by EpsE-Hcp1 and EpsE-XcpR C_M-Hcp1 is likely due to the intact fusions and not break-down products, indicating that the fusions are functional. In addition, these results show that the variability in complementation of T2S by the EpsE-XcpR C_M chimera is

mitigated when the assistant hexamer Hcp1 is present, suggesting that there is no apparent species-specific role of the C_M loop residues between the dicysteines.

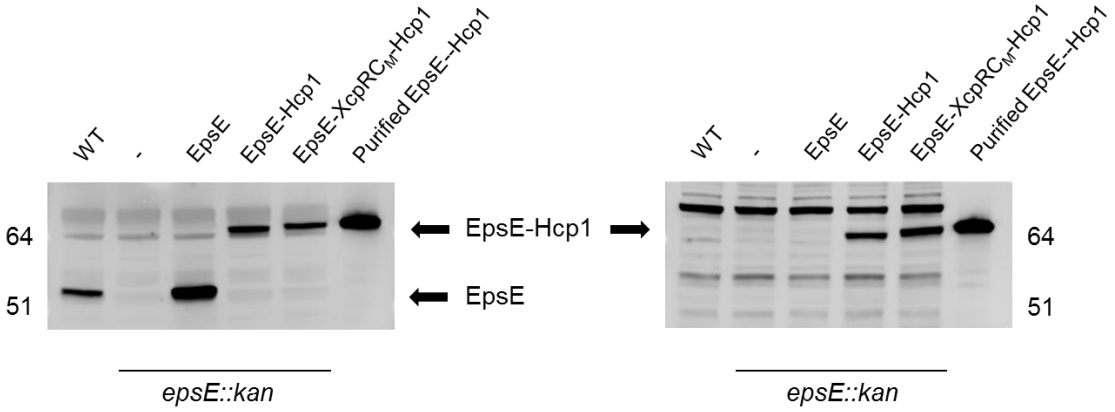

Figure 2.8 Detection of full-length EpsE-Hcp1 fusions in *V. cholerae*. Overnight cultures of *V. cholerae* TRH7000 WT or *epsE*::kan strains containing empty vector (-) or pMMB plasmids encoding EpsE, EpsE-Hcp1, or EpsE-XcpR C_M–Hcp1 were grown with 200µg/ml carbenicillin and 10µM IPTG. Cell lysates were analyzed by SDS-PAGE and immunoblotting using α-EpsE antibodies (left) or α-Hcp1 antibodies (right). Molecular mass markers are indicated and the positions of EpsE and EpsE-Hcp1 fusion are shown with arrows. Purified EpsE-Hcp1 protein was included as a positive control.

A

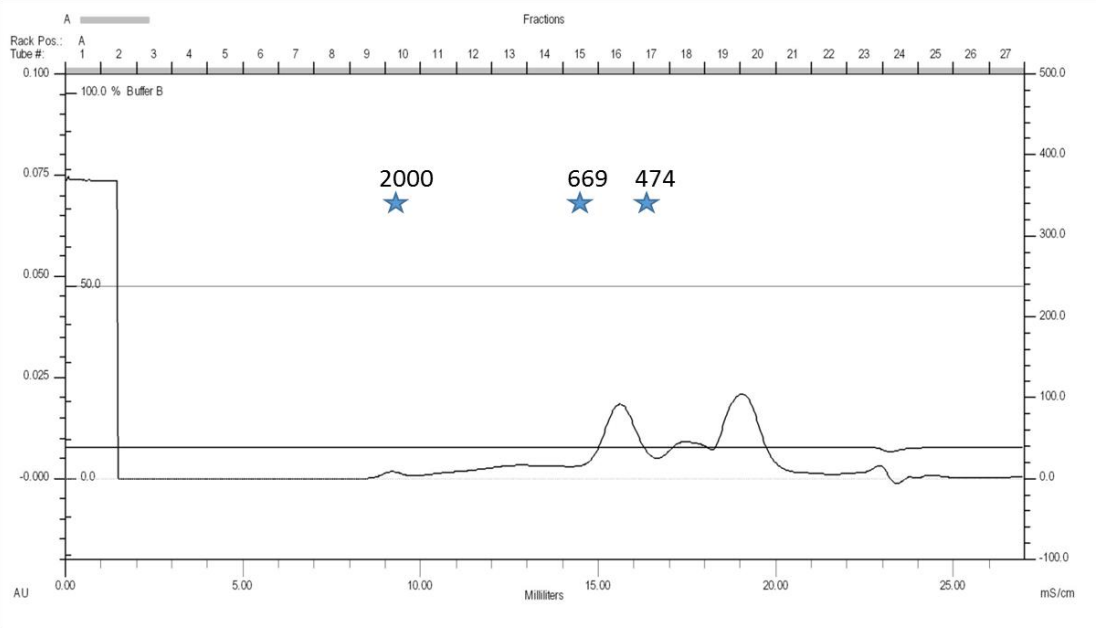

B

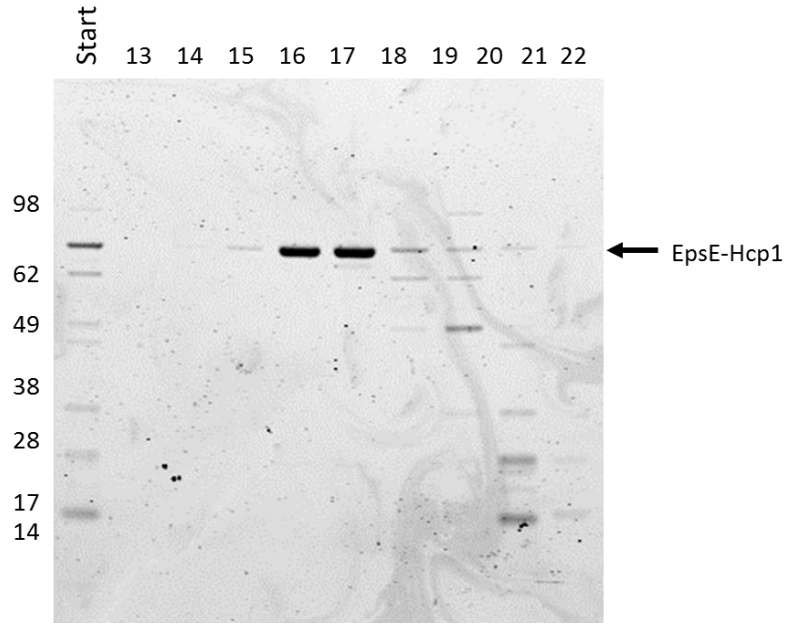

Figure 2.9 Purification of hexameric EpsE-Hcp1. A. EpsE-Hcp1 was purified by metal affinity chromatography and then subjected to gel filtration using a Superose 6 column. Stars represent protein standards with sizes in kDa indicated above. **B**. Fractions containing protein peaks were analyzed via SDS-PAGE and proteins visualized with Coomassie staining. Fractions 16 and 17 were pooled. The size of EpsE-Hcp1 is indicated with an arrow.

A

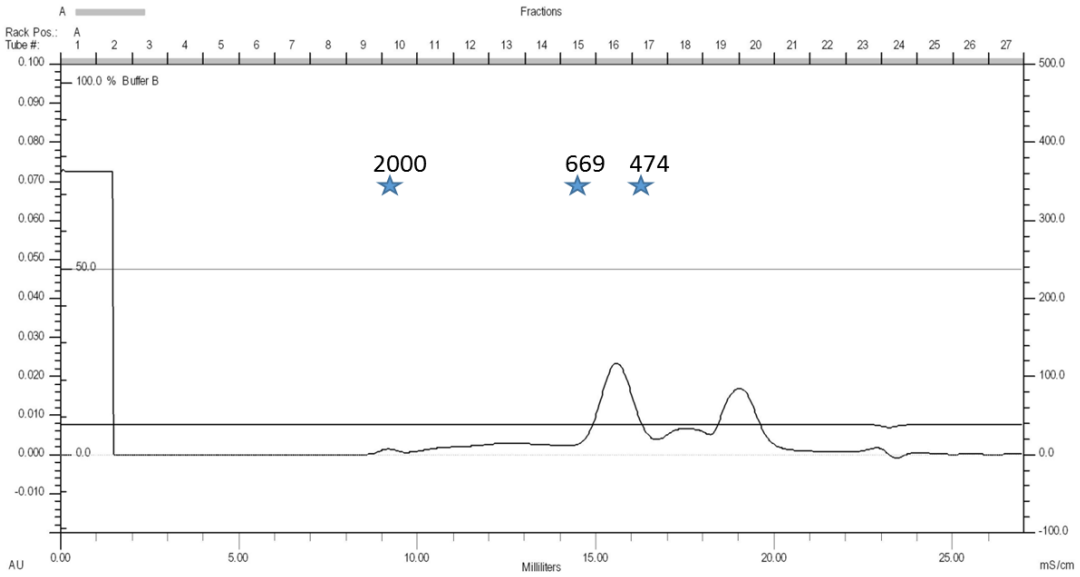

B

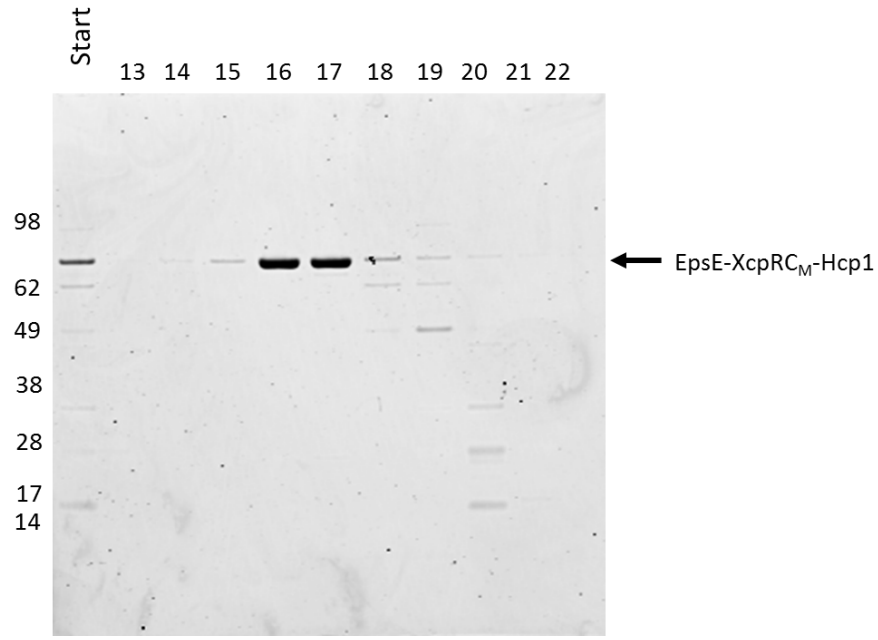

Figure 2.10 Purification of hexameric EpsE-XcpRC$_M$-Hcp1. A. EpsE-XcpRC$_M$-Hcp1 was purified by metal affinity chromatography and then subjected to gel filtration using a Superose 6 column. Stars represent protein standards with sizes in kDa indicated above. **B**. Fractions containing protein peaks were analyzed via SDS-PAGE and proteins visualized with Coomassie staining. Fractions 16 and 17 were pooled. The size of EpsE-XcpRC$_M$-Hcp1 is indicated with an arrow.

As expected, when we overexpressed and purified hexameric His_6-tagged forms of EpsE-Hcp1 and EpsE-XcpR C_M-Hcp1 from *E. coli* by metal affinity chromatography and gel filtration (Figures 2.9, 2.10) and determined their ability to hydrolyze ATP, there is no decrease in ATPase activity when the EpsE C_M loop residues are exchanged with those of the homologue XcpR (Figure 2.11).

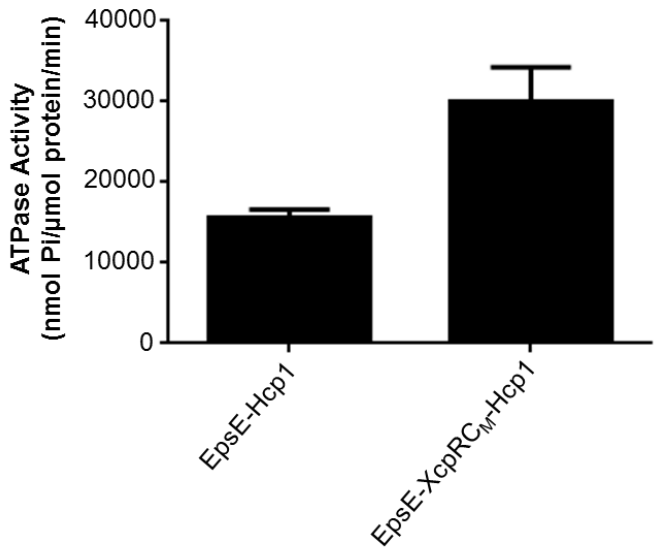

Figure 2.11 The EpsE-XcpR C_M–Hcp1 chimera fusion maintains *in vitro* ATPase activity. Purified EpsE-Hcp1 and EpsE-XcpR C_M–Hcp1 fusions were assayed for *in vitro* ATPase activity as described in *Experimental Procedures*.

Zinc binding to the C_M domain is required for T2S and EpsE ATPase activity

Given the importance of having an intact C_M domain, and yet the relative flexibility in the requirement for precise C_M loop residues for the function of EpsE, we next sought to understand the contribution of the dicysteines to EpsE and T2S. We constructed a series of EpsE C_M cysteine to serine substitution mutants and

tested their ability to complement the loss of T2-secreted protease and lipase activities and restoration of outer membrane integrity in the *epsE::kan* mutant as described above. We analyzed single (C400S, C430S), double (C397SC400S, C430SC433S), triple (C400SC430SC433S), and quadruple (C397SC400SC430SC433S) cysteine to serine substitution mutants. Similarly to the C_M domain deletion variants EpsE ΔC_M and EpsE ΔC_MPro, all EpsE C_M cysteine mutants are unable to complement the T2S defects in the *epsE::kan* strain (Figures 2.2, 2.4). While expression of the C400S and C3xS variants results in what appear to be EpsE dimers, perhaps due to the exposure of single free cysteines, these bands are not detected in the double or quadruple cysteine mutants (Figure 2.2C). In order to test whether the cysteine mutant variants of EpsE are nonfunctional simply due to misfolding, we tested for negative dominance *in vivo*. All cysteine mutants exhibited negative dominance and inhibited the ability of WT EpsE to support protease secretion, suggesting that they are not completely misfolded and are able to interact with WT EpsE and/or other components of the T2S complex such as EpsL (Figure 2.3A). We also confirmed the negative dominant phenotype of the EpsE C4xS variant by analyzing cholera toxin secretion, and show that expression of EpsE C4xS inhibits the secretion of the cholera toxin B subunit in WT *V. cholerae* to approximately the same level as in a T2S mutant (Figure 2.3B). Collectively, these results indicate the importance of cysteines for EpsE's function in T2S and suggest that all four cysteine residues are essential.

In order to analyze the metal content of the cysteine mutant proteins and the effect of these mutations on activity, we attempted to purify hexahistidine-tagged proteins; however, these variant proteins were not amenable to purification, as they aggregated when overexpressed in *E. coli*. We were also unable to purify cysteine mutant variants of the EpsE-Hcp1 fusion (data not shown). This suggests that the folding and/or stability of the mutant proteins is severely compromised when any of the cysteine residues are exchanged for serines, and lends support to the notion that zinc binding to this domain may be crucial for the overall conformation/stability of EpsE.

Because we were unable to analyze the effect of the cysteine-to-serine substitutions on purified proteins, we instead took a chemical approach to determine the contribution of zinc binding to the C_M domain. We used p-chloromercuribenzoic acid (PCMB) to release zinc and measured free zinc using the zinc-complexing agent 4-(2-pyridylazo)resorcinol (PAR). As these experiments required large amounts of purified proteins, we used the previously described hexameric N-terminally truncated ΔN1-EpsE-Hcp1 fusion (Lu *et al.*, 2013), which can be purified in much greater quantities and has about 3-fold higher *in vitro* ATPase activity than the full-length fusion (Figures 2.12, 2.13B). This form of EpsE is unable to function *in vivo* because it lacks the first 90 NTD residues known to interact with EpsL, which are necessary for EpsE to support T2S (Sandkvist *et al.*, 1995; Sandkvist *et al.*, 2000; Abendroth *et al.*, 2005) (data not shown). Figure 2.13A shows that increasing amounts of PCMB cause an increase in the amount of zinc released by ΔN1-EpsE-Hcp1 hexamers, which coordinate metal at a 1:1

ratio of zinc:EpsE, consistent with our previous findings with monomeric EpsE (Camberg & Sandkvist, 2005). Additionally, when the EpsE-Hcp1 fusion is pre-treated with a 4-fold molar excess of PCMB for 10 minutes at room temperature, it has nearly abolished ATPase activity *in vitro* compared to untreated and mock-treated controls (Figure 2.13B). Thus, zinc binding to the EpsE C_M domain is necessary for *in vitro* ATPase activity.

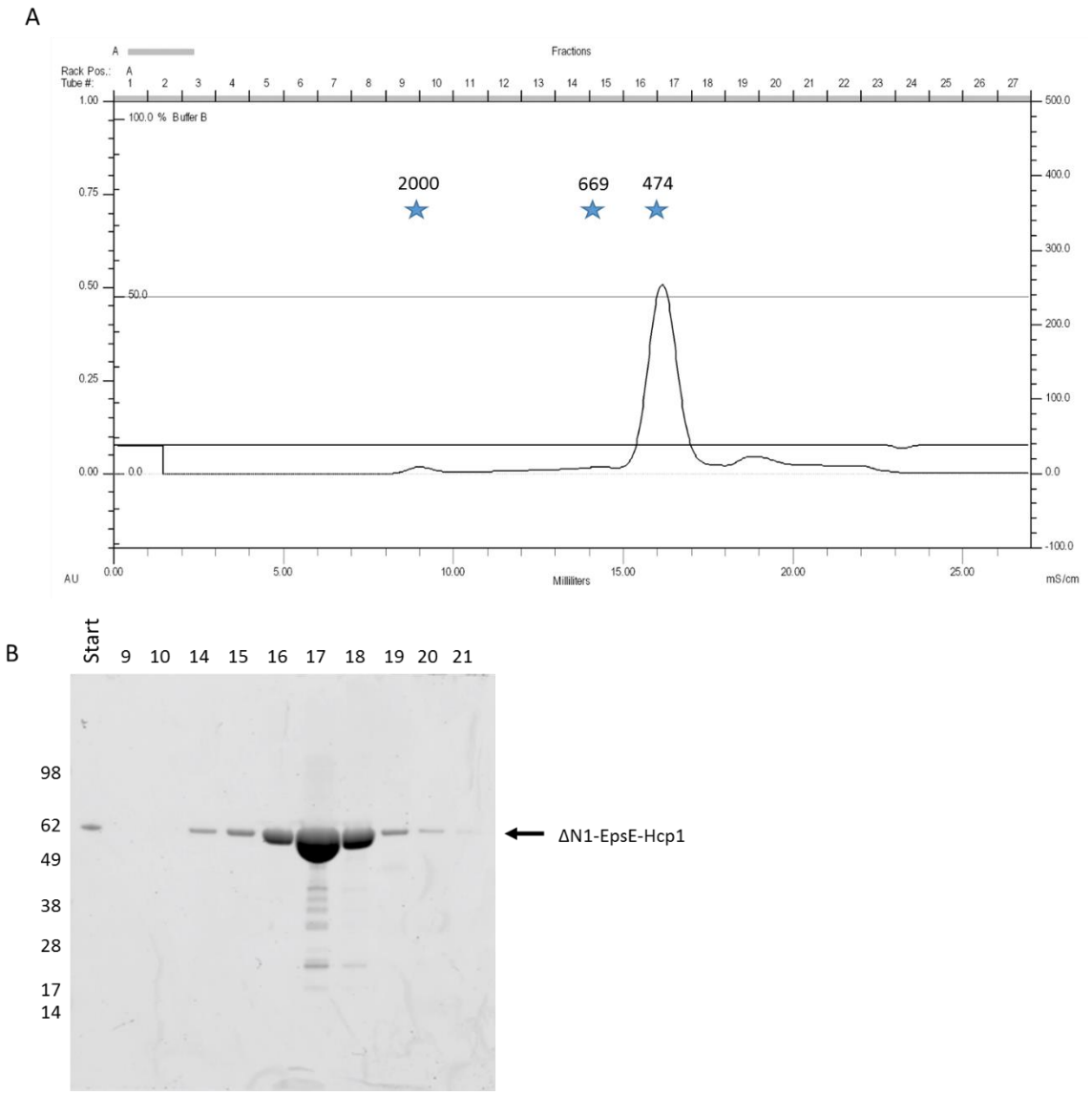

Figure 2.12 Purification of hexameric ΔN1-EpsE-Hcp1. A. ΔN1-EpsE-Hcp1 was purified by metal affinity chromatography and then subjected to gel filtration using a Superose 6 column. Stars represent protein standards with sizes in kDa indicated above. **B**. Fractions containing protein peaks were analyzed via SDS-PAGE and proteins visualized with Coomassie staining. Fraction 17 was used for further analyses. The size of ΔN1-EpsE-Hcp1 is indicated with an arrow.

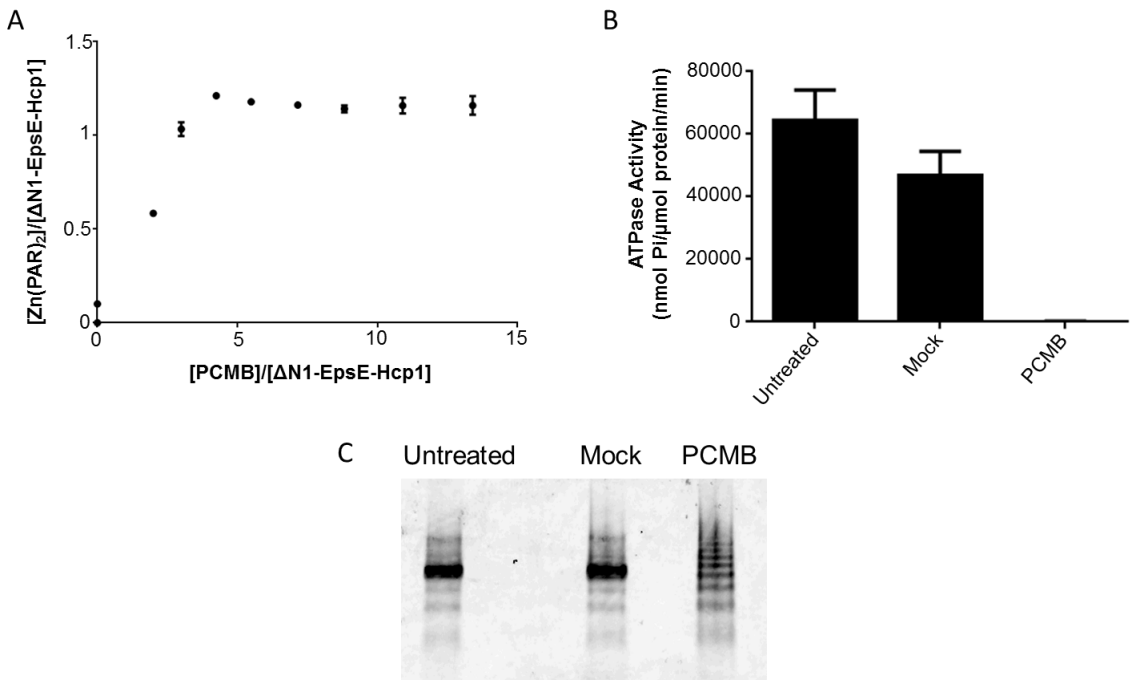

Figure 2.13 Removal of zinc results in a loss of *in vitro* ATPase activity and changes the migration pattern of ΔN1-EpsE-Hcp1. A. Zinc release titration curve. Increasing amounts of p-chloromercuribenzoic acid (PCMB) result in increased zinc release. **B.** Treatment of ΔN1-EpsE-Hcp1 protein abolishes *in vitro* ATPase activity. Proteins were either untreated or treated with a 4-fold molar excess of PCMB or mock-treated for 10 minutes at room temperature and assayed for ATPase activity as described in *Experimental Procedures*. **C**. Purified ΔN1-EpsE-Hcp1 was untreated or incubated with a 4-fold molar excess of PCMB or mock-treated for 10 minutes at room temperature. Samples were then analyzed using native-PAGE and stained with Coomassie.

Zinc stabilizes the conformation of EpsE

Based on the aggregation of EpsE C_M cysteine mutants when overexpressed in *E. coli* and the loss of ΔN1-EpsE-Hcp1's *in vitro* ATPase activity upon zinc release, we hypothesized that zinc contributes to the overall protein conformation of hexameric EpsE. In order to test this, we analyzed purified protein migration profiles using native polyacrylamide gel electrophoresis. Purified ΔN1-EpsE-Hcp1 protein was either untreated or incubated with a 4-fold molar excess

of PCMB or mock-treated for 10 minutes at room temperature. As seen in Figure 2.13C, zinc removal results in a change in the native migration pattern of the ΔN1-EpsE-Hcp1 hexamer, indicating that conformational changes occur following zinc release.

Discussion

This study demonstrates that the EpsE C_M domain is required for type II secretion in *V. cholerae*. Although many of the loop residues that form the elbow of the C_M domain in between the dicysteines are interchangeable, the tetracysteine motif ($CXXCX_{29}CXXC$) must be intact in order for EpsE to function as the molecular motor for T2S. Substitution of any of the cysteine residues resulted in EpsE variants that are unable to support secretion. These EpsE variants are produced in *V. cholerae*; however, none of them were amenable to purification due to aggregation when overexpressed in *E. coli*. It is possible that these variant proteins are misfolded when they are overproduced in isolation from the rest of the T2S complex. However, the negative dominance by the EpsE cysteine mutants when expressed in WT *V. cholerae* demonstrates that they are still able to interact with other components of the T2S complex and/or WT EpsE, suggesting that they retain some native properties and are not completely misfolded. For several of our experiments, we utilized a form of EpsE fused to the assistant hexamer Hcp1, as this construct forms hexamers in the absence of other Eps proteins, has high ATPase activity *in vitro* (Figures 2.9, 2.10, 2.11) (Lu *et al.*, 2013) and is functional *in vivo* (Figure 2.7). When zinc was chemically removed from purified ΔN1-EpsE-Hcp1 fusion protein using PCMB, we observed a loss of ATPase activity and a

change in the migration pattern using native-PAGE (Figure 2.13). Collectively, these data indicate that zinc binding to the C_M domain is necessary to support hexameric complex stability.

We have previously characterized many aspects of the function and activity of EpsE. Among others, we have shown that while monomeric EpsE is capable of hydrolyzing ATP, hexamerization results in greatly increased ATPase activity (Camberg & Sandkvist, 2005; Camberg *et al.*, 2007; Patrick *et al.*, 2011; Lu *et al.*, 2013). The role of zinc was first examined using purified GST-tagged EpsE that primarily yields monomers with low ATPase activity and only a small fraction of highly active hexamers (Camberg & Sandkvist, 2005). Titration of this purified material with *p*-hydroxymercuriphenylsulfonic acid (PMPS) in the presence of PAR revealed that EpsE binds 1 mol of zinc per mol of EpsE, which corresponds with our results in the present study showing that equimolar amounts of zinc are released by ΔN1-hexameric EpsE-Hcp1 using PCMB. When purified EpsE was treated with a four-fold molar excess of PMPS, there was only a 50% decrease in EpsE's ATPase activity, suggesting that zinc does not significantly contribute to the stability of monomeric EpsE (Camberg & Sandkvist, 2005). In contrast, our current study shows that there is a nearly complete reduction in ATPase activity of EpsE hexamers. As the ability to hydrolyze ATP is sensitive to the conformational state of EpsE, the removal of zinc has a greater impact on the ATPase activity of the hexamer than the monomer.

Previous studies examining the tetracysteine motifs of similar Type II/IV secretion ATPases have also indicated the importance of this motif, although some

key differences also exist between those reports and the current study. Possot and Pugsley (1997) showed that secretion of the T2S substrate pullulanase was decreased upon substitution of single or double cysteine to serine substitutions to the ATPase PulE, and was abrogated following a triple cysteine to serine substitution. The two different single cysteine substitutions also exhibited varying amounts of negative dominance, with C391S exhibiting 31% dominance and C419S only 3% (Possot & Pugsley, 1997). We have found that even removing a single cysteine abolishes the ability of EpsE to support T2S, and all variants display very similar levels of negative dominance. Unlike WT PulE, which cannot be purified due to the aggregation of the protein when produced in the absence of other T2S components, WT EpsE is soluble and readily amenable to purification. This allowed us to determine the difference in protein solubility upon substituting cysteine residues, which showed that all cysteines are required for EpsE solubility when overexpressed in *E. coli*.

An investigation of the tetracysteine motif in *T. thermophilus* PilF by Salzer *et al* (2014) showed these cysteines are required in order to support piliation at high temperatures. PilF requires at least three cysteine residues to coordinate zinc, and may be able to use H_2O to substitute for the fourth cysteine. These authors used cysteine to alanine substitutions, whereas we chose to substitute cysteines with serines in order to maintain more closely-related amino acid side chains. At lower growth temperatures, however, cysteine substitutions do not affect PilF function, suggesting that zinc binding is not essential for pilus assembly, but rather provides the protein stability necessary for proper function at elevated

temperatures. Our data indicates that EpsE's stability is also compromised when zinc is removed; however, EpsE is non-functional upon replacement of even one of its cysteines. Additionally, zinc is not necessary for PilF ATPase activity, whereas our data show that zinc is required for ATPase activity of EpsE. PilF requires neither ATP nor zinc-coordinating cysteine residues for hexameric complex assembly and hexamerization does not appear to be a prerequisite for ATP hydrolysis, perhaps due to its extended N-terminus, which the authors suggest may provide additional stability compared to homologues lacking these additional residues. As this study focused on an extremophile, our results are more likely to be widely applicable to other mesophilic organisms, including important pathogens that express T2S and/or T4P systems.

Zinc frequently plays an important role in protein conformation and stabilization, with zinc-coordinating domains most commonly supporting overall or domain-specific protein folding and/or stability or participating in interactions with DNA, RNA, or proteins (Krishna *et al.*, 2003; Maret & Li, 2009). Zinc may stabilize a particular conformation that is important for activity, such as a redox sensor, or to position a domain for protein-protein interactions. For example, the chaperone Hsp33 acts as a molecular "redox switch," by remaining inactive in its zinc-coordinating reduced state and becoming activated upon cellular oxidation, resulting in disulfide bonding and dimerization (Jakob *et al.*, 1999; Jakob *et al.*, 2000; Graumann *et al.*, 2001). SecA, on the other hand, contains a zinc-binding domain that stabilizes the position of basic residues involved in SecB interactions. (Fekkes *et al.*, 1999; Zhou & Xu, 2003). Similarly, the ATP-dependent chaperone

ClpX interacts with the cofactor $SspB_2$ via a hydrophobic patch of residues located in a zinc-binding domain (Thibault *et al.*, 2006).

The work presented here demonstrates that the zinc-coordinating C_M domain is necessary for the activity and function of EpsE, the motor protein that energizes T2S. One lingering question is whether the EpsE C_M domain shares any functions found in similar zinc-coordinating domains, such as Hsp33 and SecA. We have not ruled out the possibility that zinc binding to the C_M domain may offer a means for bacteria to modulate energy production for T2S in addition to, or as a consequence of, providing protein stability. EpsE is unlikely to act as a redox switch similar to Hsp33, as removal of zinc causes a conformational change resulting in a complete loss of activity. It is feasible that the C_M domain is necessary for correctly positioning residues involved in protein-protein interactions in a similar manner to SecA and ClpX; however, if the loop residues participate in protein-protein interactions, this interaction is largely insensitive to the amino acid substitutions in the EpsE-XcpR C_M loop chimera (Figure 2.5). Potentially, modulation of the C_M domain through C_M zinc coordination/abrogation or protein-protein interaction could affect EpsE activity by altering the positioning of important residues in the β-strands that enter and exit the C_M domain (Figures 2.1, 2.14). Structural analysis indicates that R441 in the strand leaving the C_M domain contacts the adenyl and ribose moieties of the nucleotide (Figure 2.14B) (Robien *et al.*, 2003). On the opposite strand, entering the C_M domain, R394 contacts a leucine residue in a neighboring subunit in 2 out of the 6 subunits in the elongated hexameric structure of ΔN1-EpsE-8aa-Hcp1 (Figure 2.14) (Lu *et al.*, 2013).

Changes in the contacts between subunits in the EpsE hexamer might prevent the adoption of important transient conformations that are essential for the functioning of EpsE in T2S. Repositioning of R394 and R441 in Zn-depleted EpsE variants could explain the loss of ATPase activity *in vitro* and/or T2S function *in vivo*.

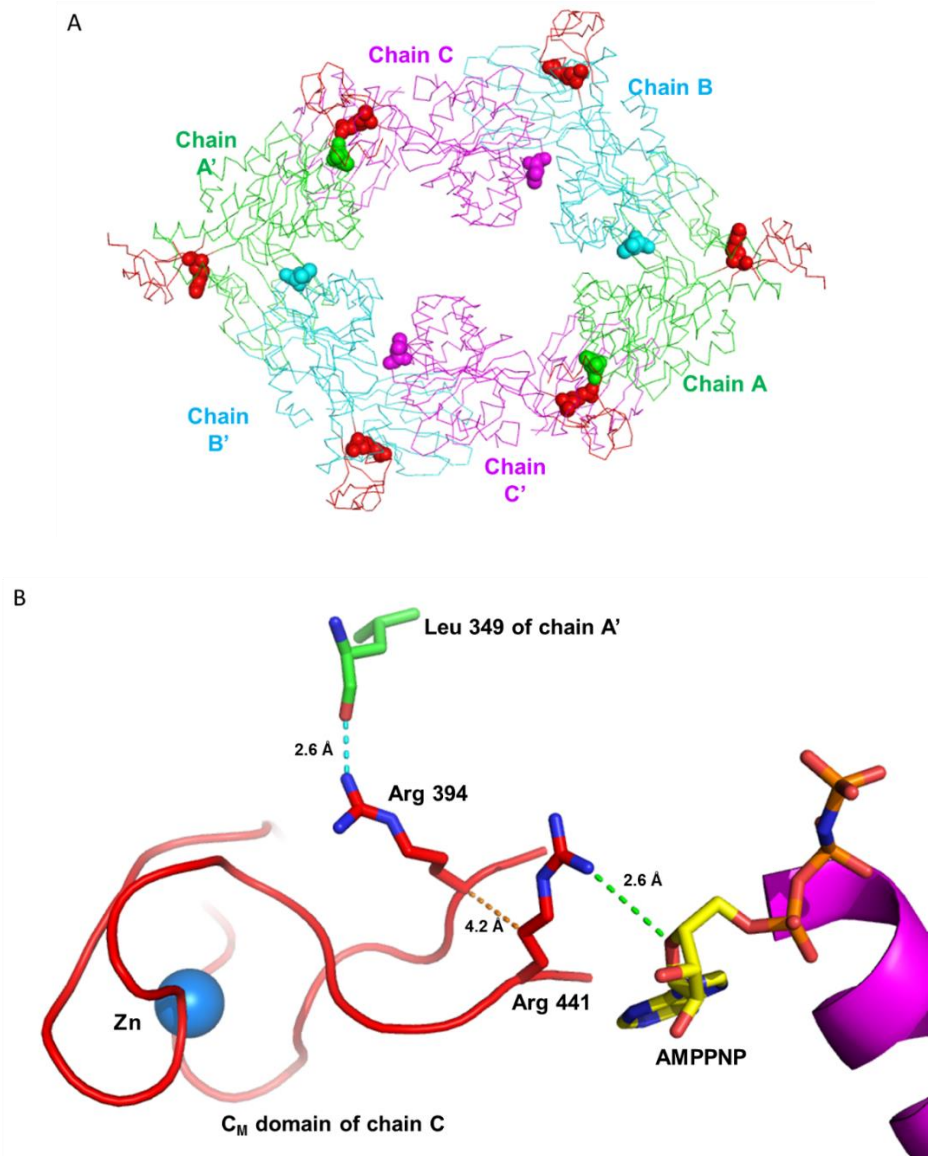

Figure 2.14 Close-up view of residues at the base of the C_M domain and potential interactions with adjacent subunits or nucleotide. A. View along the twofold axis of the *V. cholerae* ΔN1-EpsE-8aa-Hcp1 hexamer with C2 symmetry (Lu *et al*., 2013) (PDB code 4KSR). The three independent chains are related by a twofold axis and are displayed as green (chains A, A'), cyan (B, B'), and magenta (C, C') with C_M domains colored red. Arg 394 residues from each subunit are displayed as red spheres, and Leu 349 residues are displayed as spheres according to the color of the corresponding subunit. **B.** Arg 394 from chain C is shown in proximity to Leu 349 of chain A'. The proximity of Arg 441 to AMPPNP is also shown, with an alpha-helix from the EpsE C-terminal domain in purple. Distances between possible contacts are indicated by dotted lines and labeled. Zinc is superimposed from the structure of monomeric EpsE (Robien *et al*., 2003) (PDB code 1P9W) and is displayed as a blue sphere.

The T2S system shares many structural similarities not only to the closely related T4P system, but also to the archaeal flagellar system (archaellum) and competence systems of Gram-positive bacteria (Korotkov *et al.*, 2012). The assembly ATPases supporting each of these systems share many structural features, including C_M domains; therefore, results of this study should inform further research not only on T2S, but also among many different molecular motor systems across bacterial and archaeal domains (Planet *et al.*, 2001; Robien *et al.*, 2003; Korotkov *et al.*, 2012). Knowledge about EpsE structure and function relationships may also provide insight into mechanisms of the antagonistic functions of the T4P assembly and retraction ATPases.

Experimental Procedures

Bacterial Strains and Growth Conditions

Vibrio cholerae TRH7000 (El Tor, *thy* Hg^R (*ctxA-ctxB*)), *V. cholerae* 3083 (El Tor, serotype Ogawa), and *Escherichia coli* BL21(DE3) were used in this study. *V. cholerae* strains were grown at 37°C in LB broth supplemented with 100 mg/ml thymine for TRH7000. Those strains containing plasmids were grown in the presence of 200 µg/ml carbenicillin and induced with isopropyl-D-thiogalactopyranoside (IPTG) as described in the figure legends.

Cloning and Expression

The EpsE C_M domain deletion mutants were constructed using PCR with the following primers: ΔC_M: 5'-TAAGGTGCGCACCAAGCGCTGAG-3' and 5'-

TACCGTGGCCGAACCGGTAT-3'; ΔC_MPro: 5'-CCATACCGTGGCCGAACCGGTAT-3'. The EpsE ΔC_M construct is missing residues 396-437, while ΔC_MPro replaces those residues with a proline. The *epsE* fragments containing mutations were cloned into pMMB384 (wild-type *epsE* in pMMB67EH) (Sandkvist *et al.*, 1995) by exchange of an MfeI/BamHI fragment to create the pMMB EpsE variant plasmids. The pMMB plasmids were then introduced to *epsE*::*kan* and wild type (WT) *V. cholerae* strains through conjugation.

The pMMB*epsE-xcpR* C_M chimera plasmid was constructed by first amplifying the beginning of *epsE* and creating a 3' region of overlap with the beginning of the *xcpR* C_M domain (5'-GAGGGATCCTGAGCAGATGGAAGCCAAGCAATGACCGAA-3' (BamHI) and 5'-GCGCGGTAGGGCTCCTTGCAATCTGGGCATAAGG-3'.) The *xcpR* C_M fragment was amplified from pMMB-*xcpR* (Turner, 1993) using the primers 5'-CCTTATGCCCAGATTGCAAGGAGCCCTACCGCGC-3' and 5'-TGGTTACATTTAGGGCAGCCGCGGGCGCGATGCA-3'. The downstream part of *epsE* was then amplified with a 5' overlap of the end of the *xcpR* C_M domain using the primers 5'-TGCATCGCGCCCGCGGCTGCCCTAAATGTAACCA-3' and 5'-CTCCTGCAGCAAACGCGGCCATTAGGACTCCTTAGTC-3' (PstI). The three amplified fragments were used as a template for the amplification of the entire region using the first and last primers listed (to yield the *epsE-xcpR* C_M PCR product) and cloned into pMMB67EH using the BamHI and PstI restriction sites and introduced into to *epsE::kan* and WT *V. cholerae* strains through conjugation.

The protein purification expression vector pET21(d)*epsE*(2-503)-*xcpR*C_M-*epsL*(1-253)-his_6 was constructed by exchange of a NotI/BsmI fragment containing the C_M domain from the *epsE-xcpR* C_M PCR product.

The full-length EpsE-Hcp1 fusion is encoded by the expression vector pET21(d)*epsE*(1-503)-8aa-*hcp1*-his_6, and the truncated ΔN1-EpsE-Hcp1 fusion from pET21(d)*epsE*(100-503)-8aa-*hcp1*-his_6. pET21(d)*epsE*(100-503)-*xcpR*C_M-8aa-*hcp1*-his_6 was created by the exchange of a NotI/BsmI fragment from pET21(d)*epsE*(2-503)-*xcpR*C_M-*epsL*(1-253)-his_6. The pMMB*epsE-hcp1* and *epsE-xcpR*C_M-*hcp1* constructs were made by PCR amplification of the region of interest from pET21(d)*epsE*(100-503)-8aa-*hcp1*-his_6 or pET21(d)*epsE*(100-503)-*xcpR*C_M-8aa-*hcp1*-his_6, respectively, using the primers 5'-GAGGGATCCGAAGGAGATATACATGGACTTCTTC-3' (BamHI) and 5'-GAGCTGCAGATATCAGGCCTGCACGTTCTG-3' (PstI) and cloning into pMMB67EH using the BamHI and PstI restriction sites. The plasmids were conjugated into *epsE::kan* and WT *V. cholerae* as before.

EpsE point mutations were constructed using the QuikChange Site-Directed Mutagenesis kit (Stratagene) as directed. The following primers were used to construct the cysteine mutations: C400S (5'-CCTTATGCCCAGATTCCAAAGAGCCTTACGAGGC-3' and 5'-GCCTCGTAAGGCTCTTTGGAATCTGGGCATAAGG-3'), C430S (5'-CGTGCAACGGGCTCCCCTAAATGTAACC-3' and 5'-GGTTACATTTAGGGGAGCCCGTTGCACG-3'), C397SC400S (5'-GGTGCGCACCTTATCCCCAGATTCCAAAGAGCCTTAC-3' and 5'-

GTAAGGCTCTTTGGAATCTGGGGATAAGGTGCGCACC-3'), C430SC433S (5'-CGTGCAACGGGCTCCCCTAAATCTAACCACAAAGG-3' and 5'-CCTTTGTGGTTAGATTTAGGGGAGCCCGTTGCACG-3').

*epsE*C400SC430SC433S (C3xS) was constructed using site-directed mutagenesis with *epsE*C430SC433S template DNA and the primers for C400S listed above, and *epsE*C397SC400SC430SC433S (C4xS) was made similarly using *epsE*C397SC400S as a template and the primers for C430SC433S. Regions containing mutations were cloned into pMMB384 by exchange of an MfeI/BamHI fragment to create the individual pMMB EpsE variant plasmids. Plasmids were then introduced to *epsE::kan* and WT *V. cholerae* strains through conjugation.

Protease and Lipase Secretion Assays

Measurements of extracellular protease activity were performed as described (Sikora *et al.*, 2007). Briefly, the fluorogenic probe, *N*-tert-butoxy-carbonyl-Gln-Ala-Arg-7-amido-4-methylcoumarin (Sigma-Aldrich) was added to overnight culture supernatants and 10-minute kinetic protease activity was measured using fluorescence at excitation and emission wavelengths 385 nm and 440 nm, respectively.

Lipase activity was quantified as described previously by incubating *V. cholerae* overnight culture supernatants with 4-nitrophenyl myristate and measuring 4-nitrophenol release as the change in absorbance at 415 nm over a 30-minute period (Johnson *et al*., 2015). All assays were performed in triplicate,

normalized to the density of the culture at 600 nm, and mean and SEM are displayed.

SDS-PAGE and Immunoblotting

Cell lysates were boiled in SDS sample buffer and analyzed by SDS-PAGE using 4-12% Bis-Tris gels (NuPAGE, Invitrogen) and MES or MOPS running buffer. Proteins were transferred to nitrocellulose membranes (Protran, GE Healthcare) using NuPage transfer buffer (Invitrogen) and probed with either 1:10,000 α-EpsE antibodies or 1:5000 α-cholera toxin antibodies followed by 1:20,000 horseradish peroxidase-conjugated goat α-rabbit immunoglobulin G (BioRad) or 1:1,000 α-Hcp1 antibodies followed by 1:10,000 goat α-rabbit IgG-HRP. Blots were developed using Ecl2 (Pierce) and imaged using a Typhoon FLA 9500 (GE Healthcare).

Protein Purification

Constructs for purification were introduced into pET21(d)*epsE*(100-503)-8aa-*hcp1*-his_6 (ΔN1-EpsE-Hcp1) (Lu *et al.*, 2013) or pET21(d)*epsE*(1-503)-8aa-*hcp1*-his_6 (full-EpsE-Hcp1) and expressed in *E. coli* BL21(DE3) under IPTG-inducing conditions. Proteins were purified using metal affinity chromatography on cobalt resin (Talon, Clontech). Subsequently, size-exclusion chromatography was performed using a Superose 6 column (GE Healthcare) as described (Robien *et al.*, 2003; Lu *et al.*, 2013) and compared to known protein standards. Gel filtration

fractions containing protein peaks were analyzed using SDS-PAGE and visualized by staining the gel with Gel Code Blue (Thermo Scientific).

ATPase Activity Assays

Purified EpsE-Hcp1 and ΔN1-EpsE-Hcp1 fusion proteins were assayed for *in vitro* ATPase activity according to Lu *et al.*, 2013 using BIOMOL Green reagent (Enzo Life Sciences) to detect free Pi.

PAR/PCMB Assay

Zinc release was measured using a modified PAR/PCMB assay (Camberg & Sandkvist, 2005; Ilbert *et al.*, 2007). Briefly, zinc was removed from ΔN1-EpsE-Hcp1 purified protein using a titration of p-chloromercuribenzoic acid (PCMB; Sigma) in the presence of the zinc-complexing agent 4-(2-pyridylazo)resorcinol (PAR; Sigma). Zinc release was measured at 500 nm and compared to a $ZnCl_2$ standard curve. Assays were performed in duplicate and SEM is shown.

Native-PAGE

Proteins were treated with a 4-fold molar excess of PCMB or mock-treated for 10 minutes at room temperature and analyzed on a 4-20% Tris-Glycine native gel (NuPAGE, Invitrogen) with Tris-Glycine running buffer at 125V for 5 hours on ice. Proteins were visualized by staining the gel with Gel Code Blue (Thermo Scientific).

β-Lactamase activity assay

Periplasmic contents were isolated by incubating cells from overnight cultures with 2,000 U/ml polymyxin B sulfate in PBS on ice for 30 minutes, centrifuging at 8,000 rpm for 10 minutes, and isolating the supernatant (periplasmic extract) from spheroplasts. β-Lactamase activity was measured in overnight culture supernatants and periplasmic extracts as previously described with some modifications (Sikora *et al*., 2007). Nitrocefin (EMD Chemicals) was added to supernatants and periplasmic extracts in PBS buffer and the absorbance at 482 nm was measured over the course of 5 minutes at 37 °C.

Chapter 3:

Measuring *In Vitro* ATPase Activity for Enzymatic Characterization

Notes:

A modified version of this chapter is currently in press for publication.

Rule, C.S., Patrick, M., Sandkvist, M. Journal of Visualized Experiments. *In press*.

Abstract

Adenosine triphosphate-hydrolyzing enzymes, or ATPases, play a critical role in a diverse array of cellular functions. These dynamic proteins can generate energy for mechanical work, such as protein trafficking and degradation, solute transport, and cellular movements. The protocol described here is a basic assay for measuring the *in vitro* activity of purified ATPases for functional characterization. Proteins hydrolyze ATP in a reaction that results in inorganic phosphate release, and the amount of phosphate liberated is then quantitated using a colorimetric assay. This highly adaptable protocol can be adjusted to measure ATPase activity in kinetic or endpoint assays. A representative protocol is provided here based on the activity and requirements of EpsE, the AAA+ ATPase involved in type II secretion in the bacterium *Vibrio cholerae*. The amount

of purified protein needed to measure activity, length of the assay and the timing and number of sampling intervals, buffer and salt composition, temperature, co-factors, stimulants (if any), etc. may vary from those described here, and thus some optimization may be necessary. This protocol provides a basic framework for characterizing ATPases and can be performed quickly and easily adjusted as necessary.

Introduction

ATPases are integral enzymes in many processes across all kingdoms of life. ATPases act as molecular motors that use the energy of ATP hydrolysis to power such diverse reactions as protein trafficking, unfolding, and assembly; replication and transcription; cellular metabolism; muscle movement; cell motility; and ion pumping (Hanson & Whiteheart, 2005; Baker & Sauer, 2012; Maxson & Grinstein, 2014). Some ATPases are transmembrane proteins involved in transporting solutes across membranes, others are cytoplasmic and may be associated with a biological membrane such as the plasma membrane or those of organelles.

AAA+ ATPases (ATPases associated with various cellular activities) make up a large group of ATPases that share some sequence and structural conservation. These proteins contain conserved nucleotide binding motifs such as Walker-A and -B boxes and form oligomers (generally hexamers) in their active state (Hanson & Whiteheart, 2005). Large conformational changes in these proteins upon nucleotide binding have been characterized among diverse

members of the AAA+ family. EpsE is a AAA+ ATPase and member of the bacterial Type II/IV secretion subfamily of NTPases (Planet *et al*., 2001; Robien *et al*., 2003; Camberg & Sandkvist, 2005). EpsE powers type II secretion (T2S) in *Vibrio cholerae*, the causative agent of cholera. The T2S system is responsible for the secretion of a wide variety of proteins, such as the virulence factor cholera toxin that causes profuse watery diarrhea when *V. cholerae* colonizes the human small intestine (Sandkvist, 2001).

Techniques for quantitating *in vitro* ATPase activity are varied, but commonly measure phosphate release using colorimetric, fluorescent, or radioactive substrates (Brune *et al*., 1994; Carter & Karl, 1982; Henkel *et al*., 1988; Harder *et al*., 1994). We describe a basic method for determining *in vitro* ATPase activity of purified proteins using a colorimetric assay based on a commercially available malachite green-containing substrate that measures liberated inorganic phosphate (Pi). At low pH, malachite green molybdate forms a complex with Pi and the level of complex formation can be measured at 650 nm. This simple and sensitive assay may be used to functionally characterize new ATPases and to evaluate the roles of potential activators or inhibitors, to determine the importance of domains and/or specific residues, or to assess the effect of particular treatments on enzymatic activity.

Protocol

1. Perform ATP hydrolysis reaction with purified protein

1.1) Prepare stocks of all the necessary reagents for incubation with purified

protein.

1.1.1) Prepare 5x HEPES/NaCl/glycerol (HNG) buffer containing 100mM HEPES pH 8.5, 65 mM NaCl, and 5% glycerol (or other assay buffer as appropriate).

1.1.2) Prepare 100 mM $MgCl_2$ (or other metal, if ATPase is metal-dependent) in water.

1.1.3) Prepare fresh 100 mM ATP in 200mM Tris Base (do not adjust pH further) using high purity ATP. Aliquot and store the ATP stock at -20°C for no longer than a few weeks, as ATP will break down over time, and refrain from freezing and thawing the ATP stock.

1.1.4) Premix $MgCl_2$ and ATP at a 1:1 ratio just before setting up the ATP hydrolysis reaction.

1.2) Prepare and label 1.5ml tubes for collecting samples at regular intervals throughout the reaction. Prepare tubes to collect samples at time 0 and at time 15, 30, 45, and 60 minutes.

NOTE: As an alternative, collect samples only at time 0 and the endpoint.

1.2.1) Add 245 µl 1X HNG buffer to each tube in order to dilute samples collected from the ATP hydrolysis reactions 1:50.

1.3) Prepare a bath of dry ice and ethanol for quickly freezing samples to stop the reaction. In a rubber ice bucket or other safe (non-plastic) container, add several pieces of dry ice and carefully pour enough 70-100% ethanol to cover the dry ice.

1.4) Dilute purified protein in 1X HNG buffer, as appropriate (typically 5-10µM), and keep on ice.

1.5) Set up the ATP hydrolysis reactions.

1.5.1) In separate 0.5ml tubes for each sample, add the following reagents (in order): H_2O (up to a final volume of 30 µl), 6 µl 5x HNG or other buffer, 3 µl 100mM $MgCl_2$-ATP mixture, and 0.25-5 µM protein.

1.5.2) Include a buffer-only negative control condition in which no protein is added.

1.6) Remove 5µl from the reaction at time 0, dilute 1:50 in the prepared 1.5ml tube containing 245µl HNG buffer, and immediately freeze the sample in the dry ice/ethanol bath.

1.7) Incubate reactions at 37°C to allow ATP hydrolysis to occur for 1 hour. At each interval (15, 30, 45, and 60 minutes), remove 5 µl aliquots from the reaction and add to labeled sample tubes containing HNG buffer as in step 1.6.

1.8) At the end of the ATP hydrolysis reaction, move diluted samples to a -80°C freezer for storage. To ensure all samples are completely frozen, wait at least 10 minutes before proceeding.

2. Incubate samples containing free Pi with detection reagent

2.1) Thaw diluted samples containing ATP hydrolysis reaction aliquots at each time point (obtained from steps 1.6 and 1.7) at room temperature.

2.2) Set up a 96-well plate containing samples and phosphate standards.

2.2.1) In a 0.5 ml tube, dilute the phosphate standard (provided with Pi detection reagent) from 800 µM to 40 µM by adding 5.5 µl of the 800 µM standard to 104.5 µl HNG buffer. Mix well, and add 100 µl of this 40 µM Pi standard to well A1 of a 96-well plate.

2.2.2) Add 50 µl HNG buffer to wells B1-H1 for 1:1 serial dilutions of the Pi

standard.

2.2.3) Remove 50 µl of 40 µM Pi from well A1 and add to 50 µl assay buffer in well A2, mix, and remove 50 µl from well A2 and add to well A3, continuing dilutions through well G1. Discard 50 µl from well G1 after mixing to ensure each well has the same volume. Well H1 should contain only buffer to create a Pi standard from 40-0 µM.

NOTE: If an additional factor (such as an inhibitor) has been added to the samples, create a standard curve containing that factor to control for changes in phosphate release or absorbance under those conditions.

2.2.4) Add 50 µl of each sample in duplicate to the plate. Add samples from the same time point in columns vertically (sample 1 time 0 = A2, A3; sample 2 time 0 = B2, B3) and different time points horizontally. This allows for up to 8 samples and 5 time points per plate.

2.3) Use a sterile pipet to remove enough malachite green/molybdate Pi detection reagent to add 100 µl to each of the wells containing samples and standards (reagent needed (ml) = 0.1 x number of samples and standards) and add to a dish for easy pipetting using a multichannel pipet. Do not pour the detection reagent directly into the dish, as Pi contamination is likely to occur.

2.4) Using a multichannel pipet, add 100µl of the Pi detection reagent to each well and mix by carefully pipetting up and down a consistent number of times without introducing bubbles, preferably in order from the last time points to the first time points.

2.5) Incubate the plate for 25 minutes at room temperature, or according to the

manufacturer's directions.

3. Quantitate results using a microplate reader

3.1) Read the absorbance of the samples at 650 nm using an absorbance microplate reader.

3.2) Make a Pi standard curve. Using a graphing software, graph the absorbance values for the Pi standard samples versus concentration in order to find an equation used to solve for the amount of phosphate in each sample.

3.3) Calculate the ATPase activity for each sample by calibrating with the phosphate standard. Phosphate released = (OD650 – Y intercept)/slope.

3.3.1) Average the total Pi from duplicates of each sample. Subtract the buffer-only control's absorbance reading from this number. Multiply this by the dilution factor (50 in our example).

3.3.2) Determine the nmol Pi released per µmol protein. Graphing these values for each time point in a kinetic assay should yield linear fits of at least R=0.99 (Fig. 1); If not, the assay may be adjusted with more or less protein or a longer or shorter incubation time.

3.4) Represent the results as nmol Pi/µmol protein/min (Fig. 2, 3), or as nmol Pi/µg protein/min if desired.

Representative Results

The *in vitro* activity of the T2S ATPase EpsE can be stimulated by copurification of EpsE with the cytoplasmic domain of EpsL (EpsE-cytoEpsL) and

addition of the acidic phospholipid cardiolipin (Camberg *et al*., 2007). It is also possible to determine the role of particular EpsE residues in ATP hydrolysis by comparing activity of wild type (WT) to variant forms of the protein using this assay. Here, the effect of substituting two lysine residues in the EpsE zinc-binding domain is measured by comparing ATPase activity of purified WT EpsE-cytoEpsL to the EpsE K417AK419A-cytoEpsL variant. In Figure 3.1, phosphate release proceeds linearly over the course of a 1h kinetic assay, a requirement for accurate quantification of kinetic ATPase activity. Figure 3.2 shows data from the same purified protein samples as Figure 3.1 that were assayed three times in duplicate and quantitated in terms of the mean rate of phosphate release. These data show that K417 and K419 appear to be important for EpsE ATPase activity. However, comparison of unstimulated (no cardiolipin) ATPase activity rates (Figure 3.3) shows that K417 and K419 do not contribute to EpsE's basal activity but rather to the ability of the protein to be stimulated by cardiolipin. The positively-charged lysines in the EpsE zinc-binding domain may directly interact with the negatively-charged phospholipids, thus contributing to the phospholipid-mediated stimulation of EpsE ATPase activity.

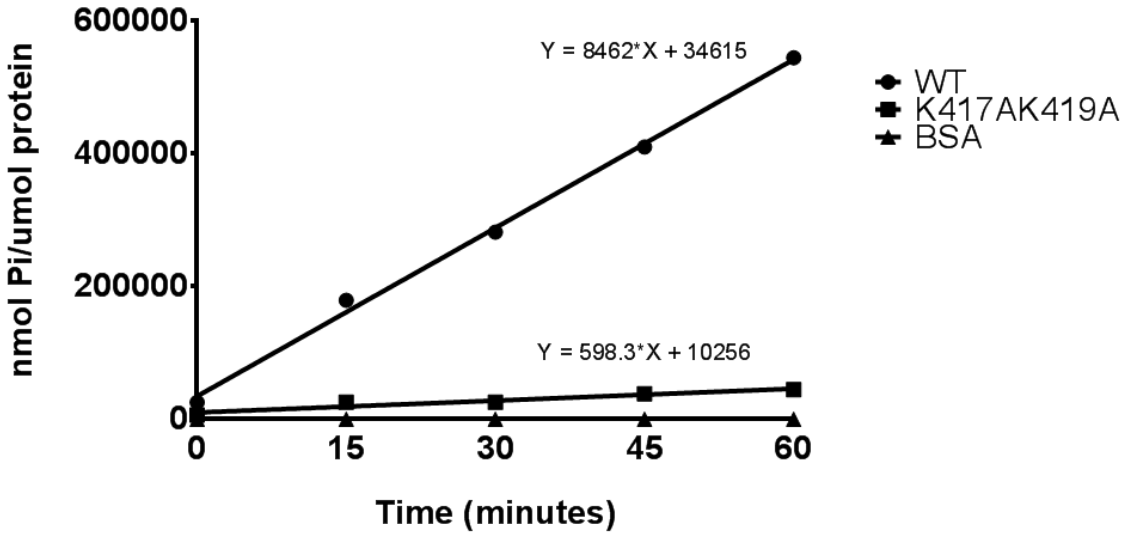

Figure 3.1 Phosphate is released linearly in a kinetic ATPase assay. One-hour kinetic cardiolipin-stimulated ATPase assay comparing phosphate release of 0.5µM WT EpsE-cytoEpsL to EpsE K417AK419A-cytoEpsL with bovine serum albumin (BSA) assayed as a negative control. Data [amount of released phosphate (y-axis) versus time (x-axis)] were plotted and subjected to linear regression analysis. The slope represents the rate of ATP hydrolysis. A representative graph with linear regression equations for the three proteins is shown.

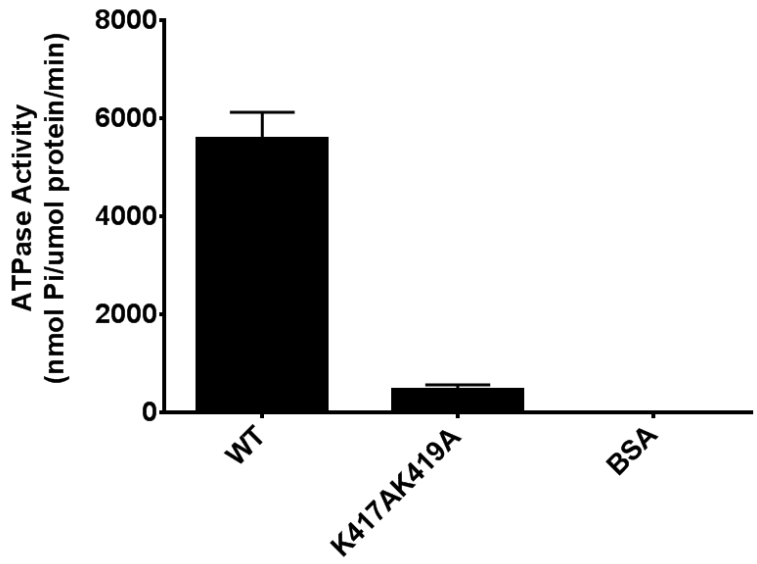

Figure 3.2 Double lysine mutations in the EpsE zinc-binding domain reduce stimulated ATPase activity. Results of the 1-hour kinetic cardiolipin-stimulated ATPase assay with the same proteins and conditions as in Figure 3.1. Assays were performed three separate times in technical duplicate and the rate of ATP hydrolysis was calculated as nmol phosphate generated per minute per µM protein using linear regression equations. The mean results with standard error are displayed.

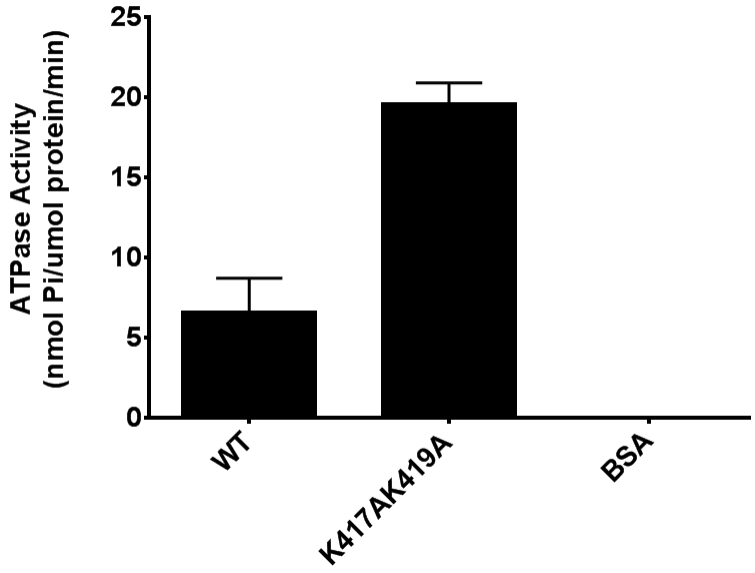

Figure 3.3 Double lysine mutations in the EpsE zinc-binding domain do not interfere with unstimulated ATPase activity. Overnight (16h) endpoint unstimulated (no cardiolipin) ATPase assay comparing the activity of 5µM WT EpsE-cytoEpsL to EpsE K417AK419A-cytoEpsL with BSA as a negative control. Assays were performed three separate times in technical duplicate and mean results with standard error are shown. The basal level of unstimulated EpsE ATPase activity assayed over a 16h period is ~1000-fold lower than 1h kinetic cardiolipin-stimulated activity.

Discussion

This is a general protocol for measuring *in vitro* ATPase activity of purified proteins for biochemical characterization. This method is easily optimized; for example, adjusting the amount of protein, buffer and salt compositions, temperature, and varying the assay length and intervals (including increasing the total number of intervals) can improve activity quantitation. Commercially available malachite green-based reagents are highly sensitive, and can detect small amounts of free phosphate (~50pmol in 100µL). Because of this assay's sensitivity,

it is crucial to use disposable plastic ware, ultrapure water, buffers, and reagents devoid of contaminating phosphate. After purifying proteins, size exclusion or ion exchange chromatography is recommended to improve protein purity and remove contaminants.

For proteins displaying weak *in vitro* ATPase activity, stimulants may be added to the reaction to enhance enzymatic activity. Many factors that stimulate ATPase activity have been characterized. For example, cardiolipin and other membrane phospholipids, client proteins of chaperones such as Hsp90, and other proteins involved in supporting particular conformations or environments in which ATPases function (McLaughlin *et al*., 2002; Shiue *et al*., 2006; Ghosh *et al*., 2011). Our laboratory first characterized EpsE by purifying monomers with weak ATPase activity compared to homologous ATPases (Camberg & Sandkvist, 2005). We later discovered that when EpsE was copurified with the cytoplasmic domain of EpsL, a transmembrane protein and binding partner of EpsE in the T2S system, addition of acidic phospholipids such as cardiolipin to the reaction mixture greatly increased the ATPase activity of EpsE (Camberg *et al*., 2007). This likely mimics the conditions EpsE experiences at the cytoplasmic membrane that may promote oligomerization.

Many techniques have been used to quantify in vitro ATPase activity of purified proteins. Radioactive γ-^{32}P has been frequently and successfully implemented to quantify ATP hydrolysis (Shiue *et al*., 2006; Savvides *et al*., 2003), however, safety is a concern and requires approval for the laboratory use of radioactivity. While highly sensitive, the short half-life of γ-^{32}P is also a

disadvantage. Other commercial phosphate detection methods are available, such as those that rely on the formation of a fluorescent product. Some of these methods are also very sensitive, but frequently require the addition of other enzymes to the reaction, resulting in reagents that are less stable over time. Additionally, kits are available that detect ADP released during ATP hydrolysis using a stable luminescence-based reagent, but these may be less ideal for ATPases with low levels of activity (Sanghera *et al*., 2009).

The assay described here consists of only one phosphate release measurement step, is highly sensitive, and can typically be performed within a few hours. It is also possible to prepare a malachite green-containing substrate to avoid purchasing a kit from a commercial vendor (Camberg & Sandkvist, 2005). One consideration before undertaking this assay is that the step between adding the phosphate detection reagent and taking absorbance readings is relatively time-sensitive and must be between 20-30 minutes. This basic protocol can be used to determine the role of stimulants (as described), antagonists, subunits, domains, and specific residues in ATPase activity (Ghosh *et al*., 2011; Savvides *et al*., 2003; Sherman *et al*., 2014; Zhang *et al*., 2015). This assay can also be extended to measure the activity of phosphatases or other enzymes that release phosphate during catalysis. Additionally, this method can be applied to high-throughput screening for ATPase inhibitors (Rowlands *et al*., 2004).

Chapter 4:

Suppressor Mutations in VesC Facilitate Genetic Inactivation of Type II Secretion in *Vibrio cholerae*

Abstract

The Type II Secretion (T2S) system is a conserved bacterial protein transport pathway responsible for the secretion of a range of virulence factors by many pathogens including *Vibrio cholerae*, the causative agent of cholera. We previously observed that disruption of the *eps* genes encoding T2S apparatus components in *V. cholerae* results in loss of secretion and several changes in cell envelope function, such as loss of outer membrane proteins, extracellular leakage of periplasmic contents, and upregulation of the RpoE extra-cytoplasmic stress response pathway resulting in growth defects. Several high-throughput genomic analyses have listed the *eps* genes among *V. cholerae* essential genes, although we and others have successfully constructed inactivating *eps* mutations. To investigate whether suppressor mutations facilitate the construction of *eps* mutants, we sequenced the genomes of three independently constructed *V. cholerae* T2S mutants with deletions in the *epsG*, *epsL* and *epsM* genes and identified at least two secondary mutations in each. Interestingly, two of the three *eps* mutants contain distinct mutations in the gene coding for the T2-secreted substrate VesC that abolish its activity. One of these mutants also carries a

mutation in a lipopolysaccharide (LPS) biosynthesis gene, while the other contains a mutation in a gene that may encode a periplasmic protein or a T2-secreted substrate. One possible mechanism by which *V. cholerae eps* mutagenesis is accomplished is through selection for VesC-inactivating mutations, which may contribute to cell envelope integrity, thus establishing permissive conditions for the disruption of the Eps system.

Introduction

Vibrio cholerae is a Gram-negative bacterial pathogen and the causative agent of the disease cholera. Upon colonization of the human small intestine, *V. cholerae* infection causes profuse diarrhea, which can lead to rapid dehydration without oral rehydration therapy (Sack *et al*., 2004; Harris *et al*., 2012). One of the major *V. cholerae* virulence factors is cholera toxin, a secreted AB_5 toxin that causes chloride ion imbalances in intestinal epithelial cells, resulting in the massive, watery, mucoid diarrhea that characterizes cholera, known as rice-water stool (Kaper *et al*., 1995). Cholera toxin is secreted to the extracellular milieu by the type II secretion (T2S) system, a widespread protein secretion pathway found in a variety of human and plant pathogens (Sandkvist *et al*., 1997; Sandkvist, 2001; Cianciotto, 2005).

The *V. cholerae* T2S apparatus is composed of 12 Eps (extracellular protein secretion) proteins, EpsC through M and PilD, which collectively span the entire cell envelope (Overbye *et al.*, 1993; Sandkvist *et al.*, 1997; Marsh & Taylor, 1998; Fullner & Mekalanos, 1999). Type II secreted proteins first cross the inner

membrane using the Sec or Tat machinery, and then transit the outer membrane via the T2S apparatus (Pugsley, 1993; Voulhoux *et al.*, 2001). The T2S system in *V. cholera*e is responsible for the secretion of cholera toxin and many hydrolytic enzymes, which contribute to both pathogenesis in the human host and survival of the bacteria in the aquatic environment as a disease reservoir (Sandkvist, 2001; Sikora, 2013; Kirn *et al*., 2005; Overbye *et al.*, 1993; Connell *et al.*, 1998; Davis *et al.*, 2000; Sikora *et al.*, 2011; Johnson *et al.*, 2014).

At least 20 substrates of the T2S system have been identified in *V. cholerae* to date, including cholera toxin, biofilm matrix proteins, chitin-binding and –degrading proteins, lipases, hemagglutinin/protease (HAP), and other proteases (Sikora *et al*., 2011; Kirn *et al*., 2005; Connell *et al*., 1998, Overbye *et al*., 1993; Davis *et al*., 2000). Three homologous serine proteases, VesA, VesB, and VesC, were identified in the *V. cholerae* secretome, and VesA was shown to be involved with processing of cholera toxin (Sikora *et al*., 2011). Recent characterization of VesB revealed a trypsin-like serine protease with an N-terminal protease domain and a C-terminal Ig-fold followed by a Gly-Gly-CTERM extension (Gadwal *et al*., 2014). These three proteases may play a role in pathogenesis, since VesB can be detected in the stool of cholera patients, VesA and VesB were identified in the cecal fluid of infected rabbits, and injection of purified VesC caused fluid accumulation and damage in a rabbit ileal loop model of infection (LaRocque *et al*., 2008; Hatzios *et al*., 2016; Syngkon *et al*., 2010). However, a Δ*vesABC* strain was still able to robustly colonize the infant mouse intestine (Sikora *et al*., 2011).

Inactivation of the T2S system in *V. cholerae* results in a reduced growth rate in rich media as well as cell envelope perturbations including loss of membrane integrity, reduced levels of outer membrane proteins including OmpS, OmpT, OmpU, OmpV, and OmpW, and induction of RpoE, an alternative sigma factor that regulates the extracytoplasmic stress response (Sandkvist *et al*., 1997; Sikora *et al*., 2007; Sikora *et al*., 2009). Similar growth defects have also been reported for *pilD* mutants of *V. cholerae*, which lack the prepilin peptidase shared by the T2S and one of the type IV pilus systems (Fullner & Mekalanos, 1999). Additional reports of analogous phenotypes among T2S mutants have been observed in *Aeromonas hydrophila*, *Vibrio vulnificus*, and *Vibrio* sp. strain 60 (Jiang & Howard, 1992; Howard *et al*., 1993; Hwang *et al*., 2011; Ichige *et al*., 1988). *Legionella pneumophila* T2S mutants grow more slowly at low temperatures, although the growth defect may be partially restored by a secreted factor, since plating T2S mutants next to WT *L. pneumophila* stimulated growth (Söderberg *et al*., 2004). In most organisms in which the T2S system has been genetically inactivated, however, neither outer membrane alterations nor reduced growth phenotypes have been reported (Baldi *et al*., 2012; Ball *et al*., 2002; Johnson *et al*., 2016).

Several high-throughput genomic analyses have indicated that the T2S genes are essential in *V. cholerae* (Judson & Mekalanos, 2000; Cameron *et al*., 2008; Chao *et al*., 2013; Kamp *et al*., 2013). Using a positive approach to identify genes required for *V. cholerae* strain N16961 growth in rich media, Judson and Mekalanos (2000) categorized *epsD* and *epsG* as essential (Judson & Mekalanos,

2000). Several *eps* genes and *pilD* were also identified as putatively essential *V. cholerae* genes by both Cameron *et al* and Kamp *et al*, as transposon insertions in these genes were not identified during genome-saturating transposon screens, presumably because bacteria containing transposon insertions in these genes cannot be recovered (Cameron *et al*., 2008; Kamp *et al*., 2013). However, transposon insertions in *eps* genes were reported in a recent Tn-seq screen (Fu *et al*., 2013). Chao *et al* (2013) categorized *V. cholerae* genes as essential, domain essential (containing both essential and non-essential coding regions), or sick. All of the genes required for T2S fell into one of these three categories except *epsI*, which had too few insertions (≤7) to accurately categorize (Chao *et al*., 2013). Combined with the observations that *eps* mutations result in outer membrane perturbations and reduced growth rates in rich media, these studies strongly indicate that the *V. cholerae* T2S genes are essential and that mutations in these genes can only be isolated under particular conditions (Sandkvist *et al*., 1997; Sikora *et al*., 2007; Sikora *et al*., 2009; Fullner and Mekalanos, 1999; Judson & Mekalanos, 2000; Cameron *et al*., 2008; Chao *et al*., 2013; Kamp *et al*., 2013; Fu *et al*., 2013).

Recently, the *rpoE* gene has been characterized as an essential gene in *V. cholerae*. Because of the ability to generate insertional *rpoE* mutations in *V. cholerae*, initial studies did not imply the gene's essentiality; however, these mutants displayed a range of different phenotypes and no *rpoE* deletion mutations could be constructed in *V. cholerae* (Davis & Waldor, 2009). Davis & Waldor (2009) used genome sequencing techniques to determine that *V. cholerae rpoE* insertion

mutants contained additional mutations, many of which reduced the production of OmpU. Their results indicated that *rpoE* mutations in *V. cholerae* may only be constructed after accumulation of additional mutations that suppress the *rpoE* mutant phenotype (Davis & Waldor, 2009). Whole-genome sequencing analysis has also been utilized to identify and characterize suppressor mutations of *relA* deletion mutants in *B. subtilis* and *gacA* deletion mutations in *V. fischeri* (Srivatsan *et al*., 2008; Foxall *et al*., 2015).

Similarly, we hypothesized that *V. cholerae* T2S mutants contain secondary mutations that may help alleviate loss of membrane integrity and cell envelope stress. Using high-throughput genome sequencing, we identified additional mutations in three different T2S mutants. We found that two out of the three sequenced T2S mutants acquired distinct mutations in the same gene, suggesting a selective pressure to alleviate the cell envelope stress induced by T2S mutations.

Results

Inactivation of the type II secretion system in Vibrio cholerae *reduces growth rates*

We have previously reported that a *V. cholerae* Δ*eps* strain lacking all *eps* genes exhibits a growth rate reduction in rich media compared to the isogenic WT strain, suggesting that loss of T2S results in a slower growth phenotype (Sikora *et al*., 2007). Interestingly, strains containing inactivating mutations in different *eps* genes show some variation in growth rate, although T2S mutants exhibit consistent reductions compared to T2S-competent WT isolates (Figure 4.1A). Although inactivation of any of the *eps* genes abolishes T2S (Figure 4.1B), the slight

differences in growth phenotypes of different *V. cholerae eps* mutants is consistent with the possibility that each mutant has acquired distinct suppressor mutations (Figure 4.1A; Sikora *et al*., 2007). Thus, comparing the growth rate of *V. cholerae* lacking T2S to isogenic WT strains may be complicated by the accumulation of different secondary mutations that may mask growth phenotypes among T2S mutants.

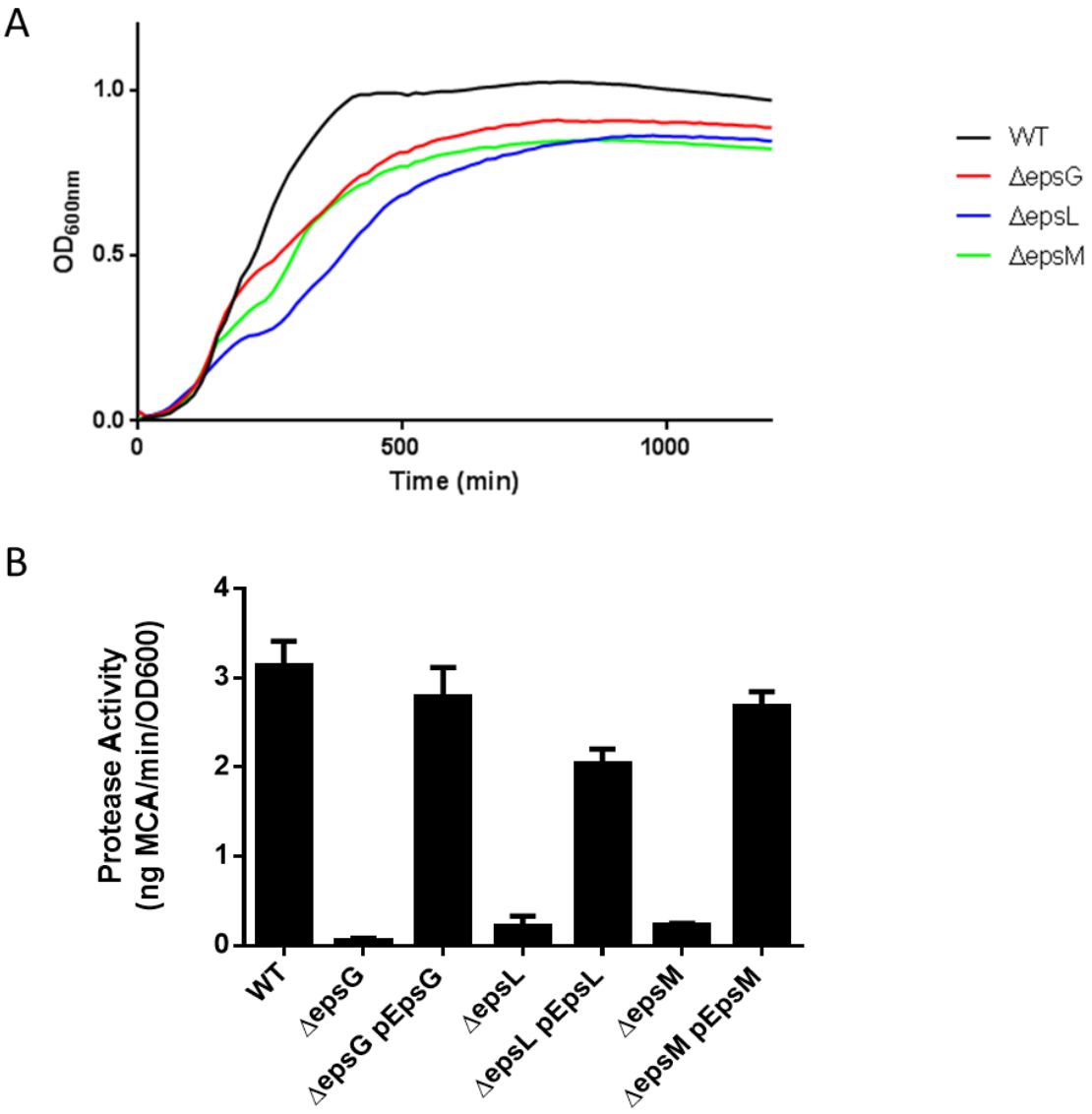

Figure 4.1 *Vibrio cholerae eps* mutants display reduced growth rates. A. Stationary phase cultures of *V. cholerae* were back-diluted to an OD_{600} of 0.05 and inoculated into microtiter plates in duplicate. OD_{600} was measured using a Bioscreen Growth Curve Analyzer every 15 minutes for 20 hours. Experiments were repeated in triplicate and means are displayed. **B.** Complementation of *eps* genes in *Vibrio cholerae* T2S mutants restores extracellular protease activity. Protease activity was measured in overnight culture supernatants using a fluorogenic probe as described in *Experimental Procedures*. Experiments were performed in triplicate with means and SEM shown.

In order to investigate directly whether T2S gene expression affects growth in *V. cholerae*, we took advantage of a previously constructed strain in which the native *eps* promoter was replaced with an arabinose-inducible promoter (P_{BAD}::*eps*) (Sikora et al., 2007). Using this inducible construct, we analyzed differences between *V. cholerae* TRH7000 P_{BAD}::*eps* and the isogenic WT strain in the presence or absence of arabinose. As shown in Figure 4.2A, *V. cholerae* P_{BAD}::*eps* exhibits a growth defect when cultured in the absence of arabinose, which is partially restored in the presence of 0.01% arabinose. To investigate whether inactivation of T2S affects *in vitro* survival of *V. cholerae*, we grew overnight cultures of WT and P_{BAD}::*eps* in the presence of arabinose, washed the cells, and plated serial dilutions of each strain on agar plates with and without arabinose. No major differences in colony forming units (cfu) counts were observed between the plates with and without arabinose, though the P_{BAD}::*eps* strain showed a marked reduction in colony size on agar plates lacking arabinose (Table 4.1, Figure 4.2B). This suggests that inactivation of *eps* genes negatively impacts growth, which may only be essential in *V. cholerae* under particular conditions. However, leaky expression from the arabinose-inducible promoter may not render the T2S system completely inactive, and some T2S complexes may be present in these cells due to overnight growth in arabinose-containing media prior to plating.

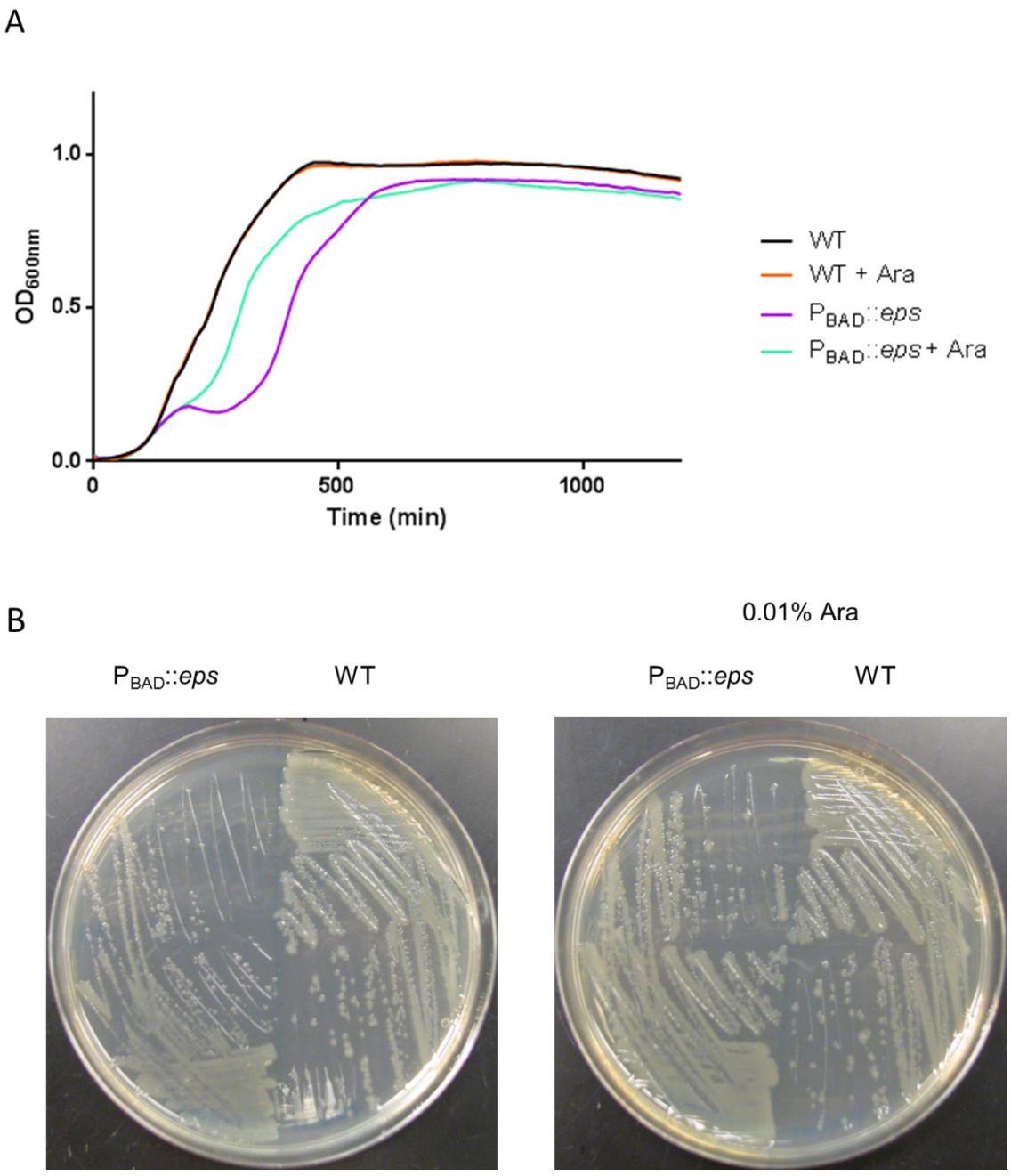

Figure 4.2 Interfering with *V. cholerae eps* gene expression results in growth defects and a small colony morphology. A. Overnight stationary phase cultures of *V. cholerae* P_{BAD}::*eps* and the isogenic WT strain were back-diluted 1:100 into media containing thymine or thymine + 0.01% arabinose and added to the wells of microtiter plates in duplicate. OD_{600} was measured using a Bioscreen Growth Curve Analyzer every 15 minutes for 20 hours. Experiments were repeated in triplicate and means are displayed. **B.** TRH7000 P_{BAD}::*eps* and the isogenic WT were streaked onto plates containing thymine and thymine + 0.01% arabinose from frozen stocks to compare colony morphology.

Table 4.1 Interfering with *V. cholerae eps* gene expression does not impact *in vitro* survival

	WT	P_{BAD}::*eps*
Thy	1.39 x 10^8 +/- 0.45	1.75 x 10^8 +/- 0.54
Thy + 0.01% Ara	1.69 x 10^8 +/- 0.3	1.37 x 10^8 +/- 0.12

Identification of secondary mutations in V. cholerae *T2S mutants*

We hypothesized that, similar to *rpoE*, the *eps* genes may be inactivated only under particular conditions, and that the process of constructing *eps* mutations selects for secondary mutations that suppress some of the phenotypes observed in these mutants, such as growth defects and outer membrane leakiness. Thus, we sought to identify additional mutations among *V. cholerae* T2S mutants using high-throughput genome sequencing. Using Illumina Hi-Seq technology, we sequenced the genomes of the *V. cholerae* El Tor strain TRH7000, a *ctxAB*::Hg^R derivative of N16961, and the isogenic Δ*epsG*, Δ*epsL,* and Δ*epsM* mutants (Figure 4.3). In order to identify genetic variants [including single nucleotide polymorphisms (SNPs) and structural variants (SVs)] between the T2S mutants and WT *V. cholerae*, we used reference-guided alignment using SeqMan software (Lasergene) with the sequenced strain N16961 as a template. We then subtracted any variants found between TRH7000 WT and N16961 in order to establish a list of differences between the WT strain and each sequenced T2S mutant, Δ*epsG,* Δ*epsL,* and Δ*epsM*. We went on to confirm the presence of secondary mutations in the Δ*epsG* and Δ*epsL* strains by PCR amplification of genomic DNA followed by

Sanger sequencing. The secondary mutations in the Δ*epsM* strain were confirmed only by bioinformatic analysis, with calls limited to variants present in >75% of reads and not located in regions of low read density (Table 4.2).

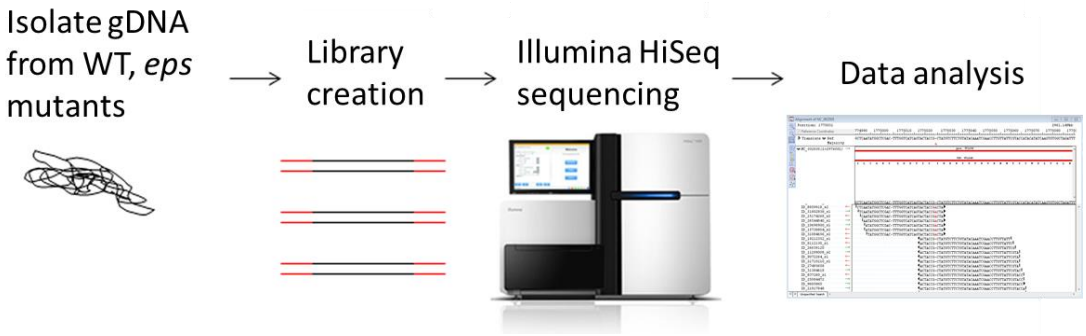

Figure 4.3 Overview of the workflow for identifying secondary mutations. Paired-end libraries were prepared from genomic DNA isolated from TRH7000 *eps* mutants and the isogenic WT strain, and sequencing was performed using an Illumina HiSeq 2000 instrument (depicted). Data analysis was performed using SeqMan NGen and SeqMan Pro software (Lasergene).

Table 4.2 Secondary mutations identified in *V. cholerae eps* mutants

Strain	Gene, Putative function	Mutation	AA Position, Change
Δ*epsG*	VC1649 (VesC), type II-secreted serine protease	Frameshift, 7bp insertion	491
	VC0259 (RfbV), lipopolysaccharide biosynthesis	Frameshift, A insertion	159
Δ*epsL*	VC1649 (VesC), type II-secreted serine protease	Missense, T→G	279, Q→P
	VCA0254, hypothetical	Frameshift, G deletion	548
Δ*epsM*	VC0286, putative gluconate transporter	Missense, T→A	100, I→F
	VC0613, beta-N-acetylhexosaminidase, chitin utilization	Missense, C→T	338, G→S
	VC1718, conserved hypothetical	Missense, G→A	190, V→M
	VC1915 (RpsA), 30S ribosomal protein S1	Frameshift, 34bp deletion	526
	Noncoding region (chromosome 2 position 972161)	G→T	

Using high-throughput sequencing, two secondary mutations were identified in two of the *V. cholerae* T2S mutants, Δ*epsG* and Δ*epsL*, and five additional mutations were identified in the Δ*epsM* mutant, as tabulated in Table 4.2. Interestingly, the Δ*epsG* and Δ*epsL* mutants have acquired distinct mutations in the *vesC* gene (VC1649), which encodes a T2-secreted protease (Syngkon *et al*., 2010; Sikora *et al*., 2011). The Δ*epsG* mutant contains a 7-bp insertion (frame-shift mutation) at position 1467 (residue 491) of *vesC* resulting in a premature stop codon at amino acid (aa) 492 of this 548-aa protein (491fs). The Δ*epsL* mutant harbors a point mutation altering residue 279 from a glutamine to a proline

(Q279P). In both Δ*epsG* and Δ*epsL* mutants, one additional gene contains a mutation besides *vesC*, and these are unique between the two strains. Specifically, the Δ*epsG* mutant contains a mutation in *rfbV* (VC0259), a gene required for LPS biogenesis (Fallarino *et al*., 1997), and the Δ*epsL* strain contains a mutation in a hypothetical gene located on the second chromosome (VCA0254). The Δ*epsM* mutant contains five secondary mutations in metabolic genes, a hypothetical gene, a gene (*rpsA*) encoding a ribosomal protein, and one located in a noncoding region of the genome (Table 4.2). We chose to follow up with the secondary mutations in the Δ*epsG* and Δ*epsL* strains for further characterization because they both contained independent mutations in the same gene, indicating one possible conserved mechanism for suppressor mutations that may facilitate inactivation of the T2S genes in *V. cholerae*.

Secondary mutations in vesC abolish protease activity

The identification of secondary mutations in the *vesC* gene among T2S mutants was particularly intriguing, as VesC is one of three homologous serine proteases, along with VesA and VesB, which have been identified as part of the *V. cholerae* T2 secretome (Sikora *et al*., 2011). We routinely measure serine protease activity towards the substrate *N*-tert-butoxy-carbonyl-Gln-Ala-Arg-7-amido-4-methylcoumarin as a readout for T2S in our laboratory, to which VesA, B, and C all contribute to various degrees (Sandkvist *et al*., 1997; Camberg *et al*., 2007; Sikora *et al*., 2007; Sikora *et al*., 2011). While VesC in culture supernatants from WT *V. cholerae* contributes to only 10-20% of the overall protease activity,

overexpression of v*esC* in the triple protease mutant, Δ*vesABC,* of *V. cholerae* N16961 results in high and reproducible activity (Sikora *et al.*, 2011). We thus used this protease assay as a way of measuring VesC's activity in order to understand the mechanism by which *vesC* mutations may contribute to suppression of *eps* mutant phenotypes.

In order to test whether the secondary mutations in *vesC* harbored by Δ*epsG* and Δ*epsL* mutants inactivate VesC, we cloned and expressed these genes in the Δ*vesABC* mutant. The protease activity in the culture supernatants was determined and compared to supernatants from Δ*vesABC* expressing genes for either WT VesC or a catalytically inactive version, VesC S225A. Neither VesC Q279P nor VesC 491fs were able to restore extracellular protease activity in the Δ*vesABC* mutant, indicating that these secondary mutations abolish VesC activity (Figure 4.4). Alternatively, the mutations may cause misfolding and/or degradation of VesC.

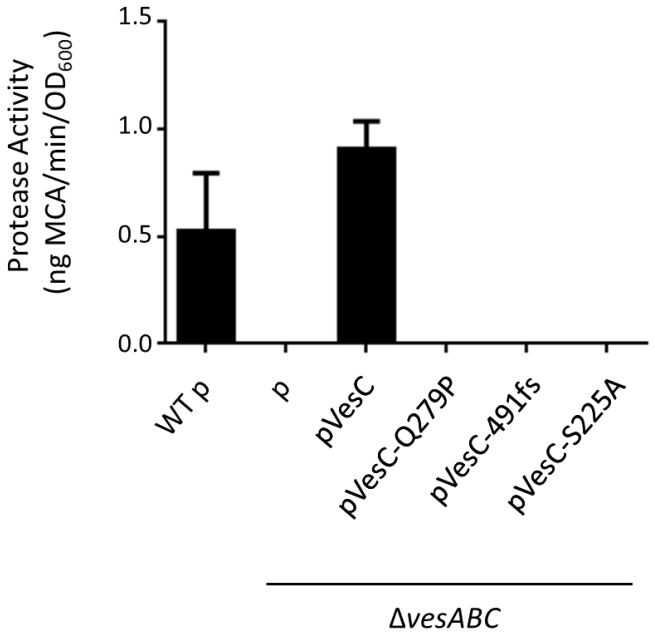

Figure 4.4 Suppressor mutations inactivate VesC. Protease activity was measured in log phase culture supernatants of N16961 WT containing an empty vector as well as the isogenic Δ*vesABC* strain containing empty vector or plasmids that code for WT VesC, VesC-Q279P, VVesC-491fs, or VesC-S225A.

To confirm that the lack of protease activity in the culture supernatants of the Δ*epsG* and Δ*epsL* mutants is due to loss of protease secretion and not simply a consequence of the secondary mutations in *vesC,* we set up two experiments. First, we verified that extracellular protease activity (primarily contributed by VesB) was restored following complementation by plasmid-encoded EpsG and EpsL, respectively. In agreement with previously published results, complementation of the Δ*epsG* and Δ*epsL* mutants resulted in extracellular protease activity similar to that of WT supernatants (Figure 4.1B; Gray *et al*., 2011). Second, WT *vesC* was overexpressed in WT TRH7000 and the isogenic Δ*epsG* and Δ*epsL* mutants.

Overexpression of *vesC* results in an increase in protease activity in WT TRH7000 supernatant, but not in the culture supernatants of the Δ*epsG* and Δ*epsL* mutants (Figure 4.5). These results are consistent with previously published proteomic analyses indicating that VesC is a T2S substrate (Sikora *et al*., 2011).

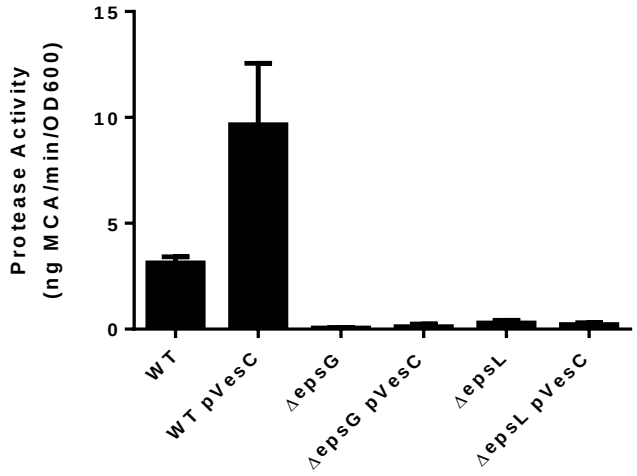

Figure 4.5 VesC expression increases extracellular protease activity in WT but not *eps* mutants. Protease activity was measured in culture supernatants from TRH7000 WT, Δ*epsG*, and Δ*epsL* mutants and the same strains overexpressing the *vesC* gene from a plasmid.

T2S mutants display altered LPS profiles

Manning and colleagues have previously shown that RfbV supports the synthesis of LPS O-antigen, as insertional inactivation of *rfbV* results in loss of the O-antigen lipid A core with an simultaneous increase in the lipid A core as visualized by SDS-PAGE and silver staining (Fallarino *et al*., 1997). Since one of the secondary mutations we identified in the Δ*epsG* mutant is located in *rfbV*, we

characterized the LPS profile of this strain by subjecting cells and culture supernatants to proteinase K treatment followed by SDS-PAGE and silver staining. We analyzed both cell and supernatant fractions, as OMVs released by *V. cholerae* contain large amounts of LPS (Kondo *et al*., 1993; Chatterjee & Das, 1967; Beveridge, 1999; Kulp & Kuehn, 2010). As shown in Figure 4.6, LPS assembly is defective in the Δ*epsG* mutant; the intact O-antigen lipid A core is absent and a faster-migrating lipid A core is accumulating. However, neither expression of EpsG nor RfbV could restore the production of intact LPS (Figure 4.6). Although EpsG complementation can restore T2S, this result suggests that some aspects of the outer membrane damage that accompanies construction of *eps* mutations is irreversible.

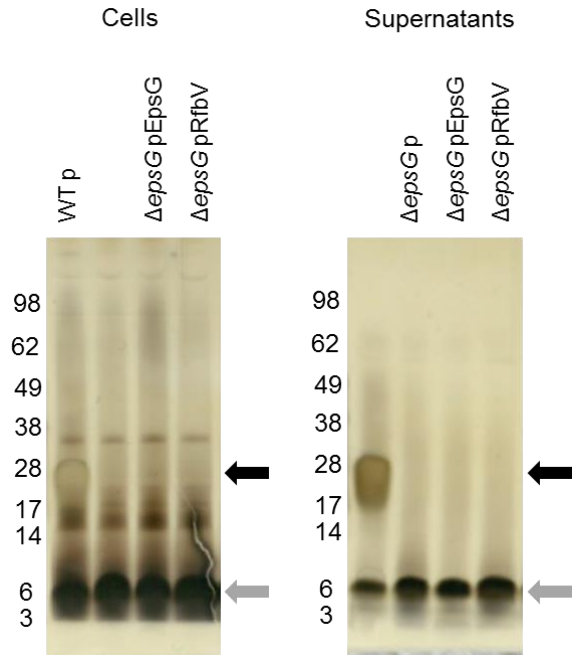

Figure 4.6 LPS biogenesis defects in Δ*epsG* cannot be complemented. Cells (left) and supernatants (right) from overnight cultures of TRH7000 WT and the Δ*epsG* mutant containing empty vector, Δ*epsG* pEpsG, and Δ*epsG* pRfbV were treated with proteinase K and analyzed using SDS-PAGE and silver staining. Fully assembled LPS is designated with a black arrow, and faster-migrating lipid A core with a gray arrow.

Discussion

This study provides a possible mechanism to parse between previous reports that the T2S (*eps*) genes are likely essential in *V. cholerae*, which has previously been suggested in several genome-wide mutational analyses of *V. cholerae* (Judson & Mekalanos, 2000; Cameron *et al*., 2008; Chao *et al*., 2013; Kamp *et al*., 2013) and the fact that we and others have successfully constructed mutations in each of the genes required for T2S. Because we have observed slight growth variations between different mutants (Figure 4.1) and occasional larger colony variants in our T2S mutant populations after streaking from frozen stocks

(Figure 4.2B), we hypothesized that *V. cholerae* T2S mutants have acquired secondary mutations that suppress some of the cell envelope defects we have characterized and allow for the construction of T2S mutations (Sikora *et al*., 2007). Indeed, we confirmed the presence of at least two secondary mutations in each of the three *V. cholerae* T2S mutants we sequenced. Two of the three *eps* mutants acquired distinct mutations in the same gene, VC1649, which encodes the T2-secreted serine protease VesC. These mutations both inactivate VesC, although one is a point mutation in the middle of the protein and the other causes a frameshift near the C-terminus (Table 4.2). Alternatively, the mutations may affect folding and/or promote degradation of VesC. This suggests that one method by which *eps* mutations can be generated in *V. cholerae* is to inactivate one of its secreted substrates, which may otherwise accumulate in the periplasm and cause damage to its cell envelope. The two sequenced *V. cholerae* T2S mutants with *vesC* mutations, Δ*epsG* and Δ*epsL*, also had one additional unique mutation in an LPS biosynthesis gene and a hypothetical gene, respectively. It is therefore feasible that multiple mutations must be acquired by *V. cholerae* in order to create conditions under which Eps inactivation is possible.

Over 20 proteins are secreted by the T2S system, yet we identified secondary mutations in the same gene, *vesC*, in two of the three sequenced *eps* mutants. Perhaps sequencing of additional *eps* mutants will reveal secondary mutations in genes encoding different T2S substrates, but the observation of two distinct mutations in the *vesC* gene is indicative of a conserved mechanism for putative *eps* mutant suppression. One feasible model of this mechanism is that

VesC-inactivating mutations in T2S mutants decrease proteolysis in the cell envelope that contributes to the outer membrane leakiness and growth defects, creating a permissive condition for acquisition of mutations in *eps* genes. VesC accumulation in the periplasm may lead to nonspecific proteolysis in the cell envelope, leading to membrane damage and leakiness as well as RpoE induction (Sikora *et al*., 2007). Alternatively, the sheer amount of VesC and other T2S substrates that accumulate upon T2S inactivation may lead to cell envelope stress. The identified mutations in VesC may thus result in misfolding and protein degradation that alleviates some cellular stress. In fact, proteomic analysis of the *V. cholerae* T2S secretome showed that VesC is the most abundant T2S substrate when grown in LB at 37°C (Sikora *et al*., 2011; Johnson *et al*., unpublished).

To better understand how the Q279P and 491fs mutations might affect VesC, we aligned the amino acid sequence of VesC with the homologues VesB, whose structure has been determined, and VesA (Figure 4.7). Both VesC and VesB consist of an N-terminal protease domain and a C-terminal non-protease domain, while VesA lacks the non-protease domain (Gadwal *et al*., 2014; Figure 4.7). The VesC non-protease domain consists of an Ig-fold domain, similar to VesB, and an additional ~130 residue extension of unknown function. The frameshift mutation in the Δ*epsG* mutant introduces an early stop codon that results in removal of the C-terminal 56 residues, truncating the protein prior to the Gly-Gly-CTERM domain (Gadwal *et al*., 2014; Figure 4.7, red arrow). Although the role of the Gly-Gly-CTERM domain is still unknown, the region's conservation suggests an important function (Haft & Varghese, 2011; Gadwal *et al*., 2014).

Additionally, we have observed that truncation of the last 30 residues of VesB results in an unstable protein with reduced activity (Gadwal *et al*., in review). The *vesC* point mutation identified in the Δ*epsL* mutant results in a Q279P substitution at the junction between the protease and non-protease domains (Figure 4.7; red box). Structural analysis indicates that the analogous glutamine residue in VesB likely forms part of an interface with residues in the protease domain (Gadwal *et al*., 2014). Since the side chain of proline is markedly different from that of glutamine, the Q279P mutation may modify this putative interaction and prevent activation or proper folding of VesC. Attempts to produce secreted VesB without its non-protease domain have been unsuccessful, supporting the suggestion that the non-protease domain plays an important role in protein stabilization and/or activation in VesB and possibly also VesC (Gadwal *et al*., 2014).

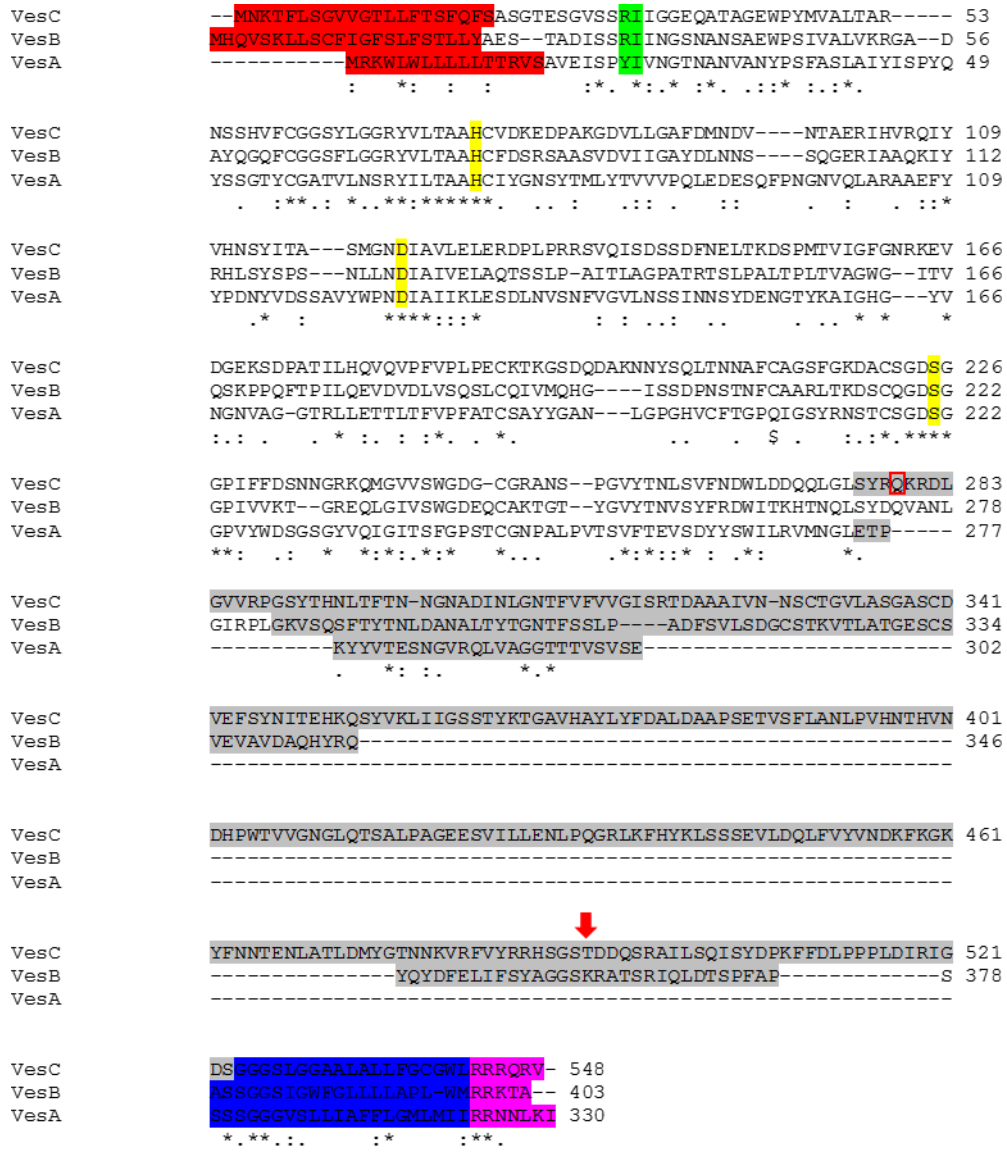

Figure 4.7 Alignment of VesC, VesB, and VesA. The signal peptides are highlighted in red, with the activation site in green and the catalytic triad residues in yellow. The non-protease domains of VesC and VesB are colored gray, blue, and pink with the membrane-spanning helix in blue and the basic tail in pink. Asterisks indicate sequence identity, and colons and periods indicate high and low levels of residue homology, respectively. The locations of the secondary mutations are labeled as such: Q279 is boxed in red, and the position of the 491fs is marked with a red arrow.

Another intriguing finding from sequencing the three *V. cholerae* T2S mutant genomes was a secondary mutation in the LPS biogenesis gene *rfbV* in the Δ*epsG* mutant. Our previous observations that a number of outer membrane proteins are diminished and the RpoE stress response system is induced suggest that LPS synthesis and/or transport may also be affected in *V. cholerae eps* mutants (Sikora *et al*., 2007). Since we have observed a lack of assembled LPS in the Δ*epsG* mutant, we reasoned that perhaps complementation of EpsG and/or RfbV would restore LPS biosynthesis. However, LPS was not assembled in either condition, suggesting that restoration of LPS assembly may require complementation with both EpsG and RfbV (Figure 4.6).

In addition to a *vesC* mutation, the Δ*epsL* mutant also contained a mutation in a hypothetical gene, VCA0254. Although the function of this gene is unknown, it encodes a protein with a putative signal sequence. It is therefore possible that this is a periplasmic protein or another yet to be identified T2S substrate; if so, this suggests that additional substrates besides VesC may contribute to cell envelope damage when the Eps system is inactivated. Five secondary mutations were also identified in the Δ*epsM* mutant, located in metabolic genes required for chitin and gluconate utilization, hypothetical, and ribosomal protein genes and a non-coding region (Table 4.2). Interestingly, the Δ*epsM* mutant was constructed differently from the Δ*epsG* and Δ*epsL* mutants, using a *λ* Red recombination-based system for genetic inactivation for the former rather than a suicide vector/sucrose selection-based approach for the latter. While further research is necessary to understand the contribution of the secondary mutations in the Δ*epsM* mutant, this

finding indicates that there may be multiple mechanisms for suppression of cell envelope defects caused by T2S gene inactivation in *V. cholerae*.

As most organisms containing T2S systems do not exhibit the same cell envelope defects upon T2S gene inactivation, the subset of T2S substrates may play an important role in this process. Specifically, this may be a phenomenon unique to organisms that contain particular T2S substrates that cause damage to the cell envelope when they accumulate in the periplasm. Although many bacteria use the T2S system to support secretion of proteases, VesC is one of three unique trypsin-like serine proteases found only in *V. cholerae*, other *Vibrio* species, and related *Aeromonas* species and may have increased nonspecific activity inside the cell compared to other T2-secreted proteases. Therefore, we speculate that perhaps the T2S genes are not essential *per se*, but rather that the phenotype observed with T2S mutants of *V. cholerae*, *V. vulnificus*, *Vibrio* sp. strain 60, and *Aeromonas hydrophila* is due to damage caused by particular T2S substrates when they accumulate in the wrong location. Additional investigation into the relationship between organisms exhibiting T2S inactivation-associated envelope defects and their corresponding suites of T2S substrates may reveal a conserved mechanism for suppression of T2S-associated phenotypes in these organisms.

Experimental Procedures

Bacterial Strains and Growth Conditions

Vibrio cholerae N16961 (El Tor), TRH7000 (thy Hg^R (ctxA-ctxB)) and mutants thereof were grown at 37°C in LB broth, which was supplemented with

100 mg/ml thymine for TRH7000 strains and 0.01% arabinose for the pBAD::*eps* strain. Plasmid-containing strains were grown in the presence of 200 µg/ml carbenicillin and gene expression was induced with 10 µM isopropyl-D-thiogalactopyranoside (IPTG) for *epsG, epsL*, *epsM*, and *rfbV* or 50 µM IPTG for *vesC* expression.

Cloning

TRH7000 pBAD::*eps*, Δ*epsL*, and Δ*epsG* strains were constructed previously (Sikora *et al*., 2007; Gray *et al*., 2011). TRH7000 Δ*epsM* was constructed by amplifying regions upstream and downstream of the *epsM* gene and introducing an internal kanamycin resistance cassette from pKD4 using the following primers: 5’ caagtcttcttggctgcggt 3’ (forward primer for upstream fragment), 5’ CGAAGCAGCTCCAGCCTACACttctccttacttgggcttcacc 3’ (reverse primer for upstream fragment), 5’ CTAAGGAGGATATTCATATGgcgtggaggctgatatga 3’ (forward primer for downstream fragment), and 5’ ccgacacgacagtaccaagctgc 3’ (reverse primer for downstream fragment). PCR products from the upstream and downstream regions were used as a template for another PCR using the first and last primers, which was used for chromosomal replacement as described (Datsenko & Wanner, 2000).

Plasmids containing either WT or T2S mutant variants of genes identified from whole-genome sequencing were constructed by amplifying the gene of interest from TRH7000 chromosomes and cloning into pMMB67EH. The primers used to amplify *vesC* (VC1649) are as follows: 5'

GAGGAGCTCtgggagttatcagaggtatc 3' (Fwd) and 5' GAGGCATGCtggctatcgatagaTCAGAC 3' (Rev). To amplify *rfbV* (VC0259), the primers 5’ gaggagctcGTGGAAGGCACTAGC (Fwd) and 5’ gaggtcgacCCGTATGTCATTGCAAG 3’ (Rev) were used. pMMB-VesC S225A was constructed from pMMB-VesC WT using PCR mutagenesis, with overlapping primers containing the point mutation: 5' CGCTTGTTCTGGTGACgcCGGTGGCCCTATCTTTTTTG 3' (Fwd) and 5' CAAAAAAGATAGGGCCACCGgcGTCACCAGAACAAGCG 3' (Rev). To introduce the S225A mutation, the VesC Fwd primer and VesC S225A Rev primer and the VesC S225A Fwd primer and the VesC Rev primer were used to amplify each half of the VesC gene and introduce the mutation, and these products were then used as the template for a third PCR with the VesC Fwd and Rev primers. All cloning was confirmed using Sanger sequencing of PCR products and plasmids.

Growth Curve Analysis

Comparisons of growth rates were performed using a Bioscreen Growth Curve Analyzer (Growth Curves USA). Overnight stationary phase cultures of *V. cholerae* were back-diluted as described in figure legends and inoculated into microtiter Bioscreen plates in duplicate wells per sample. OD_{600} was measured at 15 minute intervals for 20 hours. Experiments were repeated in triplicate and means are displayed.

Genome sequencing and analysis

Genomic DNA was isolated from *V. cholerae* using Wizard Genomic DNA Purification kits (Promega). Genomic DNA library preparation and sequencing were performed by the University of Michigan DNA Sequencing Core using Illumina HiSeq 2000. Paired-end libraries were constructed and sequencing was performed with a read-length of 100x100. Analysis was conducted using SeqMan software (Lasergene) for SNP and structural variant calling. Using SeqMan NGen, the TRH7000 WT sequence was aligned to the N16961 published reference sequence to serve as a template for analysis of T2S mutant sequences. Variants were called using SeqMan Pro software (Lasergene) and visualization and coverage analysis was performed simultaneously. Genome sequences of T2S mutants were compared to N16961 using SeqMan NGen reference-guided alignment and variant calls that were also found when comparing TRH7000 WT to N16961 were subtracted from these calls. Read depth for the variant calls was as follows: VC0259 = 244, VC1649 = 213 (Δ*epsG*); VC1649 = 226, VCA0254 = 314 (Δ*epsL*); VC0286 = 129, VC0613 = 114, VC1718 = 65, VC1915 = 82, noncoding = 54 (Δ*epsM*). Variants from the Δ*epsG* and Δ*epsL* mutants were verified using PCR and Sanger sequencing.

Protease Secretion Assay

Extracellular protease activity was measured and quantitated as described previously (Sikora *et al*., 2007). Briefly, overnight cultures supernatants were separated from cells, and the fluorogenic probe, *N*-tert-butoxy-carbonyl-Gln-Ala-

Arg-7-amido-4-methylcoumarin (Sigma-Aldrich) was added to the supernatants. Over the course of 10 minutes, protease activity was measured every minute using fluorescence at excitation and emission wavelengths 385 and 440, respectively. Assays were performed at least in triplicate and values were normalized to the density of the culture (OD_{600nm}). Mean and SEM are displayed.

SDS-PAGE and Silver Staining

LPS assembly was analyzed by SDS-PAGE and silver staining as in Fallarino *et al*., 1997. Overnight culture cells and supernatants were boiled in SDS sample buffer, cooled to room temperature, and treated with 60 µg/ml Proteinase-K for 30 minutes on ice. Samples were loaded onto 4-12% Bis-Tris gels (NuPAGE, Invitrogen) by matching the culture densities via OD_{600} and run with MES buffer for 40 minutes at 200V. Silver staining was performed according to the manufacturer's directions (SilverQuest, Invitrogen).

Chapter 5:

Discussion

The goal of my dissertation research is to better understand the molecular mechanism by which the ATPase EpsE drives T2S as well as the overall role of the T2S system in the *V. cholerae* cell envelope barrier function. Conclusions, implications, and future directions of my research will be discussed. This chapter is broken down by structural and then functional analyses of the T2S system in *V. cholerae*.

Zinc Coordination is Critical for the Function of EpsE

The research presented in Chapter 2 shows that zinc coordination by the EpsE C_M domain is necessary for T2S in *V. cholerae*, as removal of the entire C_M domain or substitutions of cysteine residues in the tetracysteine motif ($CXXCX_{29}CXXC$) abolish the ability of EpsE to complement T2S in the *epsE*::*kan* mutant. None of the cysteine mutant variants of EpsE could be purified due to aggregation when overexpressed in *E. coli*, indicating that zinc binding may play a key role in protein folding and/or stability, at least when EpsE is produced in the absence of other components of the T2S machinery. As C_M deletions and cysteine mutants exhibit negative dominance when over-expressed in WT *V. cholerae,* they

are not completely misfolded and some native properties of the EpsE mutants are likely preserved. Chemical removal of zinc from EpsE hexamers results in a loss of activity and changes in the migration pattern when analyzed by native PAGE, indicating a possible structural alteration. Exchanging the 29 C_M loop residues between the two dicysteines with those of the homologue XcpR has no effect on the function or activity of EpsE. Collectively, we conclude that zinc coordination by EpsE C_M is required for EpsE's stability and function in T2S, but that many of the loop residues in the C_M domain do not serve species-specific purposes and can be functionally interchanged with those from a homologue.

In addition to providing protein stability, it is feasible that the C_M domain may provide a means for bacteria to support pseudopilus assembly, a process that is believed to drive T2S. This could be a process unique to T2S and T4P assembly ATPases, which may explain why zinc-coordinating domains are absent in homologues involved in T4P retraction and competence. EpsE is unlikely to act as a redox switch similar to Hsp33, as cellular reduction and oxidation is an improbable mechanism for regulation of secretion because removal of zinc by PCMB (chapter 2) causes a conformational change resulting in reduced ATPase activity. It is plausible that the C_M domain is necessary for correctly positioning residues involved in protein-protein interactions in a manner similar to SecA and ClpX, although our EpsE-XcpR C_M data indicate that species-specific protein-protein interactions likely do not occur via the residues at the bottom of the EpsE C_M loop. However, several residues in the C_M loop were not exchanged in this construct, especially those positioned closer to the dicysteines (Figure 5.1). Two

areas of conservation are visible within the C_M loop, and these residues may mediate interactions between the C_M domain and other T2S components and/or the rest of the CTD (Figure 5.2).

A

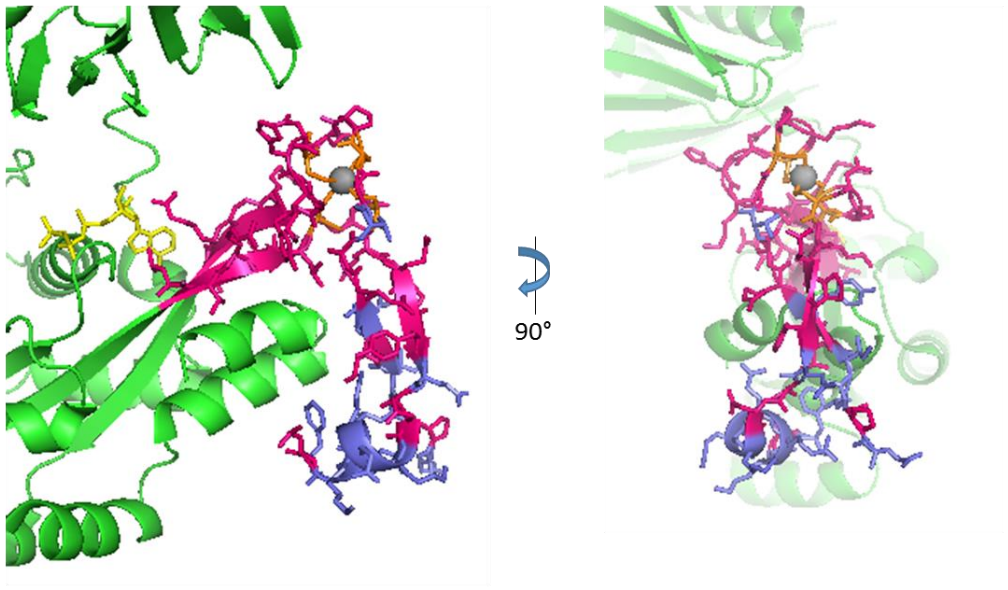

B

EpsE:	*CPDC*KEPY**E**AD**KEQRK**L**FDSKKKE**P**LI**L**Y**R**A**T**G*CPKC*
Chimera:	*CPDC*KEPY**R**AD**EAECA**L**LGVDPAA**P**PT**L**H**R**A**R**G*CPKC*

Figure 5.1 EpsE C_M residues exchanged in the EpsE-XcpR C_M chimera construct. **A.** The NTD and CTD of monomeric EpsE (PDB 1p9w) are shown in green ribbon structure, with nucleotide shown in yellow. The C_M domain is shown in ribbon and stick representation, with residues maintained in the chimera shown in magenta, and the exchanged residues colored purple. Several residues at the bottom of the C_M loop were not resolved in the crystal structure, but have also been exchanged in this construct. **B.** Alignment of the C_M domain residues in EpsE and EpsE-XcpR C_M. Bolded residues are those that differ between EpsE and XcpR loop regions and are either shown in purple in **A** or not resolved in the structure.

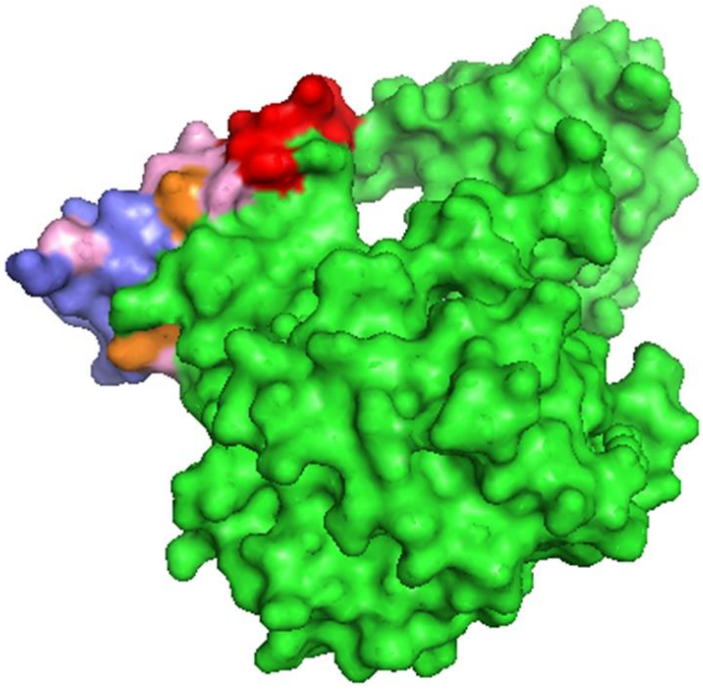

```
EpsE            KEPYEADKEQRKLFDSKKKEPLILYRATG
Chimera         KEPYRADEAECALLGVDPAAPPTLHRARG
                ****.**: :  *:  .   *  *:** *
```

Figure 5.2 Regional C_M loop residue conservation between EpsE and XcpR. The structure of monomeric EpsE (PDB 1p9w) is shown in spacefill representation with the NTD and CTD in green. The tetracysteine motif of the C_M domain is colored red. EpsE residues in the C_M loop exchanged in the EpsE-XcpR C_M chimera are shown in purple. Residues conserved between EpsE and the EpsE-XcpR C_M chimera are colored pink and orange to indicate sequence identity and similarity, respectively. A Clustal2 alignment of the C_M loop region between the two dicysteines is shown below, with stars representing sequence identity and colons and periods indicating high and low levels of sequence conservation, respectively.

Furthermore, several residues from the NTD are in close proximity to the C_M domain (Figure 5.3). In particular, R155, G159, and D158 from the NTD may contact N434 and H435 from the C_M domain, and although the former three residues are well-conserved throughout the broader class of type II/IV family of ATPases, the latter two are only present among EpsE/PilB subfamily members,

the so-called assembly ATPases that possess the C_M domain (Robien *et al*., 2003) (Figure 5.3). Many studies have demonstrated large conformational shifts of the NTD relative to the CTD during ATP binding and hydrolysis in homologous ATPases, including PilT and HP0525 (Satyshur *et al*., 2007; Yamagata & Tainer, 2007; Misic *et al*., 2010). The finding that EpsE hexamers can adopt at least two different conformations (Lu *et al*., 2013) suggests that EpsE also undergoes similar conformational shifts. Extrapolating from these studies, it is possible that residues such as D158 in the EpsE NTD may be brought closer to the C_M domain during cycles of catalysis (Figure 5.3). With several residues in close proximity to the NTD and CTD, the C_M domain may play a key role in interdomain interactions.

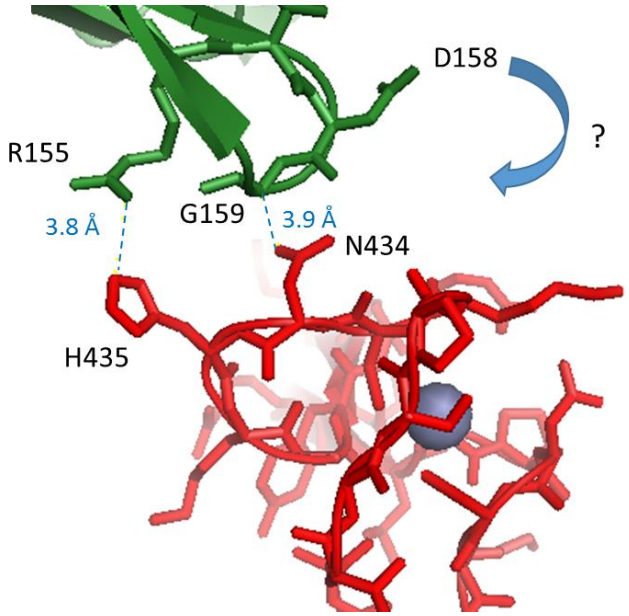

Figure 5.3 Potential interactions between residues in the EpsE NTD and C_M. The structure of monomeric EpsE (PDB 1p9w) is used to model potential NTD-C_M interdomain interactions. The NTD is represented in green ribbon structure with residues of interest shown in sticks. The C_M domain is displayed as red sticks with zinc as a gray sphere. Distances between residues are indicated with blue dotted lines and labeled. Putative NTD shifts relative to the CTD and C_M domains may also alter the position of D158, shifting it closer to the C_M domain (blue arrow).

One potential model for the role of the C_M domain in the function of EpsE is described in Chapter 2. We discussed the possibility that modulation of the C_M domain may affect activity by positioning important residues in the β-strands that enter and exit the C_M loop. For example, structural analysis indicates that two amino acids located at the base of the C_M domain may be affected by changes in the conformation of the C_M domain. On one strand, R441 contacts the adenyl and ribose moieties of the nucleotide, and on the opposite strand, R394 contacts a leucine residue of a neighboring EpsE subunit in the hexamer (Figure 2.10). We have previously shown that EpsE oligomers have increased ATPase activity (Camberg, 2005; Camberg, 2007; Patrick, 2011). Thus, conformational changes of EpsE due to C_M zinc coordination or abrogation, or alternatively, protein-protein interactions involving the C_M domain, may impact the positioning of key residues involved in ATP hydrolysis and/or subunit-subunit interactions within the hexamer.

Much of the information we have gained regarding the dynamics of the type II/IV ATPases has come from studies of the T4P retraction ATPase PilT, and although there are major similarities between PilT and EpsE, some key differences also exist. In the T4P system, two ATPases associate with the complex to extend and retract the pilus, PilB and PilT, respectively. The extension and retraction mechanisms of the T2S pseudopilus are still not completely understood, as only one ATPase is associated with the T2S system. T4P retraction ATPases such as PilT lack two structural components conserved among T2S/T4P assembly ATPases: 1) an extended N-terminal domain, known as N1, which targets these ATPases to the membrane (Sandkvist *et al*., 2000; Abendroth *et al*., 2005) and 2)

the C_M domain (Robien *et al*., 2003). My dissertation research furthers our understanding of the significance behind the presence of the zinc-coordinating C_M domain in T2S/T4P assembly ATPases to better understand not only the mechanism of energy production for T2S, but also the driving forces behind T4P extension and retraction dynamics.

A recent comprehensive model of the T4P system was constructed using cryo-EM and crystal structures of combinations of T4P proteins and their T2S and archaeal flagellar homologues (Chang *et al*. 2016). In this model, while bound to the EpsL homologue PilM, the EpsE homologue PilB transfers energy generated from ATP hydrolysis to power the rotation of the EpsF homologue PilC, which acts as a molecular glove to scoop pilin subunits from the inner membrane and add them to the growing pilus. Chang and colleagues (2016) posit that PilB and the retraction ATPase PilT are associated with the *M. xanthus* T4P complex in the same mutually exclusive manner; however, the nanometer resolution did not permit differentiation between PilB- and PilT-bound T4P complexes. Takhar *et al* (2013) showed that PilB interacts with the N-terminal cytoplasmic domain of PilC ($PilC_N$) and suggested that the C-terminal cytoplasmic domain of PilC interacts with PilT ($PilC_C$). The T4P model proposes that PilB and PilT both form “bowl-like” shapes but with PilB having an extended NTD, thus allowing for PilB-$PilC_N$ and PilT-$PilC_C$ interactions (Chang *et al*. 2016). However, It is important to note that the structure of PilB has yet to be solved, so to create this model they used the *V. cholerae* NTD of EpsE (that interacts with the cytoplasmic domain of EpsL) and *Archaeoglobus fulgidus* AfGspE, which lacks the C_M domain, to create a composite

PilB structure (Chang *et al*. 2016; Abendroth *et al*., 2005; Yamagata & Tainer, 2007). Thus, any potential role of the C_M domain in T4P assembly ATPases cannot be gleaned from this model, and further experiments are necessary to examine whether zinc coordination affects potential EpsE-EpsF interactions.

However, we can speculate that PilB may be the "default" ATPase associated with the T4P system, and that PilT only associates under particular conditions. For example, conformational changes incurred by these dynamic ATPases during cycles of catalysis may favor the incorporation of one ATPase over the other. Perhaps PilB and EpsE possess zinc-binding C_M domains and/or extended NTDs for stabilization, or to induce conformational changes that alter interactions with other T2S/T4P complex members. The dynamics of T4P and T2S (pseudo)pilus assembly are still not well understood, and it will be very informative to elucidate the roles of the N1 and C_M domains possessed by T2S and T4P assembly ATPases but not retraction ATPases.

Although the presence of the C_M domain is conserved among T2S ATPases, the tetracysteine motif that characterizes this domain is conspicuously absent in two T2S ATPases, *X. fastidiosa* and *X. campestris* XpsE (Planet *et al*., 2001; Robien *et al*., 2003). Particularly interesting is the corresponding lack of tetracysteine motifs in the PilD/XpsO pre(pseudo)pilin peptidases in these organisms, which are shared between the T2S and T4P systems (Hu *et al*., 1995). PilD homologues in most other organisms containing T2S and/or T4P systems contain a conserved tetracysteine motif that has been demonstrated to be necessary for methylase activity, but may not be absolutely required for PilD-

mediated N-terminal processing of pilins and pseudopilins (Strom *et al*., 1993; LaPointe & Taylor, 2000; Aly *et al*., 2013). It seems that *X. fastidosa* and *X. campestris* may have evolved different mechanisms to support protein stability for XpsE and XpsO. It is interesting to note that *X. campestris* XpsE contains an extended N-terminal domain that may also contribute to protein stability and result in XpsE-XpsL interactions that differ from those between EpsE and EpsL (Chen *et al*., 2005). Since PilB in *X. fastidosa* and *X. campestris* contain a tetracysteine motif, it is tempting to speculate that the shared absence of this motif in XpsE and XpsO is related and may reveal a novel interaction between T2S ATPases and prepilin peptidases. Much remains to be determined about the mechanisms that allow for proper folding, protein-protein interactions, and overall stability and function of EpsE and PilD and their homologues either in the presence or absence of zinc coordination.

Model

A working model of the role of the EpsE C_M domain is presented in Figure 5.4. During cycles of ATP binding and hydrolysis, the position of residues such as R441 and R394 at the base of the C_M domain relative to bound ATP and to other domains and/or subunits of the hexamer may be altered. Alternatively or in addition, contacts between residues from the C_M domain and the CTD and/or NTD may be modulated during this dynamic process. The positioning of key C_M residues may also be affected by interactions between EpsE and other T2S complex proteins such as EpsF, PilD, or T2S substrates, although these possibilities are

not represented in Figure 5.4. Changes in the position of R394 may support a conformation of EpsE that facilitates hexamerization and/or protein-protein interactions that favor pseudopilus extension. It is possible that R441-ATP interactions may dictate whether ATP binding and/or hydrolysis occurs, and the energy generated by this process is likely transduced by EpsE-EpsF-EpsG and/or EpsE-EpsL-EpsG interactions to power pseudopilus assembly (Gray *et al*., 2011).

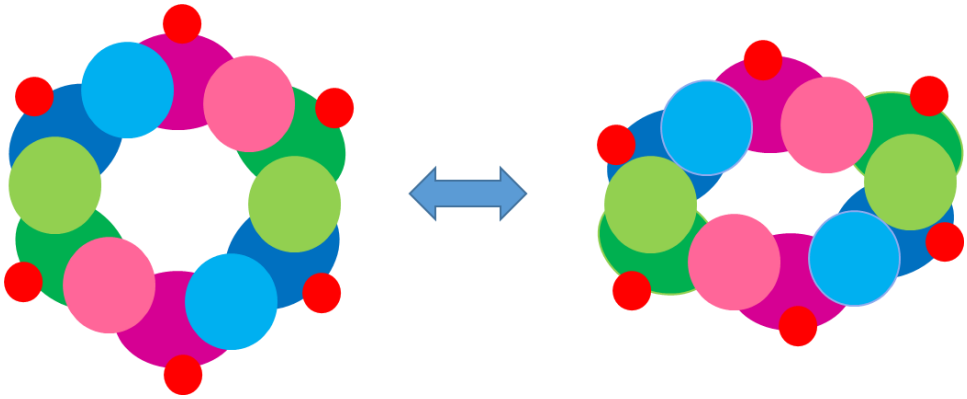

Figure 5.4 Model of possible interdomain interactions during cycles of ATP binding and hydrolysis. Representations are based on the hexameric structures of ΔN1-EpsE-6aa-Hcp1 and ΔN1-EpsE-8aa-Hcp1 (PDB 1kss and 1ksr, respectively). Subunits are colored according to structural symmetry as in Figure 1.3, with CTDs colored in a darker shade than their corresponding NTDs and all C_M domains shown in red. In the asymmetric hexamer model at right, the C_M domains from two subunits (blue) are positioned closer to NTDs and CTDs from neighboring subunits. Model is not to scale. See the text for details.

Future Directions

In order to examine the roles of R394 and R441 at the base of the C_M domain, we have begun to mutate these residues and assess the effects of mutations on *in vivo* complementation of EpsE. Additionally, we are in the process of purifying these proteins and measuring ATPase activity of both EpsE-cytoEpsL

and EpsE-Hcp1 hexamers. Preliminary data indicate that EpsE with R441A and R441D mutations is unable to complement the loss of VesB secretion in an *epsE*::*kan* strain of *V. cholerae* (Patrick, 2011). These variants were also co-purified as EpsE-cytoEpsL complexes and demonstrated a concordant loss of *in vitro* ATPase activity (Patrick, 2011). We have yet to analyze the effect of R441 mutations in EpsE hexamers *in vivo* and *in vitro*, or to construct R394 mutations in EpsE, although we expect R441A/D mutations to have similar effects on the function and activity of EpsE-Hcp1.

We also plan to investigate possible protein-protein interactions between the EpsE C_M domain and EpsF, EpsL, and PilD. Although an EpsE-PilD interaction is purely speculative at this point, we previously noted a correlation between organisms lacking the tetracysteine motif in T2S ATPases and prepilin peptidases, and it has been demonstrated that zinc binding is necessary for PilD's function (Aly *et al*., 2013). We aim to use co-immunoprecipitation to investigate potential EpsE-EpsF and/or EpsE-PilD interactions.

Potential interdomain interactions between the C_M domain and the NTD and CTD of EpsE will also be investigated through mutational analyses based on structural information. For example, mutating the residues highlighted in Figure 5.3 (R155, D158, G159, N434, H435) may provide information on specific interactions between the C_M and NTD. It would be beneficial to mutate some of the conserved residues highlighted in Figures 5.1 and 5.2 that may participate in C_M-CTD, -EpsF, and/or -PilD contacts as well. Because EpsE is a dynamic hexameric protein, we may not be able to ascertain all of the possible interdomain interactions using only

our current structural information. Alternatively, we can construct C_M loop truncations of various lengths to narrow down regions of this domain that could potentially participate in C_M interdomain or protein-protein interactions.

Despite observing complementation and activity of the EpsE-XcpR C_M chimera, we cannot definitively conclude that the EpsE C_M loop residues are unnecessary for the function or activity of T2S ATPases, since several residues are maintained in this loop swap. Mutagenesis of conserved loop residues highlighted in Figures 5.1 and 5.2 may generate tools to help elucidate whether this loop is directly involved in protein-protein interactions. To that end, we can also examine species specificity by testing whether the EpsE-XcpR C_M chimera and other C_M mutants can complement T2S in *epsE::kan V. cholerae* and a *P. aeruginosa* Δ*xcpR* mutant (Lory, unpublished). The results from these experiments will help us understand the role of the loop residues between the two dicysteines in the EpsE C_M domain.

Characterization of Secondary Mutations Acquired by *Vibrio cholerae* T2S Mutants

In Chapter 4, I identify and characterize potential suppressor mutations in *V. cholerae eps* mutants and show that two out of three sequenced strains acquired secondary mutations in the *vesC* gene, which encodes a T2-secreted protease. Since other studies have proposed that the *eps* genes are essential in *V. cholerae*, and we have previously described extensive cell envelope stability defects among *V. cholerae* T2S mutants, this knowledge has advanced our understanding of the mechanism behind these findings and provided insight into the potential role of the T2S system in the *V. cholerae* cell envelope barrier function (Judson & Mekalanos, 2000; Cameron *et al*., 2008; Chao *et al*., 2013; Kamp *et al*., 2013; Sandkvist *et al*., 1997; Sikora *et al*., 2007). My research suggests that the process of isolating *V. cholerae eps* mutations selects for secondary mutations that enable the disruption of these putatively essential genes.

Sequencing *V. cholerae eps* mutant genomes provided us with a high-throughput method for identifying possible suppressor mutations for further characterization. Since both the Δ*epsG* and Δ*epsL* mutants contain distinct mutations in *vesC*, this indicates one potential conserved mechanism for acquisition of suppressor mutations that may support *eps* gene inactivation. However, not all sequenced strains contain this mutation, and it is not known whether any other *V. cholerae* T2S mutants harbor *vesC* mutations. No *vesC* mutations have been identified in the Δ*epsM* mutant, which acquired 4 secondary mutations in a range of genes including those encoding metabolic and ribosomal proteins, and has one additional mutation in a non-coding region of the genome. It

is important to note that the Δ*epsG* and Δ*epsL* mutants were constructed using sucrose-based selection for allelic exchange using a suicide vector approach (Donnenberg & Kaper, 1991; Sikora *et al*., 2007), whereas the Δ*epsM* mutant was constructed using a single-step *λ* red recombination-based method (Datsenko & Wanner, 2000). These differences in selection may account for the variation in secondary mutations acquired by each *V. cholerae eps* mutant. In addition, the type of antibiotics used for selection may have an effect. It is also not known whether the particular *eps* gene that is inactivated influences the secondary mutations that are acquired.

Since *vesC* is not the only gene containing a secondary mutation in the Δ*epsG* and Δ*epsL* mutants, it may be that combinations of mutations are required to facilitate *eps* gene inactivation. We do not yet understand the significance of the 5 mutations in the Δ*epsM* strain, nor do we know the function of the VCA0254 gene which was mutated in the Δ*epsL* mutant. The relationship between the *eps* genes and *rfbV* is also not completely clear; however, inactivating *rfbV*, which is required for LPS assembly (Fallarino *et al*., 1997), may relieve some of the stress associated with the compromised cell envelope. These observations collectively suggest that there may be several factors that influence the acquisition of secondary mutations among *V. cholerae* T2S mutants and perhaps multiple ways to facilitate inactivation of the putatively essential *eps* genes.

The cell envelope defects of *V. cholerae eps* mutants are likely interrelated, although it is not completely clear how the acquisition of putative *eps* suppressor mutations plays a role in these phenotypes. LPS transport across the cell envelope

is accomplished by the LPS transport (Lpt) proteins LptA through G and MsbA (Silhavy *et al*., 2010, Okuda *et al*., 2016). Mislocalization of LPS or defects in LPS assembly lead to reductions in outer membrane barrier function (Ruiz & Silhavy, 2009). The outer membrane β-barrel protein LptD is regulated by the RpoE stress response pathway (Dartigalongue *et al*., 2001). RpoE acts as a sensor of envelope damage, including defects in OMP and LPS biogenesis (Alba & Gross, 2004). Interestingly, the *eps* genes are themselves regulated by RpoE (Ding *et al*., 2004; Zielke *et al*., 2014). Thus, accumulation of T2S substrates in the periplasm may cause cell envelope stress and trigger induction of RpoE, degradation of outer membrane proteins and LPS transport downregulation, collectively compromising the outer membrane barrier function. *V. cholerae eps* mutants may therefore acquire secondary mutations to mitigate some of the cell envelope stress resulting from these changes, by inactivating and/or degrading some of the T2S substrates. Alternatively or in addition, altering other cell envelope biogenesis pathways may mitigate some of the extracytoplasmic stress incurred by Eps inactivation.

Model

Our working model for this section is depicted in Figure 5.5. Under wild-type conditions, *V. cholerae* secretes VesC through the T2S system, and the protease is auto-activated once outside of the cell (left). However, when the T2S system is inactivated, VesC accumulates in the periplasm (right). Here, VesC may cause damage to the cell envelope through nonspecific proteolysis or by the sheer amount of protein accumulation in the periplasm, leading to RpoE activation and

degradation of outer membrane proteins including OmpS, OmpT, OmpU, OmpV, and OmpW (Sikora *et al*., 2007; Sandkvist *et al*., 1997). The process of constructing T2S gene disruptions may select for random mutations that inactivate VesC (A) and/or target the VesC protease for degradation (B) to alleviate some of the cell envelope stress incurred upon inactivation of the T2S system.

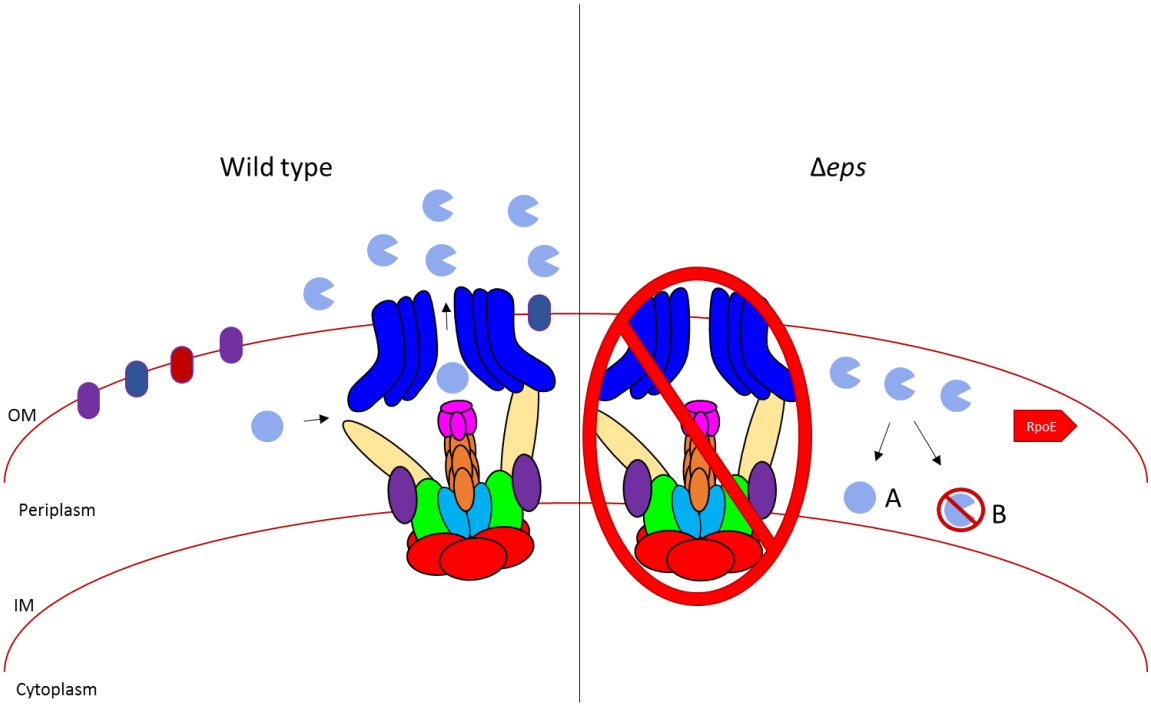

Figure 5.5 Working model of the mechanism by which secondary mutations in *vesC* may suppress *eps* mutant cell envelope phenotypes. Wild-type *V. cholerae* secretes VesC via the T2S system, which auto-activates extracellularly (left). Upon inactivation of the T2S system, VesC secretion is blocked and the protease accumulates in the periplasm (right). VesC may damage the cell envelope through nonspecific proteolysis or by massive protein accumulation, resulting in outer membrane protein perturbation and RpoE pathway induction. During the process of genetic inactivation of the T2S system, we may select for mutations that inactivate VesC (A) and/or target VesC for degradation (B) to prevent irreparable cell envelope damage in the absence of T2S.

Future Directions

Sequencing additional *V. cholerae eps* mutant genomes should provide further information on the mechanism of secondary mutation acquisition by T2S mutants. It would be particularly informative to sequence the genome of the P_{BAD}::*eps* strain, which was constructed in the presence of arabinose and thus may not have been subjected to suppressor-inducing conditions during its isolation. It would be interesting to sequence the P_{BAD}::*eps* strain grown with arabinose alongside the same strain passaged in the absence of arabinose. This might allow for the direct identification of secondary mutations acquired during the process of T2S gene inactivation in *V. cholerae*. However, it is possible that the P_{BAD} promoter is not completely turned off or that multiple experiments may yield different results, especially if there are multiple routes by which *V. cholerae eps* mutant suppression may occur, as our limited study suggests.

In order to investigate the conservation of *vesC* mutations among different *V. cholerae* T2S mutants, we aim to PCR-amplify and sequence the *vesC* genes from a variety of *eps* mutants from our laboratory collection. This will include additional T2S mutants from TRH7000, as well as those that have been constructed in N16961, 3083 and classical strains such as O395 and 569B, which are of different biotypes and have different LPS profiles (Hankins *et al*., 2012) and *eps* transposon-insertion mutants. The identification of additional *vesC* mutations among other T2S mutants would support our working model. It is possible, however, that the method of *eps* mutant construction and selection will influence the particular secondary mutations acquired by each strain.

One lingering question is whether it is easier to construct an *eps* mutation in a Δ*vesC* background. If so, this would support our model that *vesC* mutations suppress inactivation of *eps* mutations that would otherwise be lethal to *V. cholerae*. Attempts to distinguish this phenotype quantitatively have yielded mixed results, however. We have confirmed that both WT and Δ*vesC* are equally likely to undergo the initial homologous recombination event wherein a suicide vector containing a kanamycin-disrupted *eps* gene recombines with the chromosome. It is the second recombination step using sucrose selection to resolve the suicide vector sequence that is presumably the point at which selective pressure for the acquisition of secondary mutations occurs. We hypothesized that a Δ*vesC* mutant would be more likely to undergo this second recombination event. We performed this experiment twice so far, and in one instance we observed higher recombination frequencies in WT and in a subsequent experiment we found the opposite. Because the second crossover is a random occurrence, it is possible that we would need to perform the sucrose selection step multiple times with multiple cultures to accurately quantify the probability of this event. Thus, it is difficult to say with certainty that *vesC* mutations facilitate inactivation of the *eps* genes. It is also feasible that a Δ*vesC* ΔVCA0254 or a Δ*vesC* Δ*rfbV* background would be required for suppression.

Our working model is that secondary mutations in *vesC* among *eps* mutants either inactivate VesC or target it for degradation, but so far we cannot discriminate between the two possibilities. In order to do so, we will analyze culture supernatants and cells of a *V. cholerae* Δ*vesC* mutant overexpressing WT VesC

as well as the Q279P and 491fs variants by SDS-PAGE and immunoblotting once we have successfully developed VesC antiserum. If the variants of VesC can be detected in culture supernatants, the protease is likely inactivated by these mutations. The absence of VesC variants in the supernatant and cells would suggest that these mutations instead result in degradation of the protein.

Recently, our lab has noted that LPS assembly is diminished in two recently isolated *eps* mutants, and complementation of T2S corrects the assembly defect (Johnson *et al*., unpublished). In contrast, LPS assembly is not restored in the Δ*epsG* mutant expressing plasmid-encoded *epsG* (chapter 4). This is likely due to the mutation in *rfbV,* which supports O-antigen-lipid A core assembly, and complementation of the LPS assembly/transport defect may require both *epsG* and *rfbV* (Fallarino *et al*., 1997). Experiments are currently underway to probe the effects of *rfbV* overexpression on growth in *V. cholerae* to further understand the relationship between the cell envelope phenotypes of T2S mutants and secondary mutations acquired by these mutants.

Although some studies have suggested a role for the Ves proteases in pathogenesis, the precise functions of VesA, B, and C are still unknown (LaRocque *et al*., 2008; Syngkon *et al*., 2010; Hatzios *et al*., 2016). Recent characterization of the function of VesB from our laboratory hints at a role in nutrient acquisition (Gadwal *et al*., 2014). The Ves proteases may primarily mediate environmental survival of *V. cholerae*, supported by the observation that homologues of these proteins are only found among marine bacterial genera such as *Vibrio*, *Aeromonas*, and *Shewanella*. It is interesting to note that observations of cell

envelope defects have been limited to T2S mutants of *Vibrio* and *Aeromonas* species, which supports our assertion that this phenotype is related to the particular T2S substrates secreted by different organisms.

The function of the VCA0254 gene, which contained a secondary mutation in the Δ*epsL* mutant, is unknown. Interestingly, the predicted protein contains a putative signal peptide, suggesting that it may be a periplasmic protein or an as-yet unidentified T2S substrate. Domain homology analysis using BLAST reveals that a putative glycoside hydrolase domain (PFAM GH129) is also present. It is tempting to speculate that mutations are acquired in VCA0254 in a manner similar to that of *vesC*, wherein mutations that inactivate and/or degrade this protein alleviate cell envelope stress. We plan to construct a ΔVCA0254 mutant and VCA0254 overexpression constructs to investigate this possibility.

Conclusions

Collectively, my research provides additional mechanistic details of the T2S system. We have learned that zinc plays a critical role in the activity and function of EpsE, and that the C_M domain is required for T2S and likely supports protein stability. We have also assembled a working model of how secondary mutations in a T2S substrate may provide suppression of cell envelope stability defects upon inactivation of the putatively essential *eps* genes in *V. cholerae*. Thus, my dissertation encompasses insights we have gained from structural and functional analyses of the T2S system in *V. cholerae*.

References

Abendroth, J., Bagdasarian, M., Sandkvist, M. & Hol, W. G. J. The Structure of the Cytoplasmic Domain of EpsL, An Inner Membrane Component of the Type II Secretion System of Vibrio cholerae: An Unusual Member of the Actin-like ATPase Superfamily. *Journal of Molecular Biology* **344,** 619–633 (2004).

Abendroth, J., Kreger, A. C. & Hol, W. G. J. The dimer formed by the periplasmic domain of EpsL from the Type 2 Secretion System of Vibrio parahaemolyticus. *Journal of structural biology* **168,** 313 (2009).

Abendroth, J. *et al.* The three-dimensional structure of the cytoplasmic domains of EpsF from the type 2 secretion system of Vibrio cholerae. *Journal of structural biology* **166,** 303–315 (2009).

Abendroth, J., Murphy, P., Sandkvist, M., Bagdasarian, M. & Hol, W. G. J. The X-ray Structure of the Type II Secretion System Complex Formed by the N-terminal Domain of EpsE and the Cytoplasmic Domain of EpsL of Vibrio cholerae. *Journal of Molecular Biology* **348,** 845–855 (2005).

Abendroth, J., Rice, A. E., McLuskey, K., Bagdasarian, M. & Hol, W. G. The Crystal Structure of the Periplasmic Domain of the Type II Secretion System Protein EpsM From Vibrio cholerae: The Simplest Version of the Ferredoxin Fold. *Journal of Molecular Biology* **338,** 585–596 (2004).

Alam, A. *et al.* Hyperinfectivity of Human-Passaged Vibrio cholerae Can Be Modeled by Growth in the Infant Mouse. *Infection and Immunity* **73,** 6674–6679 (2005).

Alba, B. M. & Gross, C. A. Regulation of the Escherichia coli σE-dependent envelope stress response. *Molecular Microbiology* **52,** 613–619 (2004).

Albers, S.-V. & Jarrell, K. F. The archaellum: how Archaea swim. *Frontiers in Microbiology* **6,** 23 (2015).

Ali, M., Nelson, A. R., Lopez, A. L. & Sack, D. A. Updated Global Burden of Cholera in Endemic Countries. *PLoS Neglected Tropical Diseases* **9,** e0003832 (2015).

Aly, K. A. *et al.* Cell-free production of integral membrane aspartic acid proteases reveals zinc-dependent methyltransferase activity of the Pseudomonas aeruginosa prepilin peptidase PilD. *MicrobiologyOpen* **2,** 94–104 (2013).

Andro, T. *et al.* Mutants of Erwinia chrysanthemi defective in secretion of pectinase and cellulase. *Journal of Bacteriology* **160,** 1199–1203 (1984).

Aragon, V., Kurtz, S. & Cianciotto, N. P. Legionella pneumophila Major Acid Phosphatase and Its Role in Intracellular Infection. *Infection and Immunity* **69,** 177–185 (2001).

Aragon, V., Kurtz, S., Flieger, A., Neumeister, B. & Cianciotto, N. P. Secreted Enzymatic Activities of Wild-Type and pilD-Deficient Legionella pneumophila. *Infection and Immunity* **68,** 1855–1863 (2000).

Arts, J. *et al.* Interaction domains in the Pseudomonas aeruginosa type II secretory apparatus component XcpS (GspF). *Microbiology* **153,** 1582–1592 (2007).

Ayers, M. *et al.* PilM/N/O/P Proteins Form an Inner Membrane Complex That Affects the Stability of the Pseudomonas aeruginosa Type IV Pilus Secretin. *Journal of Molecular Biology* **394,** 128–142 (2009).

Baker, T. A. & Sauer, R. T. ClpXP, an ATP-powered unfolding and protein-degradation machine. *Biochimica et biophysica acta* **1823,** 15–28 (2012).

Baldi, D. L. *et al.* The Type II Secretion System and Its Ubiquitous Lipoprotein Substrate, SslE, Are Required for Biofilm Formation and Virulence of Enteropathogenic Escherichia coli. *Infection and Immunity* **80,** 2042–2052 (2012).

Ball, G., Durand, É., Lazdunski, A. & Filloux, A. A novel type II secretion system in Pseudomonas aeruginosa. *Molecular Microbiology* **43,** 475–485 (2002).

Bally, M. *et al.* Protein secretion in Pseudomonas aeruginosa: characterization of seven xcp genes and processing of secretory apparatus components by prepilin peptidase. *Molecular Microbiology* **6,** 1121–1131 (1992).

Berk, V. *et al.* Molecular Architecture and Assembly Principles of Vibrio cholerae Biofilms. *Science (New York, N.Y.)* **337,** 236–239 (2012).

Beveridge, T. J. Structures of Gram-Negative Cell Walls and Their Derived Membrane Vesicles. *Journal of Bacteriology* **181,** 4725–4733 (1999).

Bischof, L. F., Friedrich, C., Harms, A., Søgaard-Andersen, L. & van der Does, C. The Type IV Pilus Assembly ATPase PilB of Myxococcus xanthus interacts with the Inner Membrane Platform Protein PilC and the Nucleotide Binding Protein PilM. *Journal of Biological Chemistry* (2016). doi:10.1074/jbc.M115.701284

Bitter, W., Koster, M., Latijnhouwers, M., De Cock, H. & Tommassen, J. Formation of oligomeric rings by XcpQ and PilQ, which are involved in protein transport across the outer membrane of Pseudomonas aeruginosa. *Molecular Microbiology* **27,** 209–219 (1998).

Bouley, J., Condemine, G. & Shevchik, V. E. The PDZ domain of OutC and the N-terminal region of OutD determine the secretion specificity of the type II out pathway of Erwinia chrysanthemi1. *Journal of Molecular Biology* **308,** 205–219 (2001).

Broza, M. & Halpern, M. Pathogen reservoirs: Chironomid egg masses and Vibrio cholerae. *Nature* **412,** 40–40 (2001).

Brune, M., Hunter, J. L., Corrie, J. E. T. & Webb, M. R. Direct, Real-Time Measurement of Rapid Inorganic Phosphate Release Using a Novel Fluorescent Probe and Its Application to Actomyosin Subfragment 1 ATPase. *Biochemistry* **33,** 8262–8271 (1994).

Butler, S. M. & Camilli, A. Going against the grain: chemotaxis and infection in Vibrio cholerae. *Nature reviews. Microbiology* **3,** 611–620 (2005).

Camberg, J. L. *et al.* Synergistic stimulation of EpsE ATP hydrolysis by EpsL and acidic phospholipids. *The EMBO Journal* **26,** 19–27 (2007).

Camberg, J. L. & Sandkvist, M. Molecular Analysis of the Vibrio cholerae Type II Secretion ATPase EpsE. *Journal of Bacteriology* **187,** 249–256 (2005).

Cameron, D. E., Urbach, J. M. & Mekalanos, J. J. A defined transposon mutant library and its use in identifying motility genes in Vibrio cholerae. *Proceedings of the National Academy of Sciences of the United States of America* **105,** 8736–8741 (2008).

Campos, M., Cisneros, D. A., Nivaskumar, M. & Francetic, O. The type II secretion system – a dynamic fiber assembly nanomachine. *Research in Microbiology* **164,** 545–555 (2013).

Carter, S. G. & Karl, D. W. Inorganic phosphate assay with malachite green: An improvement and evaluation. *Journal of Biochemical and Biophysical Methods* **7,** 7–13 (1982).

Chami, M. *et al.* Structural Insights into the Secretin PulD and Its Trypsin-resistant Core. *Journal of Biological Chemistry* **280,** 37732–37741 (2005).

Chang, Y.-W. *et al.* Architecture of the type IVa pilus machine. *Science* **351,** (2016).

Chao, M. C. *et al.* High-resolution definition of the Vibrio cholerae essential gene set with hidden Markov model–based analyses of transposon-insertion sequencing data. *Nucleic Acids Research* **41,** 9033–9048 (2013).

Chatterjee, S. & Das, J. Electron microscopic observations on the excretion of cell-wall material by Vibrio cholerae. *J Gen Microbiol* **49,** 1–11 (1967).

Chen, Y. *et al.* Structure and Function of the XpsE N-Terminal Domain, an Essential Component of the Xanthomonas campestris Type II Secretion System. *Journal of Biological Chemistry* **280,** 42356–42363 (2005).

Chiang, P. *et al.* Functional role of conserved residues in the characteristic secretion NTPase motifs of the Pseudomonas aeruginosa type IV pilus motor proteins PilB, PilT and PilU. *Microbiology* **154,** 114–126 (2008).

Chung, I.-Y., Jang, H.-J., Bae, H.-W. & Cho, Y.-H. A phage protein that inhibits the bacterial ATPase required for type IV pilus assembly. *Proceedings of the National Academy of Sciences of the United States of America* **111,** 11503–11508 (2014).

Cianciotto, N. P. Many substrates and functions of type II secretion: lessons learned from Legionella pneumophila. *Future microbiology* **4,** 797–805 (2009).

Cianciotto, N. P. Type II secretion: a protein secretion system for all seasons. *Trends in Microbiology* **13,** 581–588

Clemens, J. *et al.* Field trial of oral cholera vaccines in Bangladesh: results from three-year follow-up. *The Lancet* **335,** 270–273 (1990).

Clemens, J. *et al.* Field trial of oral cholera vaccines in Bangladesh. *The Lancet* **328,** 124–127 (1986).

Condemine, G. & Shevchik, V. E. Overproduction of the secretin OutD suppresses the secretion defect of an Erwinia chrysanthemi outB mutant. *Microbiology* **146,** 639–647 (2000).

Connell, T. D., Metzger, D. J., Lynch, J. & Folster, J. P. Endochitinase Is Transported to the Extracellular Milieu by the eps-Encoded General Secretory Pathway of Vibrio cholerae. *Journal of Bacteriology* **180,** 5591–5600 (1998).

Dartigalongue, C., Missiakas, D. & Raina, S. Characterization of the Escherichia coli σE Regulon. *Journal of Biological Chemistry* **276,** 20866–20875 (2001).

Datsenko, K. A. & Wanner, B. L. One-step inactivation of chromosomal genes in Escherichia coli K-12 using PCR products. *Proceedings of the National Academy of Sciences of the United States of America* **97,** 6640–6645 (2000).

Davis, B. M. *et al.* Convergence of the Secretory Pathways for Cholera Toxin and the Filamentous Phage, CTXϕ. *Science* **288,** 333–335 (2000).

Davis, B. M. & Waldor, M. K. High-throughput sequencing reveals suppressors of Vibrio cholerae rpoE mutations: one fewer porin is enough. *Nucleic Acids Research* **37,** 5757–5767 (2009).

Ding, Y., Davis, B. M. & Waldor, M. K. Hfq is essential for Vibrio cholerae virulence and downregulates σE expression. *Molecular Microbiology* **53,** 345–354 (2004).

Donnenberg, M. S. & Kaper, J. B. Construction of an eae deletion mutant of enteropathogenic Escherichia coli by using a positive-selection suicide vector. *Infection and Immunity* **59,** 4310–4317 (1991).

Douet, V., Loiseau, L., Barras, F. & Py, B. Systematic analysis, by the yeast two-hybrid, of protein interaction between components of the type II secretory machinery of Erwinia chrysanthemi. *Research in Microbiology* **155,** 71–75 (2004).

Douzi, B. *et al.* The XcpV/GspI Pseudopilin Has a Central Role in the Assembly of a Quaternary Complex within the T2SS Pseudopilus. *The Journal of Biological Chemistry* **284,** 34580–34589 (2009).

Durand, É. *et al.* Type II Protein Secretion in Pseudomonas aeruginosa: the Pseudopilus Is a Multifibrillar and Adhesive Structure. *Journal of Bacteriology* **185,** 2749–2758 (2003).

Durand, É. *et al.* XcpX Controls Biogenesis of the Pseudomonas aeruginosa XcpT-containing Pseudopilus. *Journal of Biological Chemistry* **280,** 31378–31389 (2005).

Fallarino, A., Mavrangelos, C., Stroeher, U. H. & Manning, P. A. Identification of additional genes required for O-antigen biosynthesis in Vibrio cholerae O1. *Journal of Bacteriology* **179,** 2147–2153 (1997).

Fekkes, P., de Wit, J. G., Boorsma, A., Friesen, R. H. E. & Driessen, A. J. M. Zinc Stabilizes the SecB Binding Site of SecA. *Biochemistry* **38,** 5111–5116 (1999).

Felsenfeld, O. Notes on food, beverages and fomites contaminated with Vibrio cholerae. *Bulletin of the World Health Organization* **33,** 725–734 (1965).

Fong, J. C. N. & Yildiz, F. H. The rbmBCDEF Gene Cluster Modulates Development of Rugose Colony Morphology and Biofilm Formation in Vibrio cholerae. *Journal of Bacteriology* **189,** 2319–2330 (2007).

Foxall, R. L., Ballok, A. E., Avitabile, A. & Whistler, C. A. Spontaneous phenotypic suppression of GacA-defective Vibrio fischeri is achieved via mutation of csrA and ihfA. *BMC Microbiology* **15,** 180 (2015).

Fu, Y., Waldor, M. K. & Mekalanos, J. J. Tn-Seq Analysis of Vibrio cholerae Intestinal Colonization Reveals a Role for T6SS-Mediated Antibacterial Activity in the Host. *Cell host & microbe* **14,** 652–663 (2013).

Fullner, K. J. & Mekalanos, J. J. Genetic Characterization of a New Type IV-A Pilus Gene Cluster Found in Both Classical and El Tor Biotypes of Vibrio cholerae. *Infection and Immunity* **67,** 1393–1404 (1999).

Gadwal, S., Korotkov, K. V., Delarosa, J. R., Hol, W. G. J. & Sandkvist, M. Functional and Structural Characterization of Vibrio cholerae Extracellular Serine Protease B, VesB. *The Journal of Biological Chemistry* **289,** 8288–8298 (2014).

Galhardo, R. S., Hastings, P. J. & Rosenberg, S. M. Mutation as a Stress Response and the Regulation of Evolvability. *Critical Reviews in Biochemistry and Molecular Biology* **42,** 399–435 (2007).

Georgiadou, M., Castagnini, M., Karimova, G., Ladant, D. & Pelicic, V. Large-scale study of the interactions between proteins involved in type IV pilus biology in Neisseria meningitidis: characterization of a subcomplex involved in pilus assembly. *Molecular Microbiology* **84,** 857–873 (2012).

Gérard-Vincent, M. *et al.* Identification of XcpP domains that confer functionality and specificity to the Pseudomonas aeruginosa type II secretion apparatus. *Molecular Microbiology* **44,** 1651–1665 (2002).

Gerlach, R. G. & Hensel, M. Protein secretion systems and adhesins: The molecular armory of Gram-negative pathogens. *International Journal of Medical Microbiology* **297,** 401–415 (2007).

Ghosh, A. & Albers, S.-V. Assembly and function of the archaeal flagellum. *Biochemical Society Transactions* **39,** 64–69 (2011).

Ghosh, A., Hartung, S., van der Does, C., Tainer, J. A. & Albers, S.-V. Archaeal flagellar ATPase motor shows ATP-dependent hexameric assembly and activity stimulation by specific lipid binding. *The Biochemical journal* **437,** 43–52 (2011).

Gibson, J. L. *et al.* The σ(E) stress response is required for stress-induced mutation and amplification in Escherichia coli. *Molecular Microbiology* **77,** 415–430 (2010).

Grad, Y. H. & Waldor, M. K. Deciphering the Origins and Tracking the Evolution of Cholera Epidemics with Whole-Genome-Based Molecular Epidemiology. *mBio* **4,** e00670–13 (2013).

Graumann, J. *et al.* Activation of the Redox-Regulated Molecular Chaperone Hsp33—A Two-Step Mechanism. *Structure* **9,** 377–387

Gray, M. D., Bagdasarian, M., Hol, W. G. J. & Sandkvist, M. In vivo cross-linking of EpsG to EpsL suggests a role for EpsL as an ATPase-pseudopilin coupling protein in the Type II secretion system of Vibrio cholerae. *Molecular microbiology* **79,** 786–798 (2011).

Haft, D. H. & Varghese, N. GlyGly-CTERM and Rhombosortase: A C-Terminal Protein Processing Signal in a Many-to-One Pairing with a Rhomboid Family Intramembrane Serine Protease. *PLoS ONE* **6,** e28886 (2011).

Halpern, M., Gancz, H., Broza, M. & Kashi, Y. Vibrio cholerae Hemagglutinin/Protease Degrades Chironomid Egg Masses. *Applied and Environmental Microbiology* **69,** 4200–4204 (2003).

Hankins, J. V., Madsen, J. A., Giles, D. K., Brodbelt, J. S. & Trent, M. S. Amino acid addition to Vibrio cholerae LPS establishes a link between surface remodeling in Gram-positive and Gram-negative bacteria. *Proceedings of the National Academy of Sciences of the United States of America* **109,** 8722–8727 (2012).

Hanson, P. I. & Whiteheart, S. W. AAA+ proteins: have engine, will work. *Nat Rev Mol Cell Biol* **6,** 519–529 (2005).

Harder, K. W. *et al.* Characterization and kinetic analysis of the intracellular domain of human protein tyrosine phosphatase beta (HPTP beta) using synthetic phosphopeptides. *Biochemical Journal* **298,** 395–401 (1994).

Harding, C. M., Kinsella, R. L., Palmer, L. D., Skaar, E. P. & Feldman, M. F. Medically Relevant Acinetobacter Species Require a Type II Secretion System and Specific Membrane-Associated Chaperones for the Export of Multiple Substrates and Full Virulence. *PLoS Pathogens* **12,** e1005391 (2016).

Harris, J. B., LaRocque, R. C., Qadri, F., Ryan, E. T. & Calderwood, S. B. Cholera. *The Lancet* **379,** 2466–2476

Hatzios, S. K. *et al.* Chemoproteomic profiling of host and pathogen enzymes active in cholera. *Nat Chem Biol* **12,** 268–274 (2016).

Henkel, R. D., VandeBerg, J. L. & Walsh, R. A. A microassay for ATPase. *Analytical Biochemistry* **169,** 312–318 (1988).

Hirst, T. R., Sanchez, J., Kaper, J. B., Hardy, S. J. & Holmgren, J. Mechanism of toxin secretion by Vibrio cholerae investigated in strains harboring plasmids that encode heat-labile enterotoxins of Escherichia coli. *Proceedings of the National Academy of Sciences of the United States of America* **81,** 7752–7756 (1984).

Howard, S. P. & Buckley, J. T. Protein export by a gram-negative bacterium: production of aerolysin by Aeromonas hydrophila. *Journal of Bacteriology* **161,** 1118–1124 (1985).

Howard, S. P., Critch, J. & Bedi, A. Isolation and analysis of eight exe genes and their involvement in extracellular protein secretion and outer membrane assembly in Aeromonas hydrophila. *Journal of Bacteriology* **175,** 6695–6703 (1993).

Hu, N.-T., Lee, P.-F. & Chen, C. The type IV pre-pilin leader peptidase of Xanthomonas campestris pv. campestris is functional without conserved cysteine residues. *Molecular Microbiology* **18,** 769–777 (1995).

Huq, A., West, P. A., Small, E. B., Huq, M. I. & Colwell, R. R. Influence of water temperature, salinity, and pH on survival and growth of toxigenic Vibrio cholerae serovar 01 associated with live copepods in laboratory microcosms. *Applied and Environmental Microbiology* **48,** 420–424 (1984).

Huq, A. *et al.* Simple Sari Cloth Filtration of Water Is Sustainable and Continues To Protect Villagers from Cholera in Matlab, Bangladesh. *mBio* **1,** e00034–10 (2010).

Hwang, W. *et al.* Functional Characterization of EpsC, a Component of the Type II Secretion System, in the Pathogenicity of Vibrio vulnificus. *Infection and Immunity* **79,** 4068–4080 (2011).

Ichige, A., Oishi, K. & Mizushima, S. Isolation and characterization of mutants of a marine Vibrio strain that are defective in production of extracellular proteins. *Journal of Bacteriology* **170,** 3537–3542 (1988).

Ilbert, M. *et al.* The redox-switch domain of Hsp33 functions as dual stress sensor. *Nature structural & molecular biology* **14,** 556–563 (2007).

Iredell, J. R., Stroeher, U. H., Ward, H. M. & Manning, P. A. Lipopolysaccharide O-antigen expression and the effect of its absence on virulence in rfb mutants of Vibrio cholerae O1. *FEMS Immunology & Medical Microbiology* **20,** 45–54 (1998).

Jakob, U., Eser, M. & Bardwell, J. C. A. Redox Switch of Hsp33 Has a Novel Zinc-binding Motif. *Journal of Biological Chemistry* **275,** 38302–38310 (2000).

Jakob, U., Muse, W., Eser, M. & Bardwell, J. C. Chaperone Activity with a Redox Switch. *Cell* **96,** 341–352

Jiang, B. & Howard, S. P. The Aeromonas hydrophila exeE gene, required both for protein secretion and normal outer membrane biogenesis, is a member of a general secretion pathway. *Molecular Microbiology* **6,** 1351–1361 (1992).

Johnson, T. L. *et al.* The Type II Secretion System Delivers Matrix Proteins for Biofilm Formation by Vibrio cholerae. *Journal of Bacteriology* **196,** 4245–4252 (2014).

Johnson, T. L., Waack, U., Smith, S., Mobley, H. & Sandkvist, M. Acinetobacter baumannii Is Dependent on the Type II Secretion System and Its Substrate LipA for Lipid Utilization and In Vivo Fitness. *Journal of Bacteriology* **198,** 711–719 (2016).

Judson, N. & Mekalanos, J. J. TnAraOut, A transposon-based approach to identify and characterize essential bacterial genes. *Nat Biotech* **18,** 740–745 (2000).

Jutla, A. *et al.* Environmental Factors Influencing Epidemic Cholera. *The American Journal of Tropical Medicine and Hygiene* **89,** 597–607 (2013).

Jyot, J. *et al.* Type II Secretion System of Pseudomonas aeruginosa: In Vivo Evidence of a Significant Role in Death Due to Lung Infection. *The Journal of Infectious Diseases* **203,** 1369–1377 (2011).

Kamp, H. D., Patimalla-Dipali, B., Lazinski, D. W., Wallace-Gadsden, F. & Camilli, A. Gene Fitness Landscapes of Vibrio cholerae at Important Stages of Its Life Cycle. *PLoS Pathogens* **9,** e1003800 (2013).

Kaper, J. B., Morris, J. G. & Levine, M. M. Cholera. *Clinical Microbiology Reviews* **8,** 48–86 (1995).

Kirn, T. J., Jude, B. A. & Taylor, R. K. A colonization factor links Vibrio cholerae environmental survival and human infection. *Nature* **438,** 863–866 (2005).

Köhler, R. *et al.* Structure and assembly of the pseudopilin PulG. *Molecular Microbiology* **54,** 647–664 (2004).

Kondo, K., Takade, A. & Amako, K. Release of the Outer Membrane Vesicles from Vibrio cholerae and Vibrio parahaemolyticus. *Microbiology and Immunology* **37,** 149–152 (1993).

Korotkov, K. V. *et al.* Calcium Is Essential for the Major Pseudopilin in the Type 2 Secretion System. *The Journal of Biological Chemistry* **284,** 25466–25470 (2009).

Korotkov, K. V. & Hol, W. G. J. Structure of the GspK-GspI-GspJ complex from the enterotoxigenic Escherichia coli type 2 secretion system. *Nat Struct Mol Biol* **15,** 462–468 (2008).

Korotkov, K. V. *et al.* Structural and Functional Studies on the Interaction of GspC and GspD in the Type II Secretion System. *PLoS Pathogens* **7,** e1002228 (2011).

Korotkov, K. V., Krumm, B., Bagdasarian, M. & Hol, W. G. J. Structural and Functional Studies of EpsC, a Crucial Component of the Type 2 Secretion System from Vibrio cholerae. *Journal of Molecular Biology* **363,** 311–321 (2006).

Korotkov, K. V., Sandkvist, M. & Hol, W. G. J. The type II secretion system: biogenesis, molecular architecture and mechanism. *Nature reviews. Microbiology* **10,** 336–351 (2012).

Krishna, S. S., Majumdar, I. & Grishin, N. V. Survey and summary: Structural classification of zinc fingers. *Nucleic Acids Research* **31,** 532–550 (2003).

Kulp, A. & Kuehn, M. J. Biological Functions and Biogenesis of Secreted Bacterial Outer Membrane Vesicles. *Annual review of microbiology* **64,** 163–184 (2010).

LaPointe, C. F. & Taylor, R. K. The Type 4 Prepilin Peptidases Comprise a Novel Family of Aspartic Acid Proteases. *Journal of Biological Chemistry* **275,** 1502–1510 (2000).

LaRocque, R. C. *et al.* Proteomic Analysis of Vibrio cholerae in Human Stool. *Infection and Immunity* **76,** 4145–4151 (2008).

Lathem, W. W. *et al.* StcE, a metalloprotease secreted by Escherichia coli O157:H7, specifically cleaves C1 esterase inhibitor. *Molecular Microbiology* **45,** 277–288 (2002).

Lazdunski, A., Guzzo, J., Filloux, A., Bally, M. & Murgier, M. Secretion of extracellular proteins by Pseudomonas aeruginosa. *Biochimie* **72,** 147–156 (1990).

Lee, M.-S., Chen, L.-Y., Leu, W.-M., Shiau, R.-J. & Hu, N.-T. Associations of the Major Pseudopilin XpsG with XpsN (GspC) and Secretin XpsD of Xanthomonas campestris pv. campestris Type II Secretion Apparatus Revealed by Cross-linking Analysis. *Journal of Biological Chemistry* **280,** 4585–4591 (2005).

Lobitz, B. *et al.* Climate and infectious disease: Use of remote sensing for detection of Vibrio cholerae by indirect measurement. *Proceedings of the National Academy of Sciences* **97,** 1438–1443 (2000).

Lu, C. *et al.* Hexamers of the Type II Secretion ATPase GspE from Vibrio cholerae with Increased ATPase Activity. *Structure (London, England : 1993)* **21,** 1707–1717 (2013).

Maret, W. & Li, Y. Coordination Dynamics of Zinc in Proteins. *Chem. Rev.* **109,** 4682–4707 (2009).

Marsh, J. W. & Taylor, R. K. Identification of the Vibrio cholerae type 4 prepilin peptidase required for cholera toxin secretion and pilus formation. *Molecular Microbiology* **29,** 1481–1492 (1998).

Martínez, A., Ostrovsky, P. & Nunn, D. N. LipC, a second lipase of Pseudomonas aeruginosa, is LipB and Xcp dependent and is transcriptionally regulated by pilus biogenesis components. *Molecular Microbiology* **34,** 317–326 (1999).

Maxson, M. E. & Grinstein, S. The vacuolar-type H+-ATPase at a glance – more than a proton pump. *Journal of Cell Science* **127,** 4987–4993 (2014).

McLaughlin, S. H., Smith, H. W. & Jackson, S. E. Stimulation of the weak ATPase activity of human Hsp90 by a client protein1. *Journal of Molecular Biology* **315,** 787–798 (2002).

Merrell, D. S. *et al.* Host-induced epidemic spread of the cholera bacterium. *Nature* **417,** 642–645 (2002).

Misic, A. M., Satyshur, K. A. & Forest, K. T. P. aeruginosa PilT structures with and without nucleotide reveal a dynamic Type IV pilus retraction motor. *Journal of molecular biology* **400,** 1011–1021 (2010).

Mougous, J. D. *et al.* A Virulence Locus of Pseudomonas aeruginosa Encodes a Protein Secretion Apparatus. *Science (New York, N.Y.)* **312,** 1526–1530 (2006).

Nelson, E. J., Harris, J. B., Morris, J. G., Calderwood, S. B. & Camilli, A. Cholera transmission: the host, pathogen and bacteriophage dynamic. *Nature reviews. Microbiology* **7,** 693-702 (2009).

Nouwen, N., Stahlberg, H., Pugsley, A. P. & Engel, A. Domain structure of secretin PulD revealed by limited proteolysis and electron microscopy. *The EMBO Journal* **19,** 2229–2236 (2000).

Nunn, D. Bacterial Type II protein export and pilus biogenesis: more than just homologies? *Trends in Cell Biology* **9,** 402–408 (1999).

Nunn, D. N. & Lory, S. Cleavage, methylation, and localization of the Pseudomonas aeruginosa export proteins XcpT, -U, -V, and -W. *Journal of Bacteriology* **175,** 4375–4382 (1993).

Okuda, S., Sherman, D. J., Silhavy, T. J., Ruiz, N. & Kahne, D. Lipopolysaccharide transport and assembly at the outer membrane: the PEZ model. *Nat Rev Micro* doi: 10.1038/nrmicro.2016.25, (2016).

Overbye, L. J., Sandkvist, M. & Bagdasarian, M. Genes required for extracellular secretion of enterotoxin are clustered in Vibrio cholerae. *Gene* **132,** 101–106 (1993).

Pascual, M., Rodó, X., Ellner, S. P., Colwell, R. & Bouma, M. J. Cholera Dynamics and El Niño-Southern Oscillation. *Science* **289,** 1766–1769 (2000).

Patrick, M., Korotkov, K. V., Hol, W. G. J. & Sandkvist, M. Oligomerization of EpsE Coordinates Residues from Multiple Subunits to Facilitate ATPase Activity. *The Journal of Biological Chemistry* **286,** 10378–10386 (2011).

Pineau, C. *et al.* Substrate recognition by the bacterial type II secretion system: more than a simple interaction. *Molecular Microbiology* **94,** 126–140 (2014).

Planet, P. J., Kachlany, S. C., DeSalle, R. & Figurski, D. H. Phylogeny of genes for secretion NTPases: Identification of the widespread tadA subfamily and development of a diagnostic key for gene classification. *Proceedings of the National Academy of Sciences of the United States of America* **98,** 2503–2508 (2001).

Possot, O. M., Gérard-Vincent, M. & Pugsley, A. P. Membrane Association and Multimerization of Secreton Component PulC. *Journal of Bacteriology* **181,** 4004–4011 (1999).

Possot, O. M. & Pugsley, A. P. The conserved tetracysteine motif in the general secretory pathway component PulE is required for efficient pullulanase secretion1. *Gene* **192,** 45–50 (1997).

Pugsley, A. P., Poquet, I. & Kornacker, M. G. Two distinct steps in pullulanase secretion by Escherichia coli K12. *Molecular Microbiology* **5,** 865–873 (1991).

Pugsley, A. P. The complete general secretory pathway in gram-negative bacteria. *Microbiological Reviews* **57,** 50–108 (1993).

Py, B., Loiseau, L. & Barras, F. An inner membrane platform in the type II secretion machinery of Gram-negative bacteria. *EMBO Reports* **2,** 244–248 (2001).

Reichow, S. L., Korotkov, K. V., Hol, W. G. J. & Gonen, T. Structure of the cholera toxin secretion channel in its closed state. *Nature structural & molecular biology* **17,** 1226–1232 (2010).

Reindl, S. *et al.* Insights on FlaI Functions in Archaeal Motor Assembly and Motility from Structures, Conformations and Genetics. *Molecular cell* **49,** 1069–1082 (2013).

Robert, V., Filloux, A. & Michel, G. P. F. Subcomplexes from the Xcp secretion system of Pseudomonas aeruginosa. *FEMS Microbiology Letters* **252,** 43–50 (2005).

Robert, V., Hayes, F., Lazdunski, A. & Michel, G. P. F. Identification of XcpZ Domains Required for Assembly of the Secreton of Pseudomonas aeruginosa. *Journal of Bacteriology* **184,** 1779–1782 (2002).

Robien, M. A., Krumm, B. E., Sandkvist, M. & Hol, W. G. J. Crystal Structure of the Extracellular Protein Secretion NTPase EpsE of Vibrio cholerae. *Journal of Molecular Biology* **333,** 657–674 (2003).

Rondelet, A. & Condemine, G. Type II secretion: the substrates that won't go away. *Research in Microbiology* **164,** 556–561 (2013).

Rose, I. *et al.* Identification and characterization of a unique, zinc-containing transport ATPase essential for natural transformation in Thermus thermophilus HB27. *Extremophiles* **15,** 191–202 (2011).

Rossier, O., Starkenburg, S. R. & Cianciotto, N. P. Legionella pneumophila Type II Protein Secretion Promotes Virulence in the A/J Mouse Model of Legionnaires' Disease Pneumonia. *Infection and Immunity* **72,** 310–321 (2004).

Rowlands, M. G. *et al.* High-throughput screening assay for inhibitors of heat-shock protein 90 ATPase activity. *Analytical Biochemistry* **327,** 176–183 (2004).

Ruiz, N., Kahne, D. & Silhavy, T. J. Transport of lipopolysaccharide across the cell envelope: the long road of discovery. *Nature reviews. Microbiology* **7,** 677–683 (2009).

Sack, D. A., Sack, R. B., Nair, G. B. & Siddique, A. Cholera. *The Lancet* **363,** 223–233 (2004).

Salzer, R. *et al.* Zinc and ATP Binding of the Hexameric AAA-ATPase PilF from Thermus thermophilus: Role in complex stability, piliation, adhesion, twitching motility, and natural transformation. *The Journal of Biological Chemistry* **289,** 30343–30354 (2014).

Sandkvist, M., Bagdasarian, M., Howard, S. P. & DiRita, V. J. Interaction between the autokinase EpsE and EpsL in the cytoplasmic membrane is required for extracellular secretion in Vibrio cholerae. *The EMBO Journal* **14,** 1664–1673 (1995).

Sandkvist, M. *et al.* General secretion pathway (eps) genes required for toxin secretion and outer membrane biogenesis in Vibrio cholerae. *Journal of Bacteriology* **179,** 6994–7003 (1997).

Sandkvist, M., Hough, L. P., Bagdasarian, M. M. & Bagdasarian, M. Direct Interaction of the EpsL and EpsM Proteins of the General Secretion Apparatus in Vibrio cholerae. *Journal of Bacteriology* **181,** 3129–3135 (1999).

Sandkvist, M., Keith, J. M., Bagdasarian, M. & Howard, S. P. Two Regions of EpsL Involved in Species-Specific Protein-Protein Interactions with EpsE and EpsM of the General Secretion Pathway in Vibrio cholerae. *Journal of Bacteriology* **182,** 742–748 (2000).

Sandkvist, M., Morales, V. & Bagdasarian, M. A protein required for secretion of cholera toxin through the outer membrane of Vibrio cholerae. *Gene* **123,** 81–86 (1993).

Sandkvist, M. Biology of type II secretion. *Molecular Microbiology* **40,** 271–283 (2001).

Sandkvist, M. Type II Secretion and Pathogenesis. *Infection and Immunity* **69,** 3523–3535 (2001).

Sanghera, J., Li, R. & Yan, J. Comparison of the Luminescent ADP-Glo Assay to a Standard Radiometric Assay for Measurement of Protein Kinase Activity. *ASSAY and Drug Development Technologies* **7,** 615–622 (2009).

Satyshur, K. A. *et al.* Crystal Structures of the Pilus Retraction Motor PilT Suggest Large Domain Movements and Subunit Cooperation Drive Motility. *Structure (London, England : 1993)* **15,** 363–376 (2007).

Sauvonnet, N., Vignon, G., Pugsley, A. P. & Gounon, P. Pilus formation and protein secretion by the same machinery in Escherichia coli. *The EMBO Journal* **19,** 2221–2228 (2000).

Savvides, S. N. *et al.* VirB11 ATPases are dynamic hexameric assemblies: new insights into bacterial type IV secretion. *The EMBO Journal* **22,** 1969–1980 (2003).

Schnaitman, C. A. & Klena, J. D. Genetics of lipopolysaccharide biosynthesis in enteric bacteria. *Microbiological Reviews* **57,** 655–682 (1993).

Schoenhofen, I. C., Li, G., Strozen, T. G. & Howard, S. P. Purification and Characterization of the N-Terminal Domain of ExeA: a Novel ATPase Involved in the Type II Secretion Pathway of Aeromonas hydrophila. *Journal of Bacteriology* **187,** 6370–6378 (2005).

Sherman, D. J. *et al.* Decoupling catalytic activity from biological function of the ATPase that powers lipopolysaccharide transport. *Proceedings of the National Academy of Sciences of the United States of America* **111,** 4982–4987 (2014).

Shevchik, V. E., Robert-Baudouy, J. & Condemine, G. Specific interaction between OutD, an Erwinia chrysanthemi outer membrane protein of the general secretory pathway, and secreted proteins. *The EMBO Journal* **16,** 3007–3016 (1997).

Shevchik, V. E., Robert-Baudouy, J. & Condemine, G. Specific interaction between OutD, an Erwinia chrysanthemi outer membrane protein of the general secretory pathway, and secreted proteins. *The EMBO Journal* **16,** 3007–3016 (1997).

Shiue, S.-J. *et al.* XpsE oligomerization triggered by ATP binding, not hydrolysis, leads to its association with XpsL. *The EMBO Journal* **25,** 1426–1435 (2006).

Sikora, A. E., Beyhan, S., Bagdasarian, M., Yildiz, F. H. & Sandkvist, M. Cell Envelope Perturbation Induces Oxidative Stress and Changes in Iron Homeostasis in Vibrio cholerae. *Journal of Bacteriology* **191,** 5398–5408 (2009).

Sikora, A. E., Lybarger, S. R. & Sandkvist, M. Compromised Outer Membrane Integrity in Vibrio cholerae Type II Secretion Mutants. *Journal of Bacteriology* **189,** 8484–8495 (2007).

Sikora, A. E., Zielke, R. A., Lawrence, D. A., Andrews, P. C. & Sandkvist, M. Proteomic Analysis of the Vibrio cholerae Type II Secretome Reveals New Proteins, Including Three Related Serine Proteases. *The Journal of Biological Chemistry* **286,** 16555–16566 (2011).

Sikora, A. E. Proteins Secreted via the Type II Secretion System: Smart Strategies of Vibrio cholerae to Maintain Fitness in Different Ecological Niches. *PLoS Pathogens* **9,** e1003126 (2013).

Silhavy, T. J., Kahne, D. & Walker, S. The Bacterial Cell Envelope. *Cold Spring Harbor Perspectives in Biology* **2,** a000414 (2010).

Smith, D. R. *et al.* In situ proteolysis of the Vibrio cholerae matrix protein RbmA promotes biofilm recruitment. *Proceedings of the National Academy of Sciences* **112,** 10491–10496 (2015).

Söderberg, M. A., Rossier, O. & Cianciotto, N. P. The Type II Protein Secretion System of Legionella pneumophila Promotes Growth at Low Temperatures. *Journal of Bacteriology* **186,** 3712–3720 (2004).

Srivatsan, A. *et al.* High-Precision, Whole-Genome Sequencing of Laboratory Strains Facilitates Genetic Studies. *PLoS Genetics* **4,** e1000139 (2008).

Stroeher, U. H., Jedani, K. E. & Manning, P. A. Genetic organization of the regions associated with surface polysaccharide synthesis in Vibrio cholerae O1, O139 and Vibrio anguillarum O1 and O2: a review1. *Gene* **223,** 269–282 (1998).

Strom, M. S., Bergman, P. & Lory, S. Identification of active-site cysteines in the conserved domain of PilD, the bifunctional type IV pilin leader peptidase/N-methyltransferase of Pseudomonas aeruginosa. *Journal of Biological Chemistry* **268,** 15788–15794 (1993).

Syngkon, A. *et al.* Studies on a Novel Serine Protease of a ΔhapAΔprtV Vibrio cholerae O1 Strain and Its Role in Hemorrhagic Response in the Rabbit Ileal Loop Model. *PLoS ONE* **5,** e13122 (2010).

Takhar, H. K., Kemp, K., Kim, M., Howell, P. L. & Burrows, L. L. The Platform Protein Is Essential for Type IV Pilus Biogenesis. *The Journal of Biological Chemistry* **288,** 9721–9728 (2013).

Talkington, D. *et al.* Characterization of Toxigenic Vibrio cholerae from Haiti, 2010–2011. *Emerging Infectious Diseases* **17,** 2122–2129 (2011).

Tamayo, R., Patimalla, B. & Camilli, A. Growth in a Biofilm Induces a Hyperinfectious Phenotype in Vibrio cholerae. *Infection and Immunity* **78,** 3560–3569 (2010).

Thibault, G. *et al.* Specificity in substrate and cofactor recognition by the N-terminal domain of the chaperone ClpX. *Proceedings of the National Academy of Sciences of the United States of America* **103,** 17724–17729 (2006).

Thomas, J. D., Reeves, P. J. & Salmond, G. P. C. The general secretion pathway of Erwinia carotovora subsp. carotovora: analysis of the membrane topology of OutC and OutF. *Microbiology* **143,** 713–720 (1997).

Turner, L. R., Lara, J. C., Nunn, D. N. & Lory, S. Mutations in the consensus ATP-binding sites of XcpR and PilB eliminate extracellular protein secretion and pilus biogenesis in Pseudomonas aeruginosa. *Journal of Bacteriology* **175,** 4962–4969 (1993).

Vezzulli, L., Pruzzo, C., Huq, A. & Colwell, R. R. Environmental reservoirs of Vibrio cholerae and their role in cholera. *Environmental Microbiology Reports* **2,** 27–33 (2010).

Vignon, G. *et al.* Type IV-Like Pili Formed by the Type II Secreton: Specificity, Composition, Bundling, Polar Localization, and Surface Presentation of Peptides. *Journal of Bacteriology* **185,** 3416–3428 (2003).

Voulhoux, R. *et al.* Involvement of the twin-arginine translocation system in protein secretion via the type II pathway. *The EMBO Journal* **20,** 6735–6741 (2001).

Wachsmuth, I. K., Blake, P. A. & Olsvik, Ø (eds) in *Vibrio cholerae and Cholera: Molecular to Global Perspectives*. (ASM, 1994).

Whitchurch, C. B. & Mattick, J. S. Characterization of a gene, pilU, required for twitching motility but not phage sensitivity in Pseudomonas aeruginosa. *Molecular Microbiology* **13,** 1079–1091 (1994).

Yamagata, A. & Tainer, J. A. Hexameric structures of the archaeal secretion ATPase GspE and implications for a universal secretion mechanism. *The EMBO Journal* **26,** 878–890 (2007).

Yanez, M. E., Korotkov, K. V., Abendroth, J. & Hol, W. G. J. The crystal structure of a binary complex of two pseudopilins: EpsI and EpsJ from the Type 2 Secretion System of Vibrio vulnificus. *Journal of molecular biology* **375,** 471–486 (2008).

Yanez, M. E., Korotkov, K. V., Abendroth, J. & Hol, W. G. J. Structure of the minor pseudopilin EpsH from the Type 2 Secretion System of Vibrio cholerae. *Journal of molecular biology* **377,** 91–103 (2008).

Yeo, H.-J., Savvides, S. N., Herr, A. B., Lanka, E. & Waksman, G. Crystal Structure of the Hexameric Traffic ATPase of the Helicobacter pylori Type IV Secretion System. *Molecular Cell* **6,** 1461–1472

Zhang, X. *et al.* Altered cofactor regulation with disease-associated p97/VCP mutations. *Proceedings of the National Academy of Sciences of the United States of America* **112,** E1705–E1714 (2015).

Zhou, J. & Xu, Z. Structural determinants of SecB recognition by SecA in bacterial protein translocation. *Nat Struct Mol Biol* **10,** 942–947 (2003).

Zielke, R. A. *et al.* The Type II Secretion Pathway in Vibrio cholerae Is Characterized by Growth Phase-Dependent Expression of Exoprotein Genes and Is Positively Regulated by σ(E). *Infection and Immunity* **82,** 2788–2801 (2014).